ISSN 1909-8642

SHIP SCIENCE & TECHNOLOGY

CIENCIA & TECNOLOGÍA DE BUQUES

COTECMAR
COLOMBIA

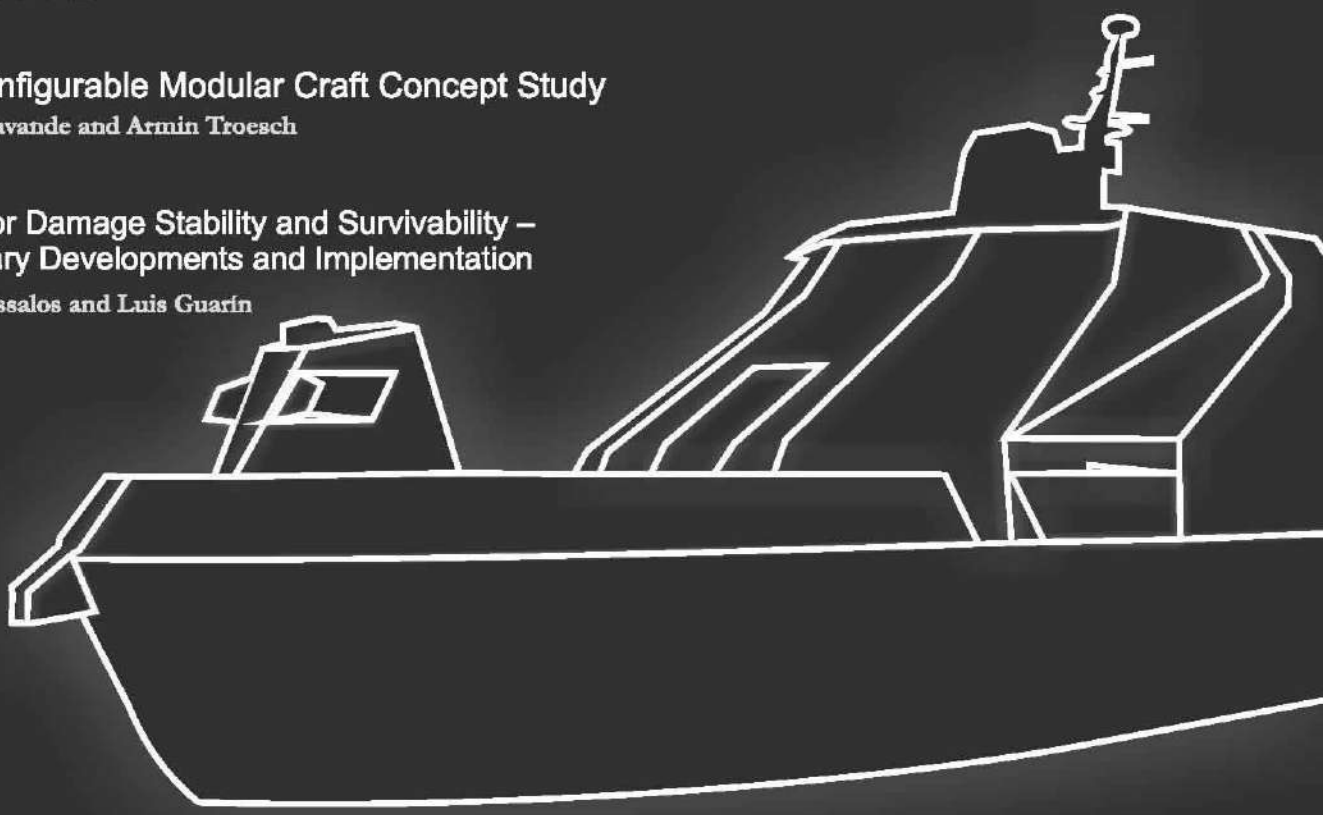

Year 3 - n.° 5 - vol. 1 - (1-128) July 2009

Cotecmar
Year 3 · n.° 5 · vol. 1 · July 2009
ISSN 1909-8642
Ship Science & Technology

SHIP
SCIENCE & TECHNOLOGY
CIENCIA & TECNOLOGÍA DE BUQUES

Number 5, volume 1 July 2009 ISSN 1909-8642

Ship Science & Technology is a specialized journal in topics related to naval architecture, and naval, marine and ocean engineering. Every six months, the journal publishes scientific papers that constitute an original contribution in the development of the mentioned areas, resulting from research projects of the Science and Technology Corporation for the Naval, Maritime and Riverine Industries, and other institutions and researchers. It is distributed nationally and internationally by exchange or subscription.

A publication of
Corporación de Ciencia y Tecnología para el Desarrollo de la Industria Naval, Marítima y Fluvial - Cotecmar
Electronic version: www.cotecmar.com/cytbuques/

Editorial Coordinator
Ensign Paolo Medina, M. Sc.

Layout and design
Mauricio Sarmiento Barreto

Cover Design
Germán Ortíz Rincón

Printed by
Publicidad & Marketing. Bogotá, D.C.

COTECMAR
COLOMBIA

SHIP
SCIENCE & TECHNOLOGY
CIENCIA & TECNOLOGÍA DE BUQUES

Number 5, volume 1 July 2009 ISSN 1909-8642

SHIP
SCIENCE & TECHNOLOGY
CIENCIA & TECNOLOGÍA DE BUQUES

Editor's Note

Cartagena de Indias, 21 July 2009

Cotecmar is currently re-formulating its Technological and Innovation Plan –PDTI, which aims to coordinate Cotecmar' scientific and technological efforts and align them with its short, medium and long term objectives. Ship Science and Technology is, together with the International Ship Design and Naval Engineering Congress - ISDNEC, a fundamental piece in Cotecmar' strategy to fulfill its mission which is the development of the naval, maritime and riverine industry in Colombia. Via the ISDNEC and the Journal, and together with the papers of contributors of Cotecmar from all over the world, the intermediate and final results of the research projects executed by Cotecmar with the aim of advancing the knowledge in Naval Engineering are shared with the community. This issue in particular, presents contributions from well known experts in the areas of ship design and optimization, ship dynamics, hydrodynamics, and safety; I am sure that you will recognize them by their names immediately.

Cotecmar has always been interested in maintaining a net of scientific collaborators capable of supporting its main activity; this Journal is just one of the many ways that Cotecmar uses to promote this net. With the aim of surpassing the barriers imposed by the language and recognizing that English has become the preferred language in technical and scientific publications, starting with this number Ship Science and Technology will be published in this language. We expect to reach more public and to generate greater exchange of scientific knowledge in the topics of interest of our publication.

I would like to take this opportunity to welcome Dr. Luís Guarín to the Editorial Committee. Dr. Gaurín, due to his active involvement in research projects related to safety at sea, is a recognized worldwide expert in this area. The readers of Ship Science and Technology with no doubt will benefit from him joining our Journal.

Commander Oscar Darío Tascón Muñoz

SHIP
SCIENCE & TECHNOLOGY
CIENCIA & TECNOLOGÍA DE BUQUES

Nota del Editor

Cartagena de Indias, 21 de Julio de 2009

Cotecmar se encuentra actualmente reformulando su Plan de Desarrollo Tecnológico y de Innovación – PDTI, a través del cual busca articular todos los esfuerzos de carácter científico y tecnológico en la consecución de sus objetivos del corto, mediano y largo plazo. Ciencia y Tecnología de Buques es, junto con el Congreso Internacional en Diseño e Ingeniería Naval – CIDIN, pieza fundamental de la estrategia de Cotecmar para cumplir con su actividad misional, la cual es el desarrollo de la industria naval, marítima y fluvial en Colombia. A través del Congreso y de la revista científica se divulgan, al lado de contribuciones de colaboradores de Cotecmar alrededor del mundo, los resultados parciales y totales de los proyectos de investigación adelantados por Cotecmar con miras a avanzar el conocimiento en temas propios y afines a la ingeniería naval. Este número en particular, presenta contribuciones de reconocidas autoridades a nivel mundial en las áreas de diseño de buques y optimización, dinámica del buque, hidrodinámica y seguridad en el mar; ustedes reconocerán por sus nombres propios a quienes me refiero en cada caso.

Ha sido siempre del interés de Cotecmar mantener una red de socios científicos que contribuya a soportar su actividad misional; la revista científica es solo una de las muchas formas que utiliza la Corporación para generar esta red. Con el interés de sobrepasar las barreras impuestas por el idioma y teniendo en cuenta que el Inglés se ha convertido en el lenguaje universal de las publicaciones de carácter técnico y científico, a partir de este número Ciencia y Tecnología de Buques se publicará en este idioma. Esperamos de esta forma llegar a más público y generar mayor intercambio de conocimiento científico en los temas de interés de nuestra publicación.

Aprovecho esta oportunidad para darle la bienvenida al Comité Editorial al Dr. Luís Guarín. Su activa participación en proyectos científicos alrededor del tema de seguridad en el mar le ha valido el reconocimiento a nivel internacional como experto en esta área. Los lectores de Ciencia y Tecnología de Buques, se beneficiaran sin duda alguna de su vinculación a nuestra publicación.

Capitán de Fragata Oscar Darío Tascón Muñoz

Applications of Optimization in Early Stage Ship Design

Aplicaciones de optimización en las primeras etapas del diseño de buques

Michael G. Parsons[a]

Abstract

Recent research at the University of Michigan developing and applying modern optimization methods to early ship design decision making is reviewed. These examples illustrate the use of fuzzy logic, genetic and evolutionary algorithms, and agent methods to solve complex multicriterion ship design problems. The first application optimizes an early stage hull form for both smooth water powering and seakeeping performance using an advanced evolutionary algorithm taking into consideration the change of vessel weight with the hull form variation. The second application supports the optimization of naval ship general arrangements using a new hybrid agent-genetic algorithm method and stochastic generation algorithm. The final example uses an evolutionary algorithm to establish the optimal commonality to use in two ship classes that are to share components and features in order to save overall fleet costs. These show how these advanced ship design methods can be used to aid early ship design decisions.

Key words: Ship design, multicriterion optimization, genetic algorithms, evolutionary algorithms, agent methods, fuzzy optimization

Resumen

Se presenta una revisión de recientes investigaciones realizadas en la Universidad de Michigan que desarrollan y aplican métodos modernos de optimización en la toma de decisiones en las primeras etapas del diseño de embarcaciones. Problemas complejos de optimización multicriterio en el diseño de buques son resueltos utilizando lógica difusa, algoritmos evolutivos y métodos de agentes. En la primera aplicación se optimiza la forma del casco en una etapa preliminar para optimizar tanto la potencia requerida en aguas tranquilas como el comportamiento en el mar usando un algoritmo evolutivo que considera el cambio en el peso del buque ocasionado por la variación en la forma del casco. La segunda aplicación utiliza un método híbrido agentes-genético y generación estocástica para soportar la optimización del arreglo general de unidades navales. Por último se utiliza un algoritmo evolutivo para optimizar la concordancia de componentes usados en dos clases de buques con el fin de reducir el costo global de la flota. Estos ejemplos muestran la ayuda que proporciona la utilización de métodos avanzados de diseño en la toma de decisiones durante las primeras etapas del diseño de buques.

Palabras claves: Diseño de buques, optimización multicriterio, algoritmos genéticos, algoritmos evolutivos, métodos de agentes, optimización difusa.

[a] Arthur F. Thurnau. Professor Emeritus Department of Naval Architecture and Marine Engineering,
e-mail: parsons@umich.edu

Introduction

Ship design involves the careful balancing and optimization of many complex, interacting issues. Formal numerical optimization methods were long unable to deliver on their promise, however, because of their limited capability to handle problems complex enough to really address the important design issues in naval ship design. This situation has changed in recent years with the evolution of computer power, the development of increasingly complex analysis and synthesis capabilities, and the development of new methods to treat complex, multicriterion optimization problems. Many of these methods evolved in the broad area of artificial intelligence and soft computing over the past three decades. The author has worked in this area for more than 20 years and taught this material in the graduate-level design class NA570 Advanced Marine Design at the University of Michigan from its introduction in 1997 until his retirement from the University in May 2008. Three areas of research using these methods are described here to illustrate some the capabilities and potential of these methods to address important ship design issues.

Multicriterion Design Optimization

Most ship design problems involve multiple conflicting criteria for selecting the best design, such as the inevitable tradeoff between performance and cost. Marine design requires the careful consideration of these competing criteria and experienced marine designers must make difficult design tradeoff decisions. Traditional numerical optimization methods were first developed for use with a single optimization criterion, objective function, measures of merit, or cost function. These early numerical optimization methods had some success in detailed design decisions, but they were significantly less effective in solving higher-level conceptual and preliminary design problems involving multiple conflicting criteria. And this is precisely the area were the greatest gains can be achieved by formal optimization.

The multicriterion optimization problem involves $K \geq 1$ criteria and can be formulated in the form:

$$\min \mathbf{F}(\mathbf{x}) = [f_1(\mathbf{x}), f_2(\mathbf{x}), f_3(\mathbf{x}), \ldots, f_K(\mathbf{x})], \quad \mathbf{x} = [x_1, x_2, \ldots, x_N]^T \tag{1}$$

subject to the equality and inequality constraints

$$h_i(\mathbf{x}) = 0, \qquad i = 1, \ldots, I \tag{2}$$

$$g_j(\mathbf{x}) \geq 0, \qquad j = 1, \ldots, J \tag{3}$$

where the K multiple optimization criteria $f_1(\mathbf{x})$ through $f_K(\mathbf{x})$ are each dependent upon the N unknown design parameters in the vector $\mathbf{x}$. In general, this problem has no single solution due to the conflicts that typically exist among the K optimization criteria.

The traditional approach to solving this type of problem with early numerical methods that could handle only one criterion was to use a weighted-sum cost function to convert the vector **F** into a related scalar cost function F. There are also a number of scalar compromise solution definitions, such as the min-max and nearest to the utopian solutions, which can be used if a particular definition reasonably reflects a design team's intent. These methods were reviewed and compared in Parsons and Scott (2004).

When conflicting multiple criteria are present, the most common definition of an optimum is Pareto optimality, which was first articulated by the Italian-French economist V. Pareto (Pareto 1906). This is also referred to today as Edgeworth-Pareto optimality (Statnikov 1999) and can be expressed as,

A design is Pareto optimal if it satisfies the constraints and is such that no criterion can be further improved without causing at least one of the other criteria to decline.

Note that this recognizes the conflicting or competitive interaction among the criteria. If there are conflicting criteria, Pareto optimality results in a set of solutions that are all considered equally good under this definition. Some additional consideration must be used to select the resulting single design to use. Compromise solutions, e.g. the min-max solution noted above, might be used to help in the selection of one particular design solution to use. The Pareto set or Pareto front that results from the minimization of two criteria $f_1(\mathbf{x})$

and $f_2(\mathbf{x})$ is illustrated schematically in Fig. 1. This shows the two criteria normalized by the best or minimum value achieved for that criterion. The Pareto front extends between the solution that yields the best for criterion one, f_{1o}, to the solution that yields the best for criterion 2, f_{2o}. It may contain gaps if the feasible region is not convex. The min-max compromise solution is one on the 45° line in this normalized presentation. Designers often focus on the "knees" of the front where there is a sharp change of slope. These solutions are considered more efficient since the loss of one criterion begins to increase more rapidly with each improvement in the other.

Fig.1. Pareto Front Extending between Solutions f_{1o} and f_{2o}

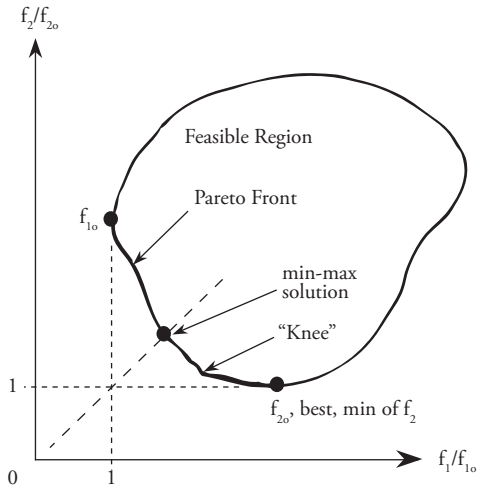

Genetic and Evolutionary Algorithms

Most recent applications of multicriterion design optimization have utilized genetic algorithms (GA's) to find the scalar solution or generate the Pareto front. GA's have evolved out of John Holland's pioneering work (Holland, 1975) and Goldberg's engineering dissertation at the University of Michigan (Goldberg, 1983). These optimization algorithms typically include operations modeled after the natural biological processes of natural selection or survival, reproduction, and mutation. They are probabilistic and have the major advantage that they can have a very high probability of locating the global optimum and not just one of the local optima if they are present in a particular problem.

GA's can readily treat a mixture of integer, discrete, and real variables in **x**. The unknown vector **x** is typically coded as a binary string called a *chromosome*. These algorithms are also called evolutionary algorithms when the unknowns are coded as real rather than binary variables. GA's operate on a *population* of potential solutions at each iteration or *generation* rather than evolve a single solution, as do most conventional optimization methods. Constraints can be handled through a penalty function or applied directly within the genetic operations. These genetic algorithms require significant computation, but this is much less important today with the dramatic advances in computing power. Accessible general references on GA's are by Goldberg (1989), Coley (1999), and Gen and Chang (2000). Independent variable coding is well treated by Michalewicz (1996).

In GA's, an initial population of solutions or individuals (chromosomes) is randomly generated in accordance with the underlying constraints and then each individual is evaluated for its fitness for survival. The definition of the fitness function is for maximization, but can achieve either minimization or maximization through the formulation. The genetic operators work on the chromosomes within a generation to create the next, usually improved generation with a higher average fitness. Individuals with higher fitness for survival in one generation are more likely to survive and breed with each other to produce offspring with even better characteristics, whereas less fit individuals will eventually die out. After a large number of generations, a globally optimal (or near-optimal) solution or the Pareto front can generally be reached.

Three genetic operators are utilized in a simplest genetic algorithm. These are *selection*, *crossover*, and *mutation* operators (Goldberg, 1989, Li and Parsons, 2001). The selection operator selects individuals from one generation to form the core of the next generation according to a set random selection scheme. Although random, the selection is biased toward better-fitted individuals so that they are more likely to be copied into the next generation. The crossover operator combines two randomly selected parent chromosomes to create two new

offspring by interchanging or combining gene segments from the parents. The mutation operator provides a means to alter a randomly selected *gene(s)* of a randomly selected single chromosome to introduce new variability into the population. Crossover and mutation provide the random search capability to locate the region of the global solution. Many algorithms include an *elitism* mechanism to ensure that the current best solution(s) is not lost through the genetic manipulations.

GA's and evolutionary algorithms have been adapted to multicriterion optimization where they are particularly attractive because they can generate the whole Pareto front in one optimization run. The algorithms are especially adapted to generate a population of solutions along the Pareto front by dominance sorting of the population at each generation to retain those that satisfy the Pareto optimum definition. Evolutionary algorithms for solving multicriterion optimization are well treated by Deb (2001), Osyczka (2002), and Zitzler et al. (2003).

Fuzzy Sets, Fuzzy Logic, and Fuzzy Systems

Many important engineering design problems involve issues that are subjective, vague, or ambiguous. Fuzzy set theory provides a way to deal with these issues. Fuzzy set theory, started by Zadeh (1965), introduced the concept that rather than requiring that something had to be a member of a set (1) or not (0), the traditional crisp sets, it could have a varying degree of membership μ(x) between zero and one. This allows subjective, vague and ambiguous things to be modeled rigorously for treatment in control systems, optimization, etc. By using fuzzy sets computations can be performed in linguistic terms (using set names) that mimic complex human reasoning. Good introductions to fuzzy sets and systems are provided in Zimmerman (1991), Kosko (1992), and Mendel (2001). Li and Parsons (1998) used fuzzy decision models to model the aggregate behavior of the world shipping community in buying, selling secondhand, and scrapping tankers (1998).

A helpful example is the concept of a person being tall. This is a subjective thing that depends upon the context – is it a basketball or horse racing jockey locker room? In traditional (crisp) set theory, a person would have to be either a "tall person" or a "not tall person." A person of normal height under normal situations might make this transition at 5'10" (1.78 m). The crisp set membership functions or truth value μ(height) for this are shown as the solid lines in Fig. 2. The membership must be either zero or one. Using fuzzy sets, one could more realistically say that a person is definitely a "not tall person" if they are 5'6" (1.68 m) or less and that they are definitely a "tall person" if they are 6'2" (1.88 m) or taller. Between these two heights there is a gradual, fuzzy transition from being not tall to being tall. The fuzzy set membership functions μ for this are shown as the dashed lines in Fig. 2.

In fuzzy optimization, fuzzy membership functions or fuzzy utilities $0 \le U(x) \le 1$ are defined for each criterion or constraint. They represent the degree to which some requirement is satisfied. The independent variable x is selected to appropriately reflect each issue. A typical fuzzy utility, as might be used to express a requirement for ship speed to accomplish a particular mission, is shown in Fig. 3. The region with U(x) = 0 is clearly unacceptable

Fig. 2. Crisp and Fuzzy Set Membership Functions for the Height of a Person

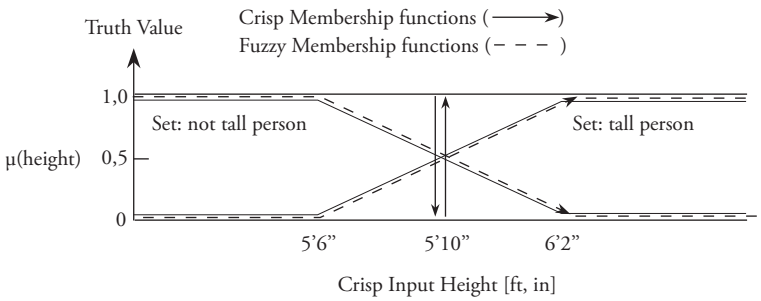

to the designer and region with U(x) = 1 is fully acceptable. The fuzzy region between the minimum acceptable threshold x_ℓ and the design goal or target x_u is a subjective, fuzzy quantity between 0 and 1. This is similar to the approach used by Brown and Salcedo (2003) to define naval design Measures of Performance (MOPs) for their use in performance and cost multicriterion optimization for a DDG. The fuzzy transition could be developed by design judgment or from expert opinion by using the Analytical Hierarchy Process (Saaty, 1996).

Fig. 3. A Typical Fuzzy Utility U(x)

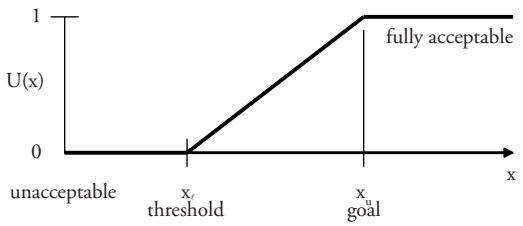

If each design goal and constraint is expressed by an appropriate utility function $U_i(\mathbf{x})$ that depends on the design choices **x**, a fuzzy optimum using minimum correlation inference (Kosko, 1992), for example, is given by the maximization of the optimization criterion (cost function) or total utility $U(U_i(\mathbf{x}))$,

$$U^* = \max_{x} U(U_i(\mathbf{x})) = \max_{x} [\min_{i} (U_i(\mathbf{x}))] \quad (4)$$

This seeks the design **x** that maximizes the worst (minimum) satisfaction of any of the applicable goals and constraints i. This approach yields a multicriterion compromise among all of the conflicting goals and constraints and treats them all in a similar manner. It has the search advantage that there can always be a "feasible" solution that can be improved.

Optimal Hull Forms for Powering and Seakeeping

The Design Problem

The naval combatant hull form that minimizes smooth water powering will generally not provide the best seakeeping performance. This design tradeoff was a major focus of the U.S. Navy DDG51 design process (Keane and Sandberg, 1984). The goal of the first research to be reviewed here (Zalek et al., 2006a; Zalek et al., 2006b; Zalek, 2007; Zalek et al., 2009) was to develop a multicriterion design optimization scheme that would take the ship design description and hull offsets produced by the U.S. Navy's Advanced Surface Ship Evaluation Tool synthesis model (ASSET, 2005) and optimize the hull form for smooth water powering and seakeeping performance. To maintain the validity of the parent ship analysis performed by ASSET, the search for the hull form parameters and variables was allowed to vary roughly ±15% from the parent design. This limitation was imposed to provide assurance that the final hull would still meet the mission effectiveness provided by ASSET, which considers much more detail about the overall design.

The example shown here will be the optimization of a frigate parent produced by ASSET. The parent hull parameters and the range of variation of the parameters permitted in the optimization are shown in Table 1. The depth D is fixed by the accumulation of deck heights and the blade number N_{pdld} is fixed by typical practice.

Table 1. Parent Frigate and Solution Variable Search Space (Zalek, 2007)

Variable	Parent $\tilde{\chi}^0$	$\tilde{S}$
L_{BP} (m)	124,36	105,71 ↔ 143,02
B (m)	13,80	11,73 ↔ 15,87
T (m)	4,79	4,06 ↔ 5,50
D (m)	9,14	9,14
C_X	0,764	0,703 ↔ 0,825
C_P	0,610	0,579 ↔ 0,640
C_{WP}	0,741	0,704 ↔ 0,778
L_{CB} (%)	-0,304	-0,804 ↔ 0,196
L_{CF} (%)	-2,076	-2,576 ↔ -1,576
D_p (m)	5,029	4,023 ↔ 6,035
A_e / A_o	0,739	0,682 ↔ 0,850
N_{pbld}	5	5
Eng_{Mn}	GE LM2500-21	GE LM2500-20,-21

The Design Modeling

The performance criteria were the minimization of required power for smooth water operations and the minimization of the probability of the vessel's failure to complete its missions due to overall seakeeping performance. The power minimization criterion was as follows:

$$F_{PWR}(\mathbf{x}) = w_1 P_{B\,Ereq}(\mathbf{x})/P_{B\,Ereq}(\mathbf{x}_o) + w_2 P_{B\,Sreq}(\mathbf{x})/P_{B\,Sreq}(\mathbf{x}_o) + w_3 V_{max}(\mathbf{x}_o)/V_{max}(\mathbf{x}) \quad (5)$$

where the weights w_i sum to one. This combines the brake power required for the endurance speed $P_{B\,Ereq}$, the brake power required for sustained sea speed $P_{B\,Sreq}$, and the maximum vessel speed V_{max}. Each is normalized by its value for the parent hull, $\mathbf{x}_o$. The inversion of the final term changes maxVmax to the equivalent min($1/V_{max}$).

The seakeeping criterion was expressed as an inoperability index to be minimized,

$$F_{SK}(x) = 1 - OI_{SK}(\mathbf{x}) \quad (6)$$

where O_{ISK}, between 0 and 1, is the U.S. Navy's seakeeping operability index as presented by Keane and Sandberg (1984):

$$OI_{SK}(\mathbf{x}) = \sum_{jk\ell m} f\{\sigma_{jk\ell}(\mathbf{x}) \le \sigma^{limit}\}_m \bullet P[\beta_j, V_k, S(\omega)_\ell, \{(X, Y, Z), \sigma^{limit}\}_m] \quad (7)$$

This operability index calculates the Expected Value (probability) of the vessel being able to complete its missions m as determined by the associated seakeeping limits σ^{limit} at locations (X, Y, Z) on the ship for the various headings β_j, speeds V_k, Sea States $S(\omega)_\ell$ that will be encountered. The summation $\mathbf{\Sigma}$ is a discrete integration overall all missions m, headings j, speeds k, and Sea States ℓ. The function *f* is either 0 or 1 for each jkℓm depending upon whether on not the ship can satisfy all the limits σ^{limit} in mission m at their associated location (X, Y, Z) in the seakeeping analysis for condition jkℓ. P is the probability of occurrence of the given heading, speed, Sea State, and mission in jkℓm.

For the example below, the speed profile V_k was adapted from data for DDG51 as shown in Table 2. The probability of occurrence of the Sea States $S(\omega)_\ell$ were for year-round conditions in the North Atlantic as shown in Table 3. The three missions (activities) m and their associated seakeeping limits and locations were as shown in Table 4. All heading angles relative to the waves β_j were considered equally likely.

Table 2. Speed Profile adapted from DDG51 (Zalek, 2007)

Speed (knots)	% Duration
7	28
10	15
15	24
18	20
20	10
28	3

Table 3. Sea State Parameters and Profile (Zalek, 2007)

Sea State	H_S (m)	T_1 (s)	% Duration
2	0,30	3,4	8
3	0,88	4,0	24
4	1,88	5,3	28
5	3,25	6,4	21
6	5,00	7,6	13
7	7,50	9,0	6

The power required was calculated using an adaptation of the model of Holtrop and Mennen (1982) and Holtrop (1984) using the wetted surface calculated from the vessel offsets. The propeller design was optimized in an inner loop calculation using an adaptation of the Wageningen B-Screw Series Propeller Optimization Program (POP) presented in Parsons et al. (1998). The seakeeping performance was calculated using an adaptation of the linear, frequency-domain, slender-body strip theory code SHIPMO.BM developed by Beck and Troesch (1989). Viscous roll damping based upon Himeno (1981) is added within SHIPMO.BM.

The ship design modeling included constraints to keep the independent variables within a reasonable distance of the parent hull initial values $\mathbf{x}_o$ as shown in Table 1 to ensure that the more complete analyses of ASSET would still be reasonably valid

for the resulting optimized hull design. In practice, ASSET would also be rerun for the optimized hull design to ensure that the overall design was viable. One unique aspect of this work was the use of the full 346 three-digit weight group models from ASSET within the optimization so that the vessel would always have realistic weight estimates as the hull form changes and satisfies weight-equals-displacement. Prior hull form optimization has typically assumed constant displacement so that this major complexity could be avoided. Zalek shows that this is a poor assumption that will yield results far from the Pareto front (Zalek, 2007). The weight was made equal to displacement within 0.05% by establishing either draft T or midship coefficient C_x internally as a dependent variable.

The longitudinal center of gravity LCG and longitudinal center of buoyancy LCB were assumed to have enough later design flexibility to provide the desired even keel trim.

Table 4. Missions and Associated Seakeeping Performance Limits (Zalek, 2007)

Activity (Weight)	Motion	Limit (RMS)	Location
Transit (50%)	Pitch, η_5	1,50º	-
	Roll, η_4	4,00º	-
	Vertical Accel	0,20g	Bridge
	Lateral Accel	0,10g	Bridge
Helo Ops (30%)	Pitch, η_5	0,75º	-
	Roll, η_4	2,00º	-
	Vertical Accel	0,20g	Flight Deck
	Lateral Accel	0,10g	Flight Deck
	Vertical Veloc	1.00 m/s	Helo Pad
Cognitive (20%)	Roll, η_4	3,00º	-
	Vertical Accel	0,10g	Bridge
	Lateral Accel	0,05	Bridge

Inequality constraints, some mandatory and others optional, were included to ensure the minimum required GMT, minimum required deck area, minimum required machinery space length and depth, minimum deck height, propeller characteristic and cavitation limits, maximum required sustained speed power, and maximum required throttle setting.

The hull form changes required to yield the design parameters were made systematically to ensure that the resulting hull was always a fair and reasonable hull. The method developed by Zalek modifies the offsets in four phases to (1) match the length on the waterline, beam, and draft; (2) match the hull prismatic coefficient and longitudinal center of buoyancy; (3) match the waterplane coefficient and longitudinal center of flotation; and then (4) modify each station's offsets to match the area and constraints derived from the first three phases (Zalek et al., 2008).

The Optimization Methodology

Zalek (2007) used a nontraditional multicriterion formulation that contains five criteria,

$$\min_{\mathbf{x}} F(\mathbf{x}) = \min_{x} \{F_{PWR}(\mathbf{x}), FSK(\mathbf{x}), D(\mathbf{x}), H(\mathbf{x}), G(\mathbf{x})\} \quad (8)$$

where $D(\mathbf{x})$ is a diversity operator that attempts for force the solutions to spread out along the Pareto front for good definition, $H(\mathbf{x})$ is a penalty term to force weight to equal displacement, and $G(\mathbf{x})$ is a penalty term to force satisfaction of the inequality constraints (Zalek, 2007; Zalek et al., 2009). The diversity operator forces each group of three nearest neighbor solutions along the Pareto front to be as far apart as possible.

The solution was obtained using a multicriterion evolutionary algorithm developed by Zalek (Zalek, 2007; Zalek et al., 2009). At each generation, the initial population of solutions and those developed by the genetic operators were subject to a non-dominance sorting in accordance with the Pareto optimality definition. The initial population was generated at random. The highest ranked solutions were placed in an archive that serves as the elitism mechanism. These were then subjected to tournament selection to produce parents for arithmetic crossover. These offspring were then added to the archive with others produced by mutation and the process was repeated to select the new non-dominated solutions that approximate the Pareto front.

Figure 4 shows the results from a typical optimization run starting with the triangle solutions in the first generation and proceeding to the diamond solutions after 120 generations, which provide a good numerical approximation to the Pareto front. The results are shown in the primary criterion space F_{PWR} and F_{SK}. The solution at the upper left provides the lowest power requirement and the solution at the lower right provides the best seakeeping performance.

Fig. 4. Progression of Evolutionary Solution toward the Pareto Front (Zalek, 2007)

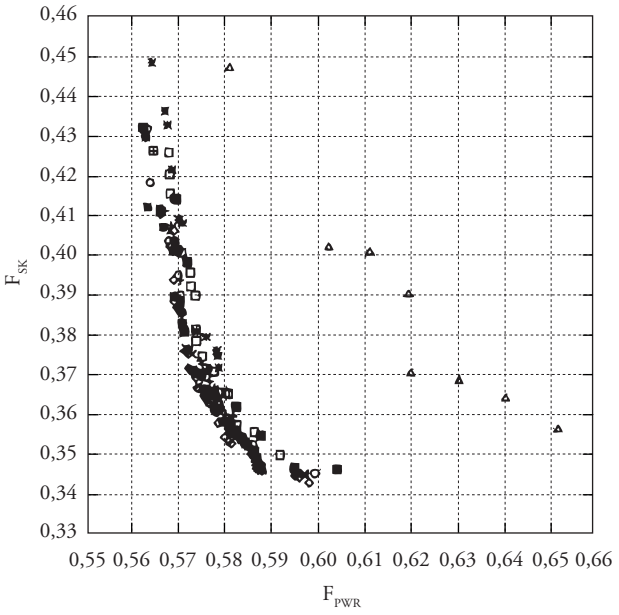

Sample Results

The resulting Pareto Front designs for the optimized ASSET produced frigate hull form are shown in the normalized optimization criterion space in Figure 5. The power weights (w_1, w_2, w_3) were (0.4, 0.4, 0.2), the endurance speed was 20 knots, and the sustained speed was 28 knots. The best powering design and the best seakeeping design are shown. The min-max compromise design is also shown. In this case, this also happens to be the nearest design to the utopian point ($F_{PWR\ min}$, $F_{SK\ min}$), which cannot be achieved due to the inequality constraints. Note that the diversity operator has produced a good definition to the entire Pareto front by ensuring that all non-dominated designs are spread out along the front.

The characteristics of the parent design produced by ASSET and the best smooth water powering, best seakeeping, and min-max compromise optimized designs are shown in Table 5. The best powering design is relatively short, narrow, and deep in the water. The best seakeeping design is almost 23 m longer, wider, and almost 1 m shallower. Both designs use the same GE LM2500-21 engine. As expected the min-max compromise design is intermediate between these two designs. Note that it achieves excellent F_{PWR} powering and FSK seakeeping performance, each within about 3.4% of the best possible. The body plans of the resulting hull forms for these designs are shown in Zalek et al. (2009).

Fig. 5. Pareto Front in Normalize Criterion Space (Zalek 2007)

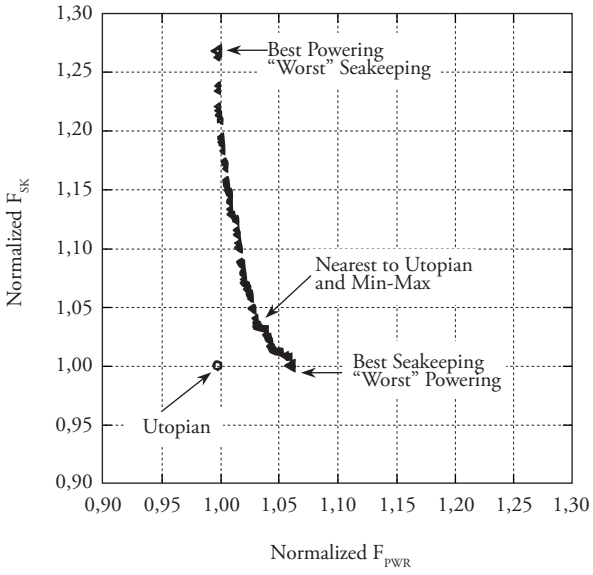

Optimal General Arrangements

The Design Problem

The creation of effective general arrangements in naval vessels is a difficult design task requiring considerable time and the consideration of many potentially conflicting design goals, requirements, and constraints. The overall goal of the second research to be reviewed here (Daniels and Parsons, 2006; Nick et al., 2006; Nick and Parsons, 2007; Daniels and Parsons, 2007; Nick, 2008; Daniels

Table 5. Comparison of Parent and Noteworthy Designs (Zalek, 2007)

Value	Parent $\tilde{\chi}^0$	Best F_{PWR}	NtU / Min-Max	Best F_{SK}
F_{PWR}	0,6776	0,5608	0,5803	0,5964
F_{SK}	0,4182	0,4329	0,3531	0,3416
L_{BP} (m)	124,36	119,41	141,90	142,34
B (m)	13,80	12,54	12,94	13,40
T (m)	4,79	5,08	4,36	4,12
D (m)	9,14	9,14	9,14	9,14
C_X	0,7640	0,7190	0,7846	0,8192
C_P	0,6100	0,5792	0,5815	0,5835
C_{WP}	0,7410	0,7393	0,7467	0,7496
L_{CB} (%)	-0,304	-0,630	-0,551	-0,622
L_{CF} (%)	-2,076	-1,800	-1,707	-1,679
D_p (m)	5,029	6,001	5,924	5,781
A_e / A_o	0,7390	0,7536	0,7713	0,7716
N_{pbld}	5	5	5	5
Eng_{Mn}	*-21	*-21	*-21	*-21

*Note: GE LM2500

and Parsons, 2008; Parsons et al., 2009) was to provide an optimization technology and design tool to assist the arrangements designer to create effective naval surface ship arrangements with the maximum amount of intelligent decision making support. The software system will assist the designer in developing rationally-based arrangements that satisfy design specific needs as well as general Navy requirements and standard practices to the maximum extent practicable. This system will be used following or as a latter part of U.S. Navy's ASSET (2005) synthesis process. It is compatible with the U.S. Navy's product modeling and database system LEAPS (2006).

The Design Modeling

The arrangement process is approached as two essentially two-dimensional tasks as shown schematically in Fig. 6. First, the spaces are allocated to Zone-decks, one deck in one vertical zone, on the ship's inboard profile using fuzzy optimization. Then the assigned spaces are arranged in detail on the deck plan of each Zone-deck in succession. The arrangement phase is divided into two coupled parts: the fuzzy optimization of the topology (relative location) of the spaces within the Zone-deck where each topology uses the best of multiple detailed geometries generated by a stochastic generation algorithm. Consideration is given to the desired overall location, adjacency, separation, access, area requirements, area utilization, and effective compartment shape. The modeling can produce rectangular, C, T, L, and Z-shaped spaces as needed to fit around each other, stair towers, vent trunks, weapons modules, etc.

Fig. 6. Structure of General Arrangement Optimization (Parsons et al., 2009)

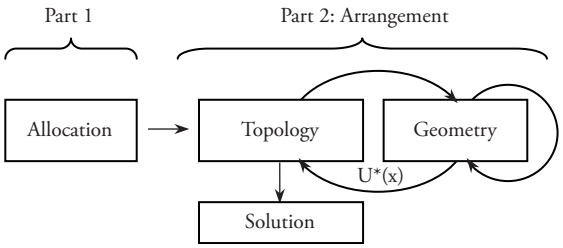

The ***allocation modeling*** used a real integer independent variable vector, chromosome, that indicates the Zone-deck k to which each space i is allocated,

$$\mathbf{x} = [x_1, x_2, \ldots, x_I]^T, \qquad 1 \le x_i \le K \tag{9}$$

This ensures that each space is assigned to one and only one Zone-deck without additional constraints. The search space is very large. A corvette-sized vessel with I = 89 assignable spaces and K = 29 Zone-decks will have a theoretical search space (possible **x** solutions) of KI = 1.4 x 10^{130}. At this strategic design stage, the efficient utilization of available arrangeable space in the Zone-decks and the desired global location, adjacency and separation of the spaces are considered. The fuzzy optimization criterion used was follows:

$$\max_{\mathbf{x}} U(\mathbf{x}) = \min_{k}(U_k) \bullet \sum_{k} U_k / K \bullet \sum_{i} [(w_i / \sum_{i} w_i) \min(U_{i1}, U_{i2}, \ldots, U_{iNi})] \le 1 \tag{10}$$

The first term uses minimum correlation inference and seeks to raise the worst of the area utilization fuzzy utilities for the Zone-decks as shown in Fig. 7 where the design seeks a utilization U_{Uk} = allocated area/available area of 95% of the available area. This model uses the formula for the Normal distribution for the each half of the continuous utility and the designer can control σ_ℓ and σ_u. The second term seeks to raise the average area utilization utility for all Zone-decks. The third term seeks to raise the weighted average of the least satisfied of the Ni global location goals and adjacency and separation constraints for each space i. Weights are used so that a Combat Information Center (CIC), for example, can have greater priority than a storeroom. Since this optimization involves assignment to discrete Zone-decks, the U_{iNi} fuzzy utilities are discrete values, between 0 and 1, that depend upon the current Zone-deck of space i and the Zone-deck of the space j to which adjacency and separation constraints are given.

Fig. 7. Fuzzy Zone-deck Area Utilization Utility (Parsons et al., 2009)

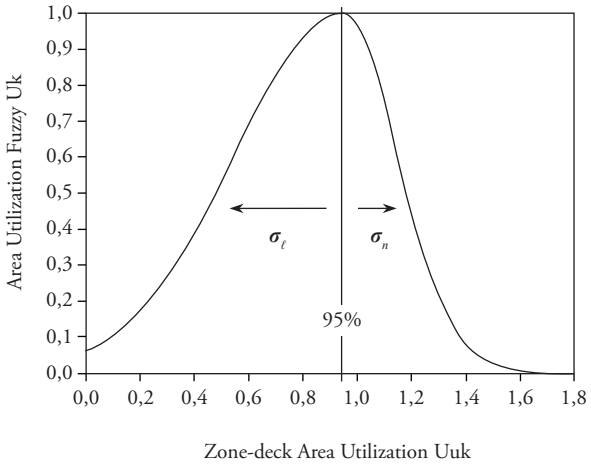

The geometry modeling involves the use of the three-box model in which each space has a centroid rectangle and can then grow up to two appendage rectangles to create L, T, C, or Z shapes as needed. The initial development was on a 1 m x 1 m grid system. An example topology chromosome for a Damage Control Deck Zone-deck to which spaces 1 through 14 have been allocated could appear as follows:

$$x_t = [1, 3, 2, \mathbf{PP}, 8, 9, 4, \mathbf{CP}, 7, 10, 5, 6, \mathbf{SP}, 13, 14\ 12\ 11] \quad (11)$$

where **PP** and **SP** indicate the prearranged location of the main fore and aft port and starboard passageways, respectively, and CP indicates the location of an arrangeable cross passage. This topology indicates that spaces 1, 3, 2 are arranged from fore to aft in the area outboard of the port passageway to which they were allocated. The best geometry generated by the stochastic growth algorithm for this topology chromosome is shown in Fig. 8 where the ST indicate stair towers and there is a fixed object trunk on the port side. Space 7 can be seen to use all three of its possible rectangles in order to fit around the stair tower and space 10.

Fig. 8. Best Geometry (U* = 0.8165) for Chromosome Equation (11) (Nick, 2008)

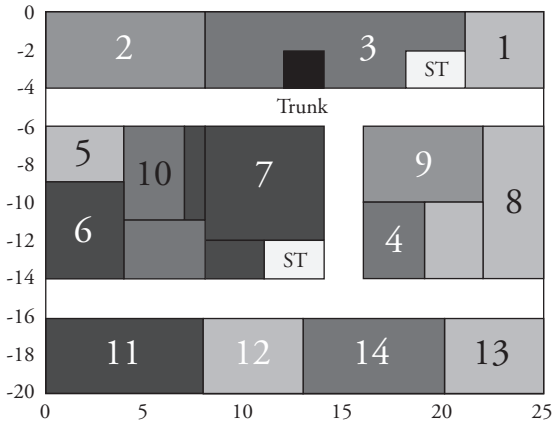

The topology fuzzy optimization used the criterion,

$$U(\mathbf{x}_t) = \sum_i \min_j (U_{icj})/I, \quad 1 \le j \le N_i \quad (12)$$

where the U_{icj} are the N_i constraint utilities for space i. The fuzzy utilities U_{icj} are for the required area, minimum overall dimension, minimum segment width, aspect ratio, perimeter, adjacencies and separations, and if two accesses are required to the space, the access separation. One or two accesses can be specified to either main passage or left free.

The stochastic growth algorithm (Nick, 2008) starts with the space "centroid" locations indicated

by the chromosome and then generates the spaces by a random process of expanding and shrinking the spaces until the total space is filled. The space, direction of change, and amount of growth (±) are determined randomly with controlled probabilities. Moves are accepted if there is room for the change. Spaces can push a stair tower if there is room. Above and below the Damage Control Deck, the stair towers become fixed objects. Multiple geometries are generated for each topology chromosome and then the one giving the best utility, equation (12), is used in the optimization.

The Optimization Methodology

Daniels (Daniels and Parsons, 2008) developed a new hybrid agent-Genetic Algorithm optimization method for the ***allocation optimization***. Agents are computer objects that are given a predefined behavior and are then allowed to operate to evolve a solution to complex problems. The allocation criterion, equation (10) has portions related to good design from the viewpoint of each Zone-decks, U_k, and portions related to good design from the viewpoint of each space, $\min(U_{i1}, U_{i2}, \ldots, U_{iNi})$. This is amenable to an agent approach if there is an agent representing the in interests of each Zone-deck k and an agent representing the interests of each space i. The overall schematic is shown in Fig. 9.

The agent approach uses K Zone-deck Design Agents that sequentially propose a prioritized list of changes to a randomly selected candidate design that will improve its own area utilization utility U_k. The Zone-deck agents can propose to add a space, divest itself of a space, or swap spaces with another Zone-deck. These proposals are evaluated by a Design Review agent and the first, if any, that improves the overall arrangement design as expressed in equation (10) is accepted. The Design Agents work on a small population of candidate designs.

The agent approach also uses I space Design Agents that simultaneously and sequentially propose changes to randomly selected candidate designs that will improve their own part of the cost function; i.e., $\min(U_{i1}, U_{i2}, \ldots U_{iNi})$. The space agents can propose to move to a new Zone-deck or swap places with a space in another Zone-deck. These proposals are evaluated by the Design Review agent and the first, if any, that improves the overall arrangement design as expressed in equation (10) is accepted.

In the agent-based approach, the agents can only improve what is already present in the current small population of candidate designs, which is initialized using a random assignment algorithm. Some form of global or divergent search is also needed for maximum performance. Combining the agents with a Genetic Algorithm Agent using mutation, crossover, and two space swap elements for a divergent search capability yielded solutions with superior overall utility (Daniels and Parsons, 2006; Daniels and Parsons, 2007). A population of 10 candidate designs was used. The hybrid agent-

Fig. 9. Overall Schematic for Hybrid Agent-Genetic Algorithm Optimization (Daniels et al., 2006)

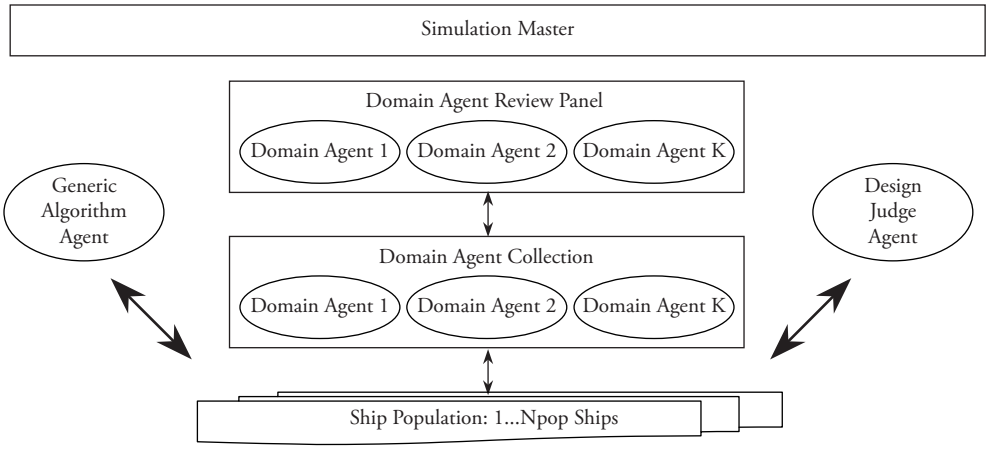

GA solutions were superior to those obtained by either a pure GA or pure agent solution and were also significantly faster than obtained with a complex GA.

The ***topology optimization*** was performed with a conventional Genetic Algorithm using roulette selection, crossover, and two space swapping (Nick and Parsons, 2007). Using a population of four topology chromosomes and generating four stochastically-generated geometries for each topology, the GA operating for 25 generations produced an 8% improvement (Figure 8) over the best of the initial random topologies.

Sample Allocation Results

The example vessel presented here is an artificial demonstration design designated the Habitability Ship. It has its origins in a non-U.S. Navy 3150 tonne, 109 m Notional Corvette design. This was a two-gender design using an Officer, PO, and Specialist (enlisted) nomenclature. Because there is publication sensitivity associated with this design and with the default constraints associated with the combat related spaces, the ship was reduced for demonstration purposes to just contain the propulsion and habitability aspects of the original design. All combat spaces, one superstructure deck, and six vertical WT zones were eliminated from the vessel and the hull form was scaled to enclose this reduced size. One engine room was eliminated. The net result is a vessel with an abnormally large fraction devoted to habitability spaces.

The Habitability Ship is shown schematically in Fig. 10. There are Port (P), Center (C), and Starboard (S) Sub-Zone-decks created by the main passageways on the after part of the Damage Control Deck. The design consists of 103 spaces, 14 of which were fixed including the bridge, bridge-related electrical equipment rooms (2), steering gear (2), anchoring and mooring, mooring area and gear storerooms (3), enclosed Rigid Inflatable Boat (RIB) stowage area, boat gear locker, main machinery room (2 levels) and auxiliary machinery room. This leaves 89 spaces to be allocated to 29 Zone-decks and Sub-Zone-decks. There were a total of 1307 goals and constraints.

The allocation for the Habitability Ship was optimized using a population of 10 candidate allocations for 1500 generations. A generation here is one round of GA operations and one cycle of space and Zone-deck agent proposals that can produce up to 5 changes each. The best solution was reached in 181 generations. This required about 20 minutes on a 2 GHz Intel Pentium Mobile PC with 1 GB RAM. No further improvement was found out to 1500 generations. In general, the arrangement is very good with a total Utility of U = 0.778. This is composed of the three component terms in equation (10) with a minimum Zone-deck area utilization utility U_1 = 0.987, average Zone-deck area utilization utility U_2 = 0.999, and weighted average minimum space utility U_3 = 0.790. The U_3 value characterizes the amount of compromise necessary for a solution. The resulting allocation of spaces is shown schematically in Figure 11 (Parsons et al., 2009).

Optimal Commonality in Multiple Classes of Ships

The Design Problem

In the automotive and consumer products industries (powered hand tools, etc.), there is a strong interest in using common base *platforms*

Fig. 10. Habitability Ship Schematic Inboard Profile (Parsons et al., 2009)

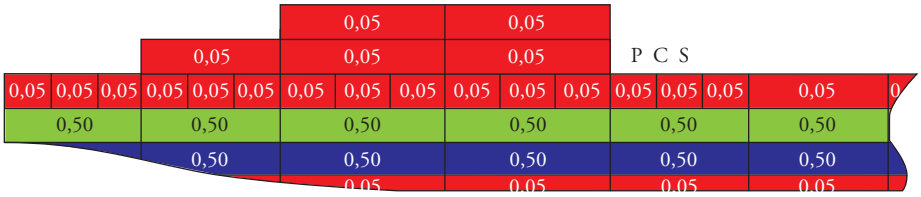

Ship Population: 1...Npop Ships

Fig. 11. Optimal Allocation of Spaces to Habitability Ship (gray unarrangable Zone-decks; lighter fixed spaces; black outside vessel)

	Subdiv 6 STERN	Subdiv 5	Subdiv 4	Subdiv 3	Subdiv 2	Subdiv 1 BOW
Level 01			ZONEDECK 29: RESIDENT SPACES: SPACE 29: Engineer Officer Cabin SPACE 36: Fan Room (Deckhouse) SPACE 48: Officer Cabin (Male)(2) & Bath GrpA SPACE 49: Officer Cabin (Male)(2) & Bath GrpA 1 SPACE 50: Officer Cabin (Male)(2) & Bath GrpA 2 SPACE 51: Officer Cabin (Male)(2) & Bath GrpA 3 SPACE 97: XO Cabin & Bath	ZONEDECK 21: RESIDENT SPACES: SPACE 12: Bridge SPACE 19: Electrical Equipment Room SPACE 20: Electrical Equipment Room 1 SPACE 52: Officer Cabin (Male)(2) & Bath GrpB		
Main Deck		ZONEDECK 36: RESIDENT SPACES: SPACE 7: Boat Gear Locker SPACE 11: Bosun Storeroom (MainDeck) 1 SPACE 22: Electrical Equipment Room 3 SPACE 30: Enclosed RIB Stowage SPACE 37: Fan Room (Deckhouse) 1 SPACE 57: Officer Cabin (Female)(2) & Bath 1 SPACE 68: PO Cabin (Female)(4) & Bath	ZONEDECK 28: RESIDENT SPACES: SPACE 6: BC Medical Facility SPACE 25: Electrical Equipment Room 6 SPACE 43: Medical Consultation Room SPACE 44: Medical Storeroom SPACE 56: Officer Cabin (Female)(2) & Bath SPACE 58: Officer Cabin (Female)(2) & Bath 2 SPACE 77: Sick Bay	ZONEDECK 20: RESIDENT SPACES: SPACE 10: Bosun Storeroom (MainDeck) SPACE 16: CO Cabin & Bath SPACE 17: CO Storeroom SPACE 28: Electrical Equipment Room 9 SPACE 53: Officer Cabin (Male)(2) & Bath GrpB 1 SPACE 54: Officer Cabin (Male)(2) & Bath GrpB 2 SPACE 55: Officer Cabin (Male)(2) & Bath GrpB 3		
DAMAGE CONTROL DECK 2nd Deck	ZONEDECK 40: Port RESIDENT SPACES: SPACE 35: Fan Room (Hull) 4 SPACE 46: Mooring Area & Gear Storeroom (Aft) ZONEDECK 39: Center RESIDENT SPACES: SPACE 8: Bosun Storeroom (Aft Mooring) SPACE 61: PO & Specialist Dining Room 1 ZONEDECK 41: Starboard RESIDENT SPACES: SPACE 23: Electrical Equipment Room 4 SPACE 47: Mooring Area & Gear Storeroom (Aft) 1	ZONEDECK 34: Port RESIDENT SPACES: SPACE 34: Fan Room (Hull) 3 SPACE 71: Daily Provision Room ZONEDECK 33: Center RESIDENT SPACES: SPACE 27: Electrical Equipment Room 8 SPACE 40: Galley & Scullery ZONEDECK 35: Starboard RESIDENT SPACES: SPACE 102: PO & Specialist Dining Room 3	ZONEDECK 26: Port RESIDENT SPACES: SPACE 15: Cleaning Gear Storeroom (Below Decks) SPACE 62: PO & Specialist Dining Room 2 ZONEDECK 25: Center RESIDENT SPACES: SPACE 33: Fan Room (Hull) 2 SPACE 72: Recreation Room SPACE 96: Wardroom ZONEDECK 27: Starboard RESIDENT SPACES: SPACE 21: Electrical Equipment Room 2 SPACE 60: PO & Specialist Dining Room	ZONEDECK 18: Port RESIDENT SPACES: SPACE 76: Ships Office SPACE 93: Training Room ZONEDECK 17: Center RESIDENT SPACES: SPACE 63: PO Cabin (Male)(4) & Bath GrpA SPACE 64: PO Cabin (Male)(4) & Bath GrpA 1 SPACE 65: PO Cabin (Male)(4) & Bath GrpA 2 ZONEDECK 19: Starboard RESIDENT SPACES: SPACE 26: Electrical Equipment Room 7 SPACE 32: Fan Room (Hull) 1 SPACE 90: Electrical Switchboard Room 1	ZONEDECK 12: Port RESIDENT SPACES: SPACE 9: Bosun Storeroom (Fwd Mooring) SPACE 24: Electrical Equipment Room 5 SPACE 31: Fan Room (Hull) SPACE 38: Foul Weather Gear Locker ZONEDECK 11: Center RESIDENT SPACES: SPACE 81: Specialist Cabin (Male)(6) GrpB ZONEDECK 13: Starboard RESIDENT SPACES: SPACE 94: Library	ZONEDECK 7: RESIDENT SPACES: SPACE 3: Anchoring & Mooring SPACE 45: Mooring Area & Gear Storeroom (Fwd)
1st Platform	ZONEDECK 38: RESIDENT SPACES: SPACE 5: Battery Locker and Charging SPACE 69: POL & Paint Locker (Storage) SPACE 70: POL & Paint Locker (Service) SPACE 75: Sewage Treatment Machinery Room SPACE 87: Steering Gear Room SPACE 88: Steering Gear Room 1 SPACE 92: Electrical Switchboard Room 3 SPACE 95: Trash Room	ZONEDECK 32: RESIDENT SPACES: SPACE 18: Cool Cold Dry Provisions SPACE 41: General Stowage SPACE 42: Linen Locker SPACE 59: Laundry (Officer & PO) SPACE 73: Refrigerator Machinery Room SPACE 86: Laundry (Specialist)	ZONEDECK 24: RESIDENT SPACES: SPACE 99: MMR Diesel (1stPlatform)	ZONEDECK 16: RESIDENT SPACES: SPACE 66: PO Cabin (Male)(4) & Bath GrpB SPACE 67: PO Cabin (Male)(4) & Bath GrpB 1 SPACE 74: SD Storeroom SPACE 78: Specialist Cabin (Male)(6) GrpA SPACE 79: Specialist Cabin (Male)(6) GrpA 1 SPACE 80: Specialist Cabin (Male)(6) GrpA 2 SPACE 85: Specialist Cabin (Female)(6) 1	ZONEDECK 10: RESIDENT SPACES: SPACE 82: Specialist Cabin (Male)(6) GrpB 1 SPACE 83: Specialist Cabin (Male)(6) GrpB 2 SPACE 84: Specialist Cabin (Female)(6)	ZONEDECK 6: RESIDENT SPACES: SPACE 13: Chain Locker SPACE 89: Electrical Switchboard Room
Hold	ZONEDECK 37: RESIDENT SPACES:	ZONEDECK 31: RESIDENT SPACES: SPACE 0: Aft Pump Room SPACE 91: Electrical Switchboard Room 2 SPACE 101: Mechanical Workshop (General)	ZONEDECK 23: RESIDENT SPACES: SPACE 98: MMR Diesel (Hold)	ZONEDECK 15: RESIDENT SPACES: SPACE 1: Air Conditioning Room SPACE 39: Fwd Pump Room SPACE 100: AMR	ZONEDECK 9: RESIDENT SPACES: SPACE 2: Air Conditioning Room 1	ZONEDECK 5: RESIDENT SPACES: SPACE 4: Auxiliary Propulsion Room SPACE 14: Chain Locker Sump
Doublebottom		ZONEDECK 30: RESIDENT SPACES:	ZONEDECK 22: RESIDENT SPACES:	ZONEDECK 14: RESIDENT SPACES:	ZONEDECK 8: RESIDENT SPACES:	ZONEDECK 4: RESIDENT SPACES:

for various design *variants* that are offered in order to save development and production costs. Methods have been in development to optimize these decisions (e.g. Gonzalez-Zugasti et al., 2000; Simpson et al., 2001; Fujita and Yoshida, 2004; Fellini et al., 2005; Fellini et al., 2006). Simpson (2004) provides an extensive review of this work.
The overall goal of the final research to be reviewed here (Corl, 2007; Corl et al., 2007a; Corl et al. 2007b) was to apply these ideas to determining the optimum commonality to use in multiple classes of ships. This involved the extension of these methods to a multicriterion approach using evolutionary optimization methods. The methodology was tested using the missions of the U. S. Coast Guard Deepwater High and Medium Endurance fleets (U.S.C.G., 1995). The design criteria were the mission performance/cost for the high endurance cutter, the mission performance/cost for the medium endurance cutter, and the fleet-wide saving from the use of commonality. The strategic design question is how much commonality to use to maximize savings without excessive degradation of the performance/cost of the two design variants.

The Design Modeling

The test application was to utilize the missions of the U.S. Coast Guard's Deepwater Cutter fleet that consists of the Maritime Security Cutter Large (WMSL), formerly the National Security Cutter (NSC), and the Maritime Security Cutter Medium (WMSM), formerly known as the Offshore Patrol Cutter (OPC). The first NSC was launched in September 2007 and the OPC was being redesigned at the time of this work. Table 6 shows the actual design characteristics of these two designs for reference (U.S.C.G. website 2006).

Three criteria were defined for this modeling:

Table 6. Nominal Characteristics of Actual NSC and OPC Fleets (Corl et al., 2007b)

Characteristics	NSC	OPC
Number of Cutters	8	25
Length Overall	127,4 m (418')	Estimate 106,7 m (350')
Maximum Beam	16,46 m (54')	Estimate 15,54 m (51')
Navigational Draft	6,4 m (21')	Estimate 6,4 m (21')
Displacement	4368,3 t (4300 LT)	Est. 3047,6 t (3000 LT)
Sprint Speed	28 kts	26,5 kts
Sprint Speed Range	2600 nm	1550 nm
Sprint Speed Endurance	3,91 days (94 hrs)	2,5 days (60 hrs)
Economical Speed	8 kts	9 kts
Economical Speed Range	12000 nm	9000 nm
Endurance	60 days	45 days
Propulsion Plant	2 Diesels, 1 Gas Turbine	4 Main Diesel Engines
Bow Thruster	Yes	Yes
Gun for Weapon System	57mm Gun	57mm Gun
Gunfire Control	Mk-160/Mk 46/SPQ-9B	Mk-160/Mk 46/SPQ-9B
Operating Days away from Port	230	230
Mission Days/Year	200-220	200-220
Bertching Capacity Limit	148	106
Number of Helicopter Hangars	2	2

$f_1(\mathbf{x}_1, \mathbf{x}_C)$ = NSC Mission Vessel Mission Effectiveness/ Average Ship Cost for 8 (13)

$f_2(\mathbf{x}_2, \mathbf{x}_C)$ = NSC Mission Vessel Mission Effectiveness/ Average Ship Cost for 25 (14)

$f_3(\mathbf{x}_1, \mathbf{x}_2, \mathbf{x}_C)$ = net fleet savings from use of commonality $\mathbf{x}_C$ (15)

The first two criteria are written as a benefit/cost ratio so that any over-design caused by the use of commonality will be penalized as wasteful. Independent variable vectors $\mathbf{x}_1$ and $\mathbf{x}_2$ defined the NSC mission vessel design and the OPC mission vessel design, respectively. Vector $\mathbf{x}_C$ defines the common components used in these designs.

The vessel designs were developed using an adaptation of the U.S. Coast Guard's Performance Based Cost Model (NSWC, Carderock Division, 1998), which was developed by the U.S. Navy using components of its Advanced Surface Ship Evaluation Tool (ASSET, 2005) and the Canadian equivalent SHOP5 with Cost Estimating Relationships (CER's) in constant 1998 U.S. dollars based upon the U.S. Coast Guard's WHEC 378, WMEC 270, WMEC 210, and Great Lakes Icebreaker. The model is capable of synthesizing frigate-sized, deepwater cutters of over 1500 t including acquisition, operational, and support costs. The engines and ship service generators come from catalogs of available designs. This model was modified to reduce the number of inputs to the eight as listed in Table 7 with all needed constraints included internal to the synthesis. For example, the GMT was estimated using the parametric models from Parsons (2003)

The independent variables in Table 7 compose $\mathbf{x}_1$ and $\mathbf{x}_2$ describing the NSC mission vessel and the OPC mission vessel, respectively. The ranges considered for these variables were roughly ±10% from the values for the actual NSC and the OPC designs. The power plants considered were (**1**) a four (two cruise, two sprint) diesel engine CODAD plant or (**2**) a two cruise diesel, one spint gas turbine (CODOG) plant, with both using twin screws, mechanical gearing, and controllable pitch propellers. The weapon suites were (W**1**) a 46mm gun, (W**2**) a 57mm gun, and (W**3**) both a 57mm gun and a Phalanx Close in Weapon System (CIWS).

Table 7. Independent Variables and Ranges (Corl et al., 2007b)

Independent	Variable Ranges
Power Plant Type	1 or 2
Midship Coefficient	0,75 - 0,99
Block Coefficient	0,45 - 0,85
Lenght	82,3-143,3 m (270'-470')
Maximum Speed	19-31 knots
Range @ Cruising Speed	8000-14000 nm
Number of Helicopter Hangars	1 or 2
Weapon System Type	1, 2 or 3

The vessel performance used a modeling similar to Brown and Salcedo (2003) who presented a multicriterion optimization methodology for mission performance versus cost. Following their model for mission effectiveness, the mission performance/cost for vessel i was as follows:

$$[\text{Performance/Cost}]_i = \sum_j MP_{ij} \min_k [U_{ijk}(y_k)]/\text{Cost}_i \quad (16)$$

where the MP_{ij} are the mission profile percent time each vessel will spend in mission j. The ability of each ship i to successfully accomplish each mission j is assumed to depend upon K performance characteristics, y_k. The contribution of each performance characteristic yk of ship i to the success of its mission j is characterized by a fuzzy membership function or fuzzy utility $0 \leq U_{ijk}(y_k) \leq 1$. The overall mission effectiveness is obtained by minimum correlation inference (Kosko, 1992). The Costi is the average cost of ship i.

The missions of the types of vessels were taken from U.S. Coast Guard planning (U.S.C.G., 1995). The NSC and OPC missions both include National Defense, drug interdiction, and living marine resources (LMR) missions. The NSC also performs general defense operations while the OPC performs alien migration interdiction operations.

For each of the J = 4 missions, four ship attributes were selected to describe each ship's ability to perform these missions. The K = 4 attributes were maximum speed (knots), number of helicopter hangers (1 or 2), weapons systems, and endurance range (nm). For each mission, four fuzzy utility functions were developed for methodology testing. Those for the drug interdiction missions are shown in Fig. 12. This mission places a premium on fast aerial assets for surveillance with less emphasis on weapon systems as shown. Endurance is relatively less important in the Caribbean where most of these operations occur.

Fig. 12. Fuzzy Utilities for Drug Interdiction Mission (Corl et al., 2007b)

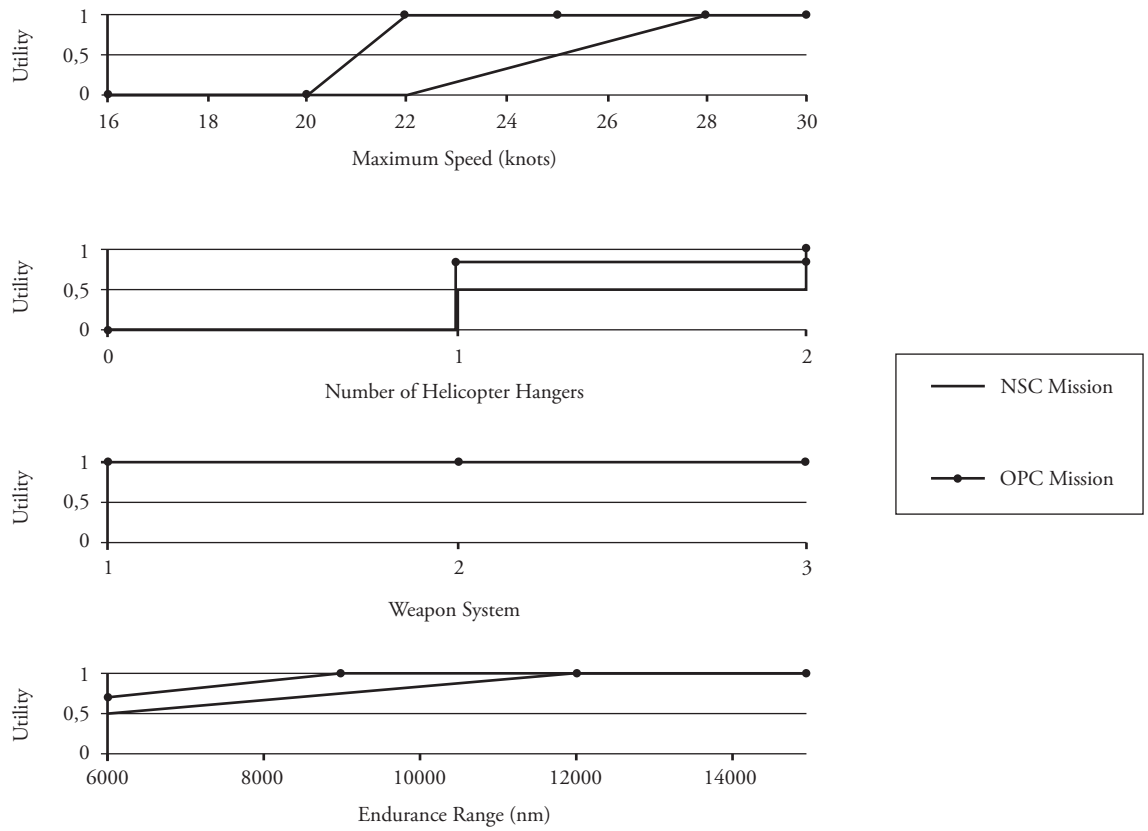

The net fleet savings function $f_3(\mathbf{x}_1, \mathbf{x}_2, \mathbf{x}_C)$ should consider all net fleet-wide savings realized from the use of commonality through savings in training, logistical support, bulk procurement, detailed design development, and construction, etc. In this study, only the savings from bulk purchase savings and construction learning curve savings were included.

The Optimization Methodology

The commonality decisions are a set of integers in $\mathbf{x}_C$ that specify which ship components will be common between both ship classes. If a given component is designated as common, both ships are constrained to use that component. By varying the number and option choice of the common components, the design space can be populated. The various combinations of these common components are used to determine which set of common components result in Pareto optimal designs for Ship A (NSC mission) and Ship B (OPC mission). As the various combinations of commonality are applied to the designs, the optimization fills out the three criterion Pareto front or Pareto surface. Figure 13 shows a schematic of the expected *discrete* Pareto front that will be obtained for this multicriterion optimization.

Every set of commonality components ℓ will result in a solution for Ship A_ℓ and Ship B_ℓ that will be located on a line of commonality. If a single ship were being considered for both missions, this line would be the two-objective Pareto Front for Ship A_ℓ performance/cost and Ship B_ℓ performance/cost. For specific commonalities, Ships A_1 and B_1 might use the same cruise engines; Ships A_2 and B_2 might share the same cruise engines and weapon system. As more things become common, the savings can increase and the ship designs will tend toward each other on the Pareto surface as more effectiveness is sacrificed for commonality. When every item on the ships is common, the result will be one design for both missions (point C in Fig 13). Once every combination of common components is used in the optimization, the discrete Pareto front will be fully populated. The Pareto Front will not be continuous because of the discrete nature of the commonality variable. Rather, the Pareto front will be a collection of pairs of discrete points as shown in Fig. 13.

Fig. 13. Expected Discrete Pair Pareto Surface (Corl, 2007)

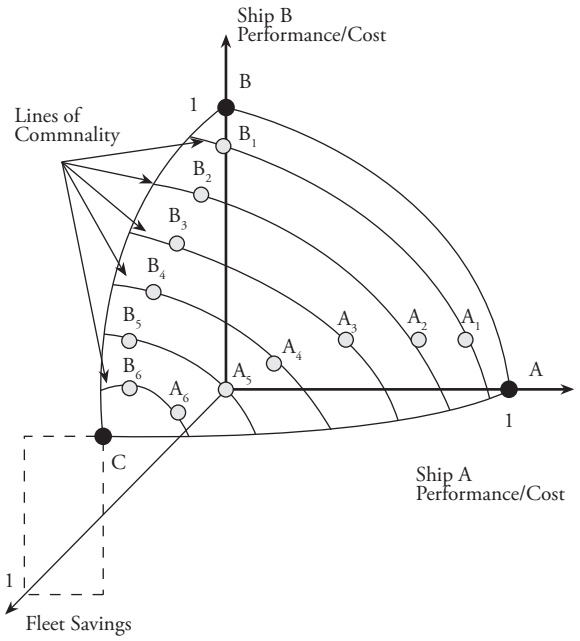

The optimization was performed with an adaptation of the evolutionary algorithm developed by Zalek (2007). Penalty functions for constraint satisfaction were not needed since all constraints were implemented within the synthesis model. The non-domination solution sorting was performed first for the primary criteria only and then for the sum of the primary criteria and a diversity measure D, if neither solution was dominant. This caused the method to emphasize developing non-dominated solutions early in the generations and then focus more on filling out the Pareto front through diversity pressure as the generations evolved. For testing, this was applied to the two criterion optimization of one ship design to satisfy both the NSC mission and the OPC mission. The typical progression of these solutions through 108 generations is shown in Fig. 14. The dense line through the center of the figure is the dividing line between designs with one helicopter hanger (below and to the right, the less capable OPC end) and two helicopter hangers (above and to the left, the more demanding NSC end).

Sample Results

The two criterion analysis for a single design to do both missions was studied to establish which choices of weapons, cruise engines, and ship service generators occurred in the Pareto optimal designs. This was used to guide which options to include in the commonality study. The results showed that only two cruise engines (C7 or C9 from the synthesis model catalog of engines), three ship service generators (G0, G1, or G3), and two weapon systems (W1 or W3) were ever Pareto optimal as shown in Fig. 15. These cruise engine and ship service generator results were used to reduce the scope of the commonality study. It was also noticed that when the number of helicopter hangers was set, there was very little variation in the resulting superstructure volume. It was with either a small superstructure (one helicopter hanger) or a large superstructure (two helicopter hangers). Also, the number of helicopter hangers resulted in little variation in the beam and depth of the hull, with either a small beam and depth or a larger beam and depth. Thus, a common superstructure (small or large) and common midship section hull blocks (small or large) were included as commonality options.

Fig. 14. Progression of Evolutionary Solution toward the Pareto Front (Corl et al., 2007b)

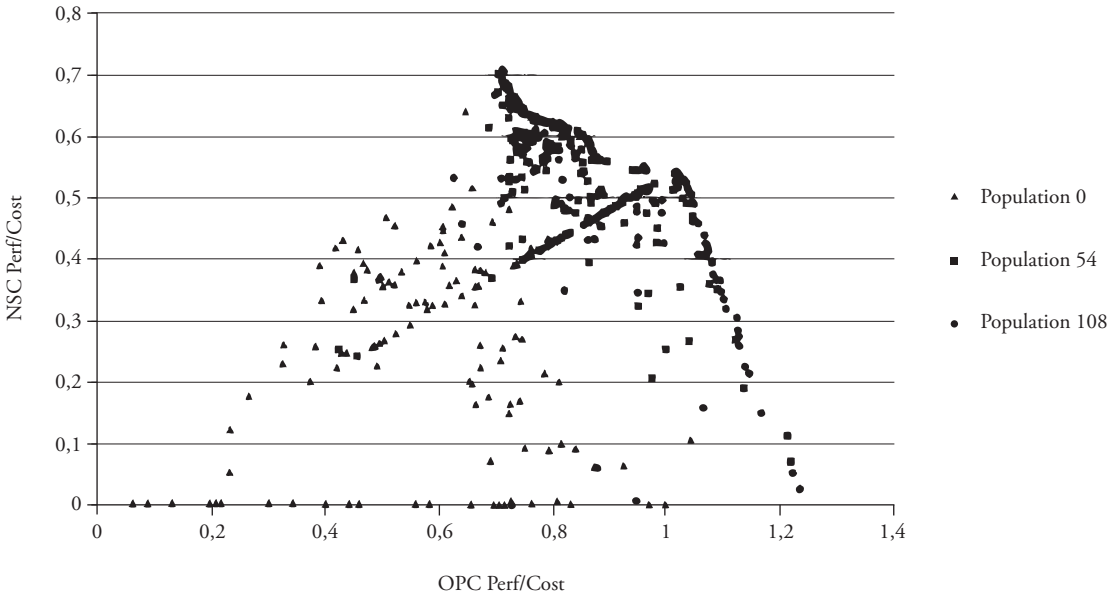

Fig. 15. Natural Commonality within Pareto Front Solutions (Corl et al., 2007b)

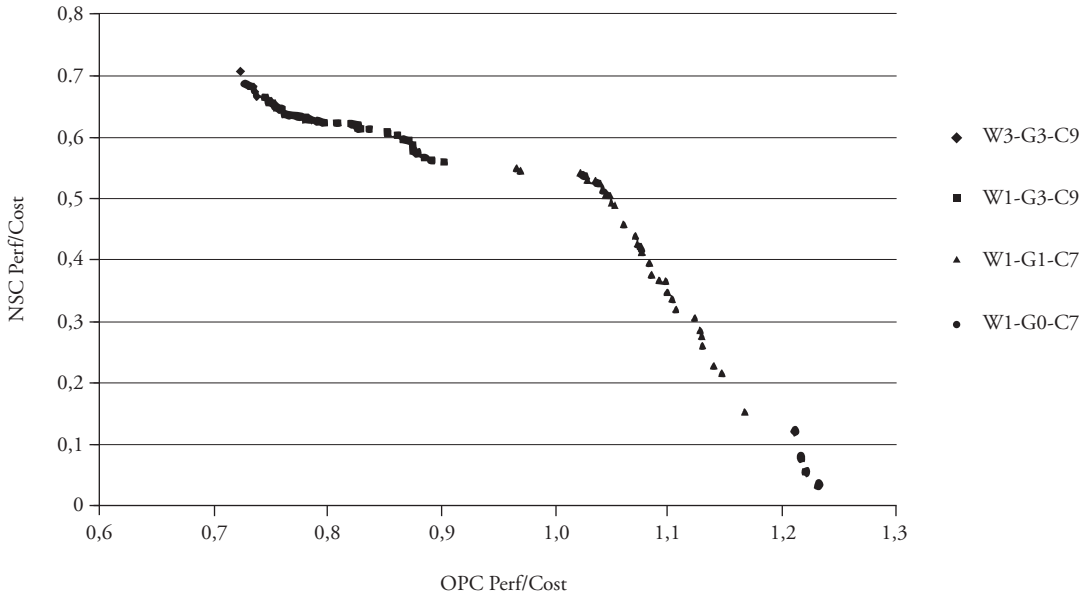

The modeling for the commonality was then an integer vector of the form $\mathbf{x}_C = [0\ 2\ 0\ 1\ 3]^T$ where the positions indicate the commonality decision for weapons, ship service generators, cruise engines, superstructure, and midship section hull blocks, respectively; the zero indicates no commonality is imposed; and a non-zero entry indicates the index number of the commonality choice imposed on the designs.

The multicriterion evolutionary algorithm was adapted further to obtain two separate, higher-quality solutions near the end of the f_1 and f_2 Pareto front, since the end points were all that was needed as shown in Fig. 13. The analysis was then run for all 288 possible combinations of commonality decisions. These results produced three bands of similar designs: 128 NSC mission vessels with two helicopter hangers, 160 NSC mission vessels with

one helicopter hanger, and 288 OPC mission vessels with one helicopter hanger. Of these results, 129 of the pairs resulted in *negative* net fleet savings when more expensive components were being imposed on the less demanding OPC mission vessels. This is a common fallacy of most of previous work on platforms where it is usually assumed that all commonality is good. Because the optimization criterion used here involves performance/cost and no increase in the performance utilities occurs with more than the goal level, over-design results in a loss in performance/cost.

When the 159 remaining positive net fleet savings commonality pairs were sorted to determine those non-dominated designs that lie on the Pareto surface, only 20 different commonality combinations remained. Of these there were only 12 uniquely different design pairs from a naval architectural standpoint. These are as shown in Fig. 16 with the baseline, no commonality designs that yield no net fleet savings (best NSC, and best OPC). The design pair NSC_{15} and OPC_{15} (using the 46 mm gun, the smaller cruise engines, the smallest ship service generators, the small superstructure and the small midship section blocks in common) yield the greatest overall fleet savings from their commonality. Note, however, that the NSC_{15} design has a significant performance loss compared to the baseline design, primarily from to its use of only one helicopter hanger. The NSC_{18} and OPC_{18} designs (using the smallest ship service generators and the large superstructure in common) have the largest net fleet savings before the shift from two helicopter hangers to one. Thus, they are at a "knee" of the surface and are particularly attractive designs.

Fig. 16. Three-Criterion Discrete Pareto Surface (Corl et al., 2007b)

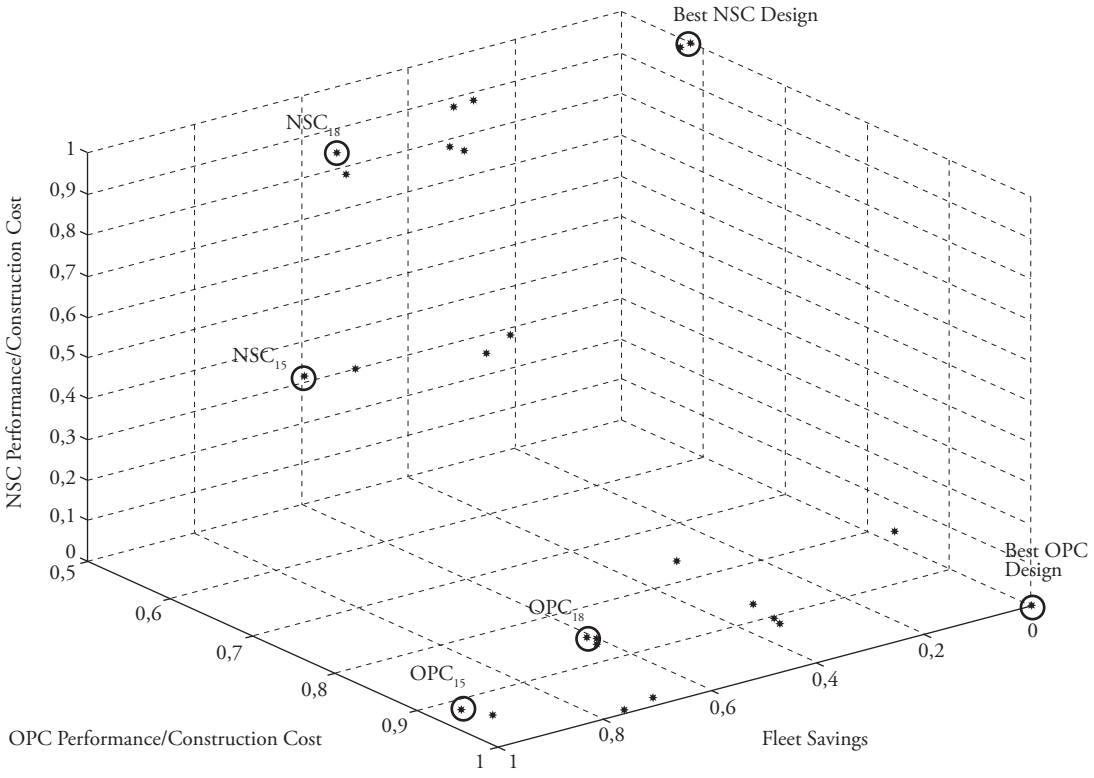

The characteristics of the NSC_{18}/OPC_{18} pair and the NSC_{15}/OPC_{15} pair of designs are shown in Table 8. Note that the NSC15 design has a significant (52.4%) performance loss compared to the baseline design, primarily due to its use of only one helicopter hanger. Note also that the two 15

designs are probably close enough that it might be better to produce one design for both missions and save even more by complete commonality. Note that the NSC_{18}/OPC_{18} pair provide 97% of the NSC baseline performance, 100% of the OPC baseline performance, and still provide 60.7% of the maximum net fleet savings observed.

Table 8. Characteristics for Selected Designs on Pareto Front (Corl et al., 2007b)

Point	L m(ft)	B m(ft)	V_{max} kts	KW_{max} (SHP)	V_{cruise} kts	KW_{cruise} (SHP)	Range nm	W	H	C	G	OPC Perf	NSC Perf	Cost $mil	Fleet Savings $mil
OPC_{18}	107,6 (353)	16,46 (54)	22,0	5757 (7720)	18,0	2895 (3882)	9158	1	2	8	0	100,0	0,314	89,8	45,5
NSC_{18}	121,6 (399)	16,46 (54)	27,9	16687 (22377)	18,0	3585 (4807)	12074	3	2	9	3	100,0	97,0	141,7	45,5
OPC_{15}	91,4 (300)	12,19 (40)	22,2	5333 (7152)	18,0	2537 (3402)	9046	1	1	7	0	89,7	2,946	72,9	75,0
NSC_{15}	92,4 (303)	12,19 (40)	25,5	9642 (12930)	18,0	2767 (3710)	9019	1	1	7	0	89,9	47,6	91,1	75,0

Conclusions

Three recent advanced ship design research efforts at the University of Michigan were reviewed to illustrate some of the capability of modern evolutionary and fuzzy optimization to address complex, multicriterion naval ship design problems encountered in early design. The work of Zalek used a multicriterion evolutionary algorithm to optimize the hull form of a naval combatant for smooth water powering and seakeeping performance. The work of Nick and Daniels used single criterion fuzzy optimization with either a hybrid agent/GA method or a GA to optimally allocate spaces to Zone-decks and then arrange these spaces in a naval surface vessel. The work of Corl used a multicriterion evolutionary algorithm to optimize the commonality to use in vessels for two different missions in order to maximize the net fleet savings from the commonality. Extensive references are provided to aid those interested in investigating this work further.

Acknowlegements

The optimal hull form and optimal general arrangement projects described here were sponsored by the U. S. Navy, Office of Naval Research through Luise Couchman and Kelly Cooper as part of the Naval Engineering Modeling and Optimization (NEMO) program. The optimal arrangements project was also sponsored by the U.S. Navy, Naval Surface Warfare Center Carderock Division through Robert Ames. The optimal commonality research was sponsored by the U. S. Coast Guard and the U.S. Navy, Office of Naval Research through Kelly Cooper. These efforts could not have been undertaken without this support. Special acknowledgement and thanks go to my four graduate students Stephen Zalek, Eleanor Nick, Anthony Daniels, and LCDR Michael Corl, U.S.C.G. whose graduate research is described here. Richard B. Couch Professor of Naval Architecture and Marine Engineering Robert F. Beck co-chaired Zalek's dissertation with the author.

References

Multicriterion Optimization

PARSONS, M. G., AND SCOTT, R. L. (2004). "Formulation of Multicriterion Design Optimization Problems for Solution with Scalar Numerical Optimization Methods." *Journal of Ship Research*, 48:1, March.

PARETO, V. (1906). *Manuale di Economica Politica*. Societa Editrice Libraria, Milano, IT, also in Manual of Political Economy, The MacMillan Press Ltd. 1971.

STATNIKOV, R. B. (1999). *Multicritria Design: Optimization and Identification*. Dordrecht: Kluwer Academic Publishers.

Genetic Algorithms and Evolutionary Algorithms

COLEY, D. A. (1999). *An Introduction to Genetic Algorithms for Scientist and Engineers*. Singapore: World Scientific.

DEB, K. (2001). *Multi-Objective Optimization using Evolutionary Algorithms*. New York: John Wiley & Sons.

GEN, M. AND CHANG, R. (2000). *Genetic Algorithms and Engineering Optimization*. New York: Wiley Interscience.

GOLDBERG, D. E. (1983). "Computer Aided Gasline Operation using Genetic Algorithms and Rule Learning." Ph.D. Dissertation, University of Michigan.

GOLDBERG, D.E. (1989). *Genetic Algorithms for Search, Optimization, and Machine Learning*. Reading, MA: Addison-Wesley.

HOLLAND, J. (1975), *Adaptation in Natural and Artificial Systems*. Ann Arbor: University of Michigan Press and (1992) Cambridge: MIT Press.

LI, J., AND PARSONS, M. G. (2001). "Complete Design of Fuzzy Systems using a Real-Coded Genetic Algorithm with Imbedded Constraints." *Journal of Intelligent and Fuzzy Systems*, 10:1.

MICHALEWICZ, Z. (1996). *Genetic Algorithms + Data Structures = Evolutionary Programs*. Berlin: Springer-Verlag.

OSYCZKA, A. (2002). *Evolutionary Algorithms for Single and Multicriteria Design Optimization*. Berlin: Physica-Verlag.

ZITZLER, E., LAUMANNS, M. AND BLEULER, S. (2003). "A Tutorial on Evolutionary Multi-objective Optimization." http://citeseer.ist.psu.edu/zitzler03tutorial.html.

Fuzzy Logic, Fuzzy Sets and Fuzzy Systems

BROWN, A. AND SALCEDO, J. (2003). "Multiple-objective Optimization in Naval Ship Design." *Naval Engineers Journal*, 115:4,49-61.

KOSKO, B. (1992). *Neural Networks and Fuzzy Systems: A Dynamical Systems Approach to Machine Learning*. Englewood Cliffs, NJ: Prentice-Hall.

LI, J. AND PARSONS, M. G. (1998). "An Improved Method for Shipbuilding Market Modeling and Forecasting." *Transactions* of the Society of Naval Architects and Marine Engineers, 106:157-183.

MENDEL, J. M. (2001). *Uncertain Rule-Based Fuzzy Logic Systems: Introduction and New Directions*. Upper Saddle River, NJ: Prentice Hall PTR

SAATY, T. L. (1996). T*he Analytical Hierarchy Process*. Pittsburgh: RWS Publishing.

ZADEH, L. (1965). "Fuzzy Sets." *Information and Control*, 8:338-353.

ZIMMERMAN, H.-J. (1991). *Fuzzy Set Theory – and Its Applications*. 2nd Ed. Boston: Kluwer Academic.

Optimal Hull Forms

ASSET (2005). "Advanced Surface Ship Evaluation Tool." Version 5.2.0, Naval Surface Warfare Center, Carderock Division.

BECK, R. F. AND TROESCH, A. W. (1989). "SHIPMO.BM User's Manual." University of Michigan, Department of Naval Architecture and Marine Engineering. Report No. 89-2.

HIMENO, Y. (1981). "Prediction of Ship Roll Damping – State of the Art." University of Michigan, Department of Naval Architecture and Marine Engineering. Report No. 239.

HOLTROP, J. (1984). "A Statistical Re-analysis of Resistance and Propulsion Data." *International Shipbuilding Progress*, 31:363, 272-276.

HOLTROP, J. AND MENNEN, G. G. J. (1982). "An Approximated Power Prediction Method." *International Shipbuilding Progress*, 29:335, 166-170.

PARSONS, M. G., LI, J. AND SINGER, D. J. (1998). "Michigan Conceptual Ship Design Software Environment User's Manual." University of Michigan, Department of Naval Architecture and Marine Engineering. Report No. 338.

KEANE, R. AND SANDBERG, W. C. (1984). "Naval Architecture of Combatants: A Technological Survey." *Naval Engineers Journal*. 92.

ZALEK, S. F. (2007). "Multicriterion Evolutionary Optimization of Ship Hull Forms for Propulsion and Seakeeping." Ph.D. Dissertation. Naval Architecture and Marine Engineering, University of Michigan. January.

ZALEK, S. F., PARSONS, M. G. AND PAPALAMBROS, P. Y. (2006a). "Multi-Criteria Design Optimization of Monohull Vessels for Propulsion and Seakeeping." *Proceedings* of the 9th International Marine Design Conference. Ann Arbor, MI. 2:533-557.

ZALEK, S. F., PARSONS, M. G. AND BECK, R. F. (2006b). "Evolutionary Multicriterion Optimization for Propulsion and Seakeeping." Proceedings of the 26th Symposium on Naval Hydrodynamics. Rome, IT. 2:69-85.

ZALEK, S. F., BECK, R. F. AND PARSONS, M. G. (2008). "Nonlinear Hull Form Transformation for Use with Design Optimization." Summer Computer Simulation Conference. Edinburgh, UK. June.

ZALEK, S. F., PARSONS, M. G. AND BECK, R. F. (2009). "Naval Hull Form Multicriterion Hydrodynamic Optimization for the Conceptual Design Phase." to appear in *Journal of Ship Research*.

Optimal General Arrangements

DANIELS, A. AND PARSONS, M. G. (2006). "An Agent-based Approach to Space Allocation in General Arrangements." *Proceedings* of the 9th International Marine Design Conference. Ann Arbor, MI. 2:673-695.

DANIELS, A. AND PARSONS, M. G. (2007). "Development of a Hybrid Agent-Genetic Algorithm Approach to General Arrangements." *Proceedings* of the 4th International Conference on Computer Applications and Information Technology in the Marine Industries (COMPIT'2007). Cortona, IT, April.

DANIELS, A. AND PARSONS, M. G. (2008). "Development of a Hybrid Agent-Genetic Algorithm Approach to General Arrangements." *Ship Technology Research (Schifftechnik)*, 55.

LEAPS (2006). "Leading Edge Architecture for Prototyping Systems." Version 3.4. Naval Surface Warfare Center, Carderock Division.

NICK, E. (2008). "Fuzzy Optimal Allocation and Arrangement of Spaces to Zone-decks in Naval Surface Ship Design." Ph.D. Dissertation. Naval Architecture and Marine Engineering, University of Michigan. April.

NICK, E. AND PARSONS, M. G. (2007) "Fuzzy Optimal Arrangement of Spaces within a Zone-deck Region of a Ship." *Proceedings* of PRADS 2007. Houston, TX.

NICK, E., PARSONS, M. G. AND NEHRLING, B. (2006). "Fuzzy Optimal Allocation of Spaces to Zone-decks in General Arrangements." Proceedings of the 9th International Marine Design Conference. Ann Arbor, MI. 2:651-671.

PARSONS, M., CHUNG, H., NICK, E., DANIELS, A., LIU, S. AND PATEL, J. (2009). "Intelligent Ship Arrangements (ISA): a New Approach to General Arrangement." to appear in *Naval Engineers Journal*.

Optimal Commonality in Multiple Classes of Ships

CORL, M. J. (2007). "Methodology for Optimizing Commonality Decisions in Multiple Classes of Ships." Ph.D. Dissertation. Naval Architecture and Marine Engineering, University of Michigan. June.

CORL, M. J., KOKKOLARAS, M. AND PARSONS, M. G. (2007a). "Platform-Based Design of a Family of Ships Considering both Performance and Savings." *Proceedings* of the International Conference on Engineering Design, ICED'07. Paris, France. August 28-31.

CORL, M. J., PARSONS, M. G., AND KOKKOLARAS, M. (2007b). "Methodology for the Optimization of Commonality in Multiple Ship Classes." *Transactions* of the Society of Naval Architects and Marine Engineers. 115: 68-93.

FELLINI, R., KOKKOLARAS, M., PAPALAMBROS, P. Y. AND PEREZ-DUARTE, A. (2005). "Platform Selection under Performance Loss Constraints in Optimal Design of Product Families." *Journal of Mechanical Design*, 127:4: 524-535.

FELLINI, R., KOKKOLARAS, M. AND PAPALAMBROS, P. Y. (2006). "Quantitative Platform Selection in Optimal Design of Product Families, with Application to Automotive Engine Design." *Journal of Engineering Design*, 17:5: 429-446.

FUJITA, K. AND YOSHIDA, H. (2004). "Product Variety Optimization: Simultaneously Designing Module Combination and Module Attributes." *Concurrent Engineering: Research and Applications*. 12:2: 105-118

GONZALEZ-ZUGASTI, J.P., OTTO, K. N. AND BAKER, J. D. (2000). "A Method for Architecting Product Platforms." *Research in Engineering Design*, 12: 61-72.

NAVAL SURFACE WARFARE CENTER CARDEROCK DIVISION (1998). "User's Guide USCG Performance Based Cost Model."

PARSONS, M. G. (2003). "Parametric Design." Ch. 11 in *Ship Design and Construction*, I, T. Lamb (ed.), New York: Society of Naval Architects and Marine Engineers.

SIMPSON, T.W. (2004). "Product Platform Design and Customization: Status and Promise." *Artificial Intelligence for Engineering Design, Analysis, and Manufacturing*. 18: 3-20.

SIMPSON, T.W., MAIER, J. R. A. AND MISTREE, F. (2001). "Product Platform Design: Method and Application." n, 13: 2-22.

U.S. COAST GUARD MEMORANDUM (1995). "Mission Analysis Report (MAR) N-001-95 Deepwater Missions."

Mission Configurable Modular Craft Concept Study

Estudio conceptual de un buque modular configurable por misión

Brant R. Savander,[a]
Armin Troesch[b]

Abstract

This work illustrates how modern high speed craft design tools may be effectively used to evaluate innovative concepts for which empirical data may be limited. The example presented here was motivated by the US Navy's interest in a finding a replacement for, or complement to, the USN Special Operations Forces' Mark V high speed craft. Given the conflicting demands of restricted size and weight imposed by air transportability and broad mission requirements, a modular, multi-hull configuration is proposed and studied. The boat parameter space that influences calm water performance, sea keeping accelerations, and structural loads is explored. A proposed trimaran concept shows how intelligent placement of outer, or wing hulls can, in principle, mitigate shock loads and lower resistance, but with the cost of increased structural complexity and potentially a heavier craft.

Key words: Planing, high-speed craft, multi-hulls, seakeeping

Resumen

Este trabajo muestra cómo las herramientas modernas de diseño de buques de alta velocidad pueden ser usadas para evaluar conceptos innovadores para los que los datos empíricos pueden ser limitados. El ejemplo presentado fue motivado por el interés de la Marina de los EE.UU. en reemplazar o complementar el buque de alta velocidad Mark V. Dados los requerimientos contradictorios de tamaño y peso reducido impuestos para poder ser transportados por aire frente a la capacidad de realizar un amplio rango de misiones, se propone y analiza una configuración modular multicasco. Se realiza la exploración del espacio de diseño de las variables que influencian el desempeño en aguas tranquilas, el comportamiento en el mar y las cargas estructurales. El diseño conceptual tipo trimarán muestra como la disposición adecuada de los cascos externos puede reducir las cargas de impacto y la resistencia del buque a cambio de un aumento en la complejidad estructural y potencialmente el peso de la embarcación.

Palabras claves: Cascos de planeo, embarcaciones de alta velocidad, multicascos, comportamiento en el mar.

[a] Maritime Research Associates,
e-mail: savander@mresearch.us

[b] Department of Naval Architecture and Marine Engineering
University of Michigan

Introduction & Background

A concept design study is documented herein for an air transportable vessel that is to be utilized by special operations forces. Further, the design will allow the vessel to be readily reconfigured to meet the demands of a broad range of mission requirements. Modularity of both the hull and systems components are assessed to support the needs for reconfiguration and air transportability.

Several configurations of mono-hull and multi-hull systems were developed through a high level concept design study, allowing foundation and technical bases to be established for a more detailed preliminary design, Gale (2003), at a later stage. The high level concept design work scope includes preliminary geometry and weight definitions, steady hydrodynamic performance assessment, seakeeping analysis, and structural analysis. Each of the concept designs are documented with emphasis given to air transportability and range of potential mission configurations.

Two central design themes emerged in the process of completing this study. The first design theme was a more conservative approach which focused on redesign of a monohull, similar to the current Mark V, that allowed for air-transportability in a C17 aircraft. This concept is not included in the subsequent sections of this paper.

The second design theme is much less conservative and exhibits significant technical risk. The risk is offset by the potential for increased performance and capabilities that may be desirable for implementation of the SeaPower 21 capstone concept, Clark (2002), through the underlying pillars of Sea Shield, Sea Strike, and Sea Basing. This design approach utilizes modularity to integrate several vessels, many similar to craft in the current SOF (Special Operation Forces) fleet, into one high speed platform. The platform in assembled form is based upon a trimaran concept with a 80 ft centerhull and two 40 ft wing units. The wing units can also be referred to as side hulls. RHIB and CRRC units can be included in the aft bay of the 80 ft centerhull. Additionally, the aft deck area of the wing units could store PWC sized craft. The wing units are detachable and are envisioned to have both manned and unmanned modes of operation.

The trimaran design emphasizes the use of modularity technology to allow a variety of craft, similar to current Mark V, HSAC, RHIB, CRRC, and PWC, which are all capable of independent operations to be assembled into one common high speed vessel. This common vessel relies on the combination and integration of high speed multi-hull and modularity technology with potential unmanned surface vehicle capability. The multi-hull concept is discussed in detail in the section Trimaran Concept Development.

Analysis Methodology

The multi-hull MCMCC concepts were developed through a high level concept design stage. These concepts have coupled high speed and modularity attributes. As a result, emphasis was placed on determining the acceleration loading while operating in a seaway. The acceleration response of the vessel was predicted using the low aspect ratio theory approach defined by Zarnick (1978), Zarnick (1979), and Akers, et al. (1999). Each planing hull form was initially designed, in an iterative manner, based upon steady hydrodynamic performance following Savander, et al. (2002).

The multi-hull concept was first developed at the preliminary level as defined by performance and mission requirements. This information provided the basis for the hull form geometry definition which was defined using steady planing hull hydrodynamic analysis. At the conclusion of the steady hydrodynamic analysis, the hull form was analyzed in a seaway. The loading defined in the seaway calculations were used as input into the preliminary structural design and analysis. The structural computations included local beam element modeling and rules based analysis following the American Bureau of Shipping rules.

Preliminary Concept Design Methodology

The concept design stage is used in this work to establish the feasibility of several different

competing vessel types and configurations to meet the objectives of a Mission Configurable Modular Combatant Craft, MCMCC. Specifically, the MCMCC is to be used by Special Operation Forces (SOF) for a range of potential missions.

The SOF also require that all vessel types considered in this study be air-transportable. The array of potential air transport options are defined in the Table 1 with the two most common options, the C17 and C130, depicted Figure 1. The underlying theme of the entire study was to explore the concept of "modularity" and how modularity could achieve two general objectives.

Table 1. Air Transport options

Air Transport Options				
	C5	**C17**	**C141**	**C130**
Length	121 ft.	85 ft. 2 in.	93 ft. 3 in.	40 ft. 4 in.
Width	19 ft.	18 ft.	10 ft. 3 in.	10 ft.
Height	13.5 ft.	12 ft. 4 in. fwd of wing. 13 ft. 6 in. aft of wing.	9 ft. 1 in.	9 ft.
Payload	216,000 lbs.	170,900 lbs.	94,508 lbs	45,000 lbs

Fig. 1. Most viable air transport options for transformable craft.

C17

C130

C5

C141

The first objective was to determine the feasibility of a vessel that could be,

- disassembled into modules or sub-assemblies;
- packaged for air transport;
- air transported to a remote forward insertion point;
- complete the specified mission;
- return to a remote forward extraction point;
- disassembled and re-packaged for air transport at extraction point; and,
- air transported back to a home base.

The second objective was to utilize the modularity attribute to allow the vessel to be configured to perform a wider array of missions than would be practical for a non-modular vessel. The concept of

modularity produced two general design themes, as also discussed in the Introduction and Background section.

The approach documented in this paper was to develop a multi-hull vessel that exhibited increased performance when compared to a mono-hull vessel like the Mark V. The goal was to increase the speed, range, and seakeeping performance by adding one or more hulls to the monohull configuration. Initially, both a catamaran and a trimaran concept were contemplated. The trimaran concept was selected for concept design development over the catamaran due to several advantages in air transportability and modes of operation.

Steady Hydrodynamic Analysis Methodology

A hydrodynamic model which is based upon slender body theory, as presented in Savander, et al. (2002), was used to compute the steady hydrodynamic performance of the hull forms discussed in this report. This analysis methodology was derived as an extension of the works of Tulin (1957), Vorus (1996), and Savander (1997). An overview of the method is contained below.

The formulation utilizes the traditional ideal flow assumptions that ignore the effects of viscosity and compressibility. The three-dimensional field equation written in terms of the perturbation potential is reduced to a series of two dimensional problems by assuming sufficiently small longitudinal variation in hull geometry to allow for application of slenderness assumptions. As the hull form passes through a fixed transverse frame of reference, as shown in Figure 2, each transverse section of the hull appears to be falling through the free surface. The cross-sectional impact velocity, $V(t)$, can be defined by specification of the hull trim angle, keel curvature, and hull forward velocity. The longitudinal coordinate is related to the sectional time variable by the relation $x = Ut$.

Two distinct flow phases, "chines-dry" (CD) and "chines-wet" (CW), are encountered and are shown in Fig. 2. The chines-dry term refers to the impact phase which is characterized by the free surface and body contour intersection remaining inboard of the chine. In reference to Fig.2, a hull cross-section is shown moving downward through the water surface with velocity, $V(t)$. The zero pressure point, $z_c(x)$, and jet head position, $z_b(x)$, proceed to move outboard with increasing keel depth, $y_{wl}(x)$. The chines-wet, or post impact immersion, phase is encountered when $z_c(x) = z_{cb}(x)$. The jet head position can continue to move outward with continued immersion depth during the CW phase. The CW phase continues until the transom is encountered at which point the calculation is terminated.

The boundary value problem that is solved includes satisfaction of a coupled system defined by a

Fig. 2. Planing surface passing through a transverse plane located in an earth fixed coordinate system

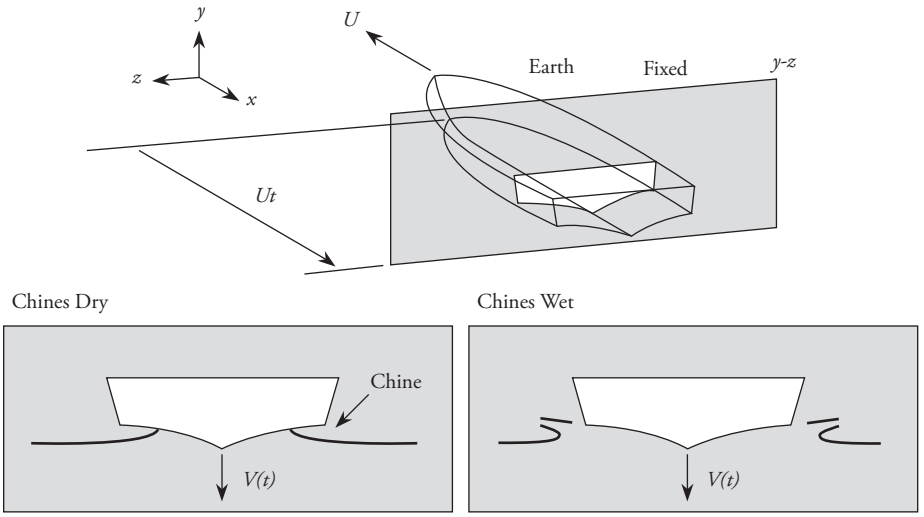

Fig. 3. Hydrodynamic definitions utilized in the cross-flow plane. (Refer to Fig. 2.)

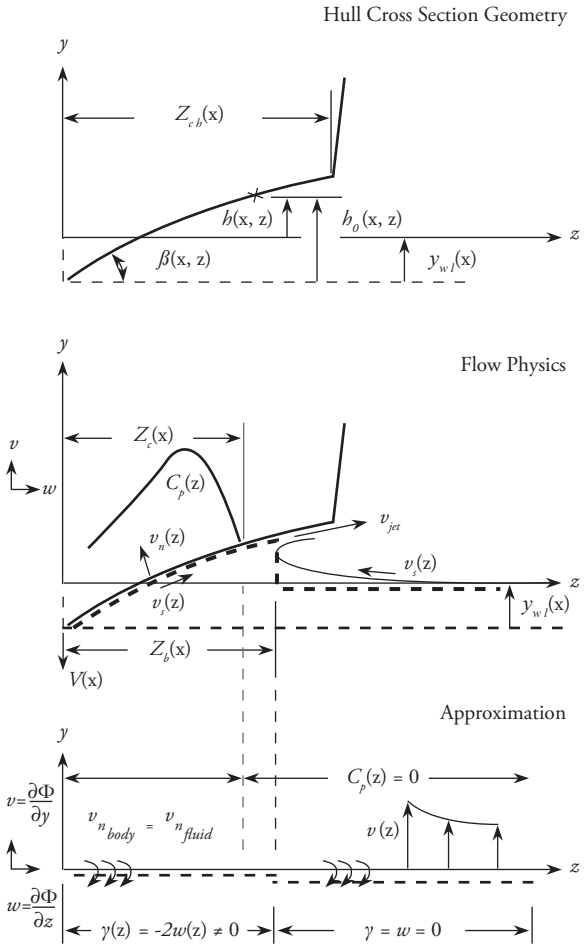

kinematic, dynamic, and displacement continuity condition. The kinematic boundary condition requires the following condition,

$$\vec{v}_{fluid} \cdot \hat{n} = \vec{v}_{body} \cdot \hat{n} . \tag{1}$$

be satisfied. The condition defined in Eq. (1) requires that the normal component of the hull surface velocity equal the fluid normal velocity on the hull contour. This condition is satisfied through use of a vortex lattice system and application of the Biot-Savart Law. The integral equation that results for the unknown vortex sheet strength, $\gamma(x,z)$, is,

$$\frac{1}{2}\gamma(x,\zeta)\tan(x,\zeta) + \frac{1}{2\pi}\int_{z_o=-b(x)}^{b(x)} \frac{\gamma(x;\zeta_o)}{\zeta_o - z}\, d\zeta_o \tag{2}$$

$$= -\tan(\alpha(x) - F(x,\zeta)$$

$\zeta \in [0,1]$, where, $b(x) = z_b(x) / z_c(x)$, and $\zeta = z / z_c(x)$

The local keel trim angle is defined by, $\alpha(x)$. The inclusion of the general term, $F(x,\zeta)$, in Eq. (2) was first presented by Savander (1997). This function could also represent any function that varies in (x,ζ). Therefore, $F(x,\zeta)$ can be written in the following form,

$$F(x,\zeta) = \frac{\partial}{\partial x} h_o(x,z) + \sum_{i=1}^{M} H_i(x,\zeta) \tag{3}$$

Solution of (2) following Savander, et al (2002) yields,

$$g(x,z) = \frac{2}{\pi}\zeta\kappa(x,\zeta)\sqrt{1-\zeta^2}\cos\beta(x,z)$$

$$\left\{ \int_{\zeta_o=1}^{b(x)} \frac{\gamma(x,\zeta_o)\, d\zeta_o}{\kappa(x,\zeta_o)\left(\zeta_o^2 - \zeta^2\right)\sqrt{\zeta_o^2 - 1}} \right. \tag{4}$$

$$+ 2\int_{\zeta_o=0}^{1} \frac{F(x,\zeta_o)\cos(x,\zeta_o)\, d\zeta_o}{\kappa(x,\zeta_o)\left(\zeta_o^2 - \zeta^2\right)\sqrt{\zeta_o^2 - 1}}$$

$$\left. - F(x,\zeta_o)\sin 2\beta(x,\zeta) \right.$$

and

$$\tan\alpha(x) + \frac{1}{\pi}\int_{\zeta_o=1}^{b(x)} \frac{\gamma(x,\zeta_o)\, d\zeta_o}{\kappa(x,\zeta_o)\sqrt{\zeta_o^2 - 1}} \tag{5}$$

$$+ \frac{2}{\pi}\int_{\zeta_o=0}^{1} \frac{F(x,\zeta_o)\cos\beta(x,\zeta_o)\, d\zeta_o}{\kappa(x,\zeta_o)\sqrt{\zeta_o^2 - 1}} = 0$$

The kappa function shown in Eq. (4) and Eq. (5) is given as,

$$\kappa(x,\zeta) = \prod_{k=1}^{N} \left| \frac{\zeta^2 - t_k^2}{\zeta^2 - t_{k-1}^2} \right|^{\frac{\beta_k(x)}{\pi}} \tag{6}$$

where $\zeta \in (0,1)$ and $t_k \in (0,1)$. The dynamic boundary condition that must be satisfied is defined as,

$$C_p(x,y,z)_{y=h} = 0 \qquad z \in [z_c, z_b], \tag{7}$$

which results in the following two relations,

$$\frac{\partial}{\partial x} z_b(x) = \frac{2V(x)v(b,x)+v^2(b,x)+w^2(b,x)+G\,h(b,x)}{2w(b,x)} \tag{8}$$

and

$$\begin{aligned} & C_p(\zeta,x) \\ & w^2(1,x) - w^2(\zeta,x) \\ & +2V(x)v(1,x) - 2V(x)v(\zeta,x) \\ & +v^2(1,x) - v^2(\zeta,x) \\ & +2\frac{\partial}{\partial x} z_c(x) \left\{ \int_{\zeta_o=\zeta}^{1} w(\zeta_o,x)\,d\zeta_o + \zeta w(\zeta,x) - w(1,x) \right\} \\ & +2z_c(x) \int_{\zeta_o=\zeta}^{1} \frac{\partial}{\partial x} w(\zeta_o,x)\,d\zeta_o \\ & +G\,h(1,x) - G\,h(\zeta,x) \end{aligned} \tag{9}$$

with non-dimensional gravity defined as,

$$G = \frac{gBc}{U^2} \tag{10}$$

where, g, is dimensional acceleration due to gravity, and B_c is the maximum full chine beam. The final relation requires that the hull surface contour match the free surface, as shown in Figure 4. This condition is referenced as the displacement continuity condition. The mathematical statement of this condition can be shown to be,

$$y_{wl}(x) = \frac{2}{\pi} \int_{\zeta_o=0}^{1} \frac{\left(h_o(\zeta_o) - \sum Hi^*\right) \cos\beta(\zeta_o,x)}{\kappa(\zeta_o)\sqrt{1-\zeta_o^2}}\,d\zeta_o \tag{11}$$

The method used for satisfaction of the kinematic, dynamic, and displacement continuity conditions, as outlined in formulas (4) through (11) is described in detail in the System Solution section of Savander, et al. (2002). Force and moment equilibrium, as shown in Fig. 4 yields the following relations,

$$\begin{aligned} & D_d + D_v + D_s = T\cos(\tau + \alpha_s) \\ & L_d + L_s + T\sin(\tau + \alpha_s) = \Delta \end{aligned} \tag{12}$$

and

$$\begin{aligned} & L_d x_d + L_s x_s + D_d y_d + D_v y_v + D_s y_s \\ & + T(x_p \sin\alpha_s + y_p \cos\alpha_s) = \Delta\, T(L_{cg}\cos\tau - y_{g}\sin\tau) \end{aligned} \tag{12a}$$

All terms used in Eq. (12), and Eq.(12a) are provided in Figure 4, and are also further discussed in the nomenclature section of Savander, et al. (2002).

The relations Eq. (12), and Eq.(12a) are solved numerically for trim angle, τ, transom draft, t_d, and propulsor thrust, T, for specified vessel weight, center of gravity, and propulsion system orientation, (Δ, V_{cg}, L_{cg},α_s,x_p,y_p) for each given speed, U.

Seakeeping Analysis Methodology

The seakeeping performance, in the head sea condition, of the concepts developed in this work were analyzed with the approach originally defined

Fig. 4. Force and moment equilibrium model.

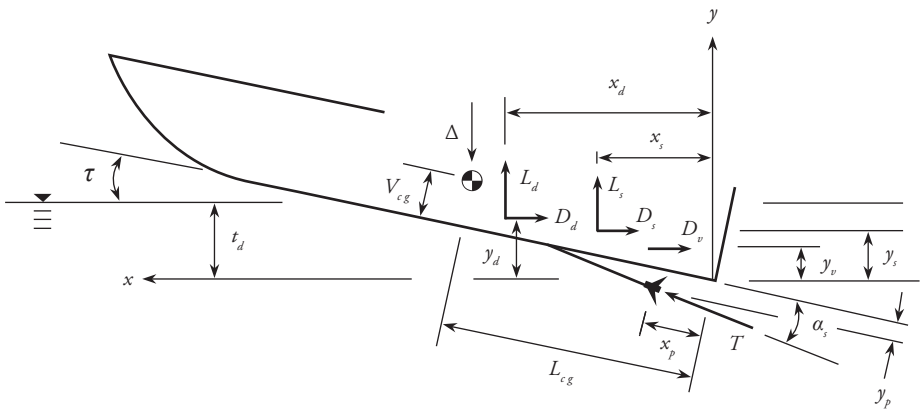

in Zarnick (1978) and (1979) and extended later by Akers et al (1999). Specifically, that method was re-created for the analysis of hull forms with longitudinal variation in deadrise travelling in regular waves. The theory is based upon utilizing a slenderness assumptions to use a combination of concepts from both strip and low aspect ratio theory. Following implementation of Zarnick (1978), the method was also extended to allow for analysis of both monohulls and multihulls in regular and random wave environments.

A theoretical summary of this formulation is provided below for convenience. Details associated with the theoretical formulation and numerical implementation are well defined in Zarnick (1978), Zarnick (1979), and Akers et al (1999) and are not repeated here.

Prediction of the rigid body motion of a high speed planing hullform operating in head or following seas is a challenging computation. The dynamic response and potentially large magnitude of the acceleration loading on the vessel structure and occupants makes this analysis of significant importance. Specifically, Zarnick (1978) highlights this point,

> "A program for planing craft would be quite useful to the small craft designer, providing a means for systematically exploring the effects of numerous design variations on performance of the craft in waves."

Further, Zarnick goes on to forsee the potential application of his method to more complex hullforms, similar to the application to trimarans, and states,

> "With minor modification, the program could also be used to examine the merits of a hybrid craft design, e.g. a combination of planing craft and hydrofoil."

Following Zarnick (1978), Figure 5 shows the coordinate system definitions utilized in the formulation. Specifically, (*x,y*) defined an inertial earth fixed coordinate system. The non-inertial body fixed system is located at the vessel center of gravity and is defined by (ξ,ζ). The vessel weight and propeller thrust is given by *W* and *T*, respectively. The hydrodynamic normal force is *N* with *D* defining the hydrodynamic drag.

Fig. 5. Seakeeping model coordinate system.

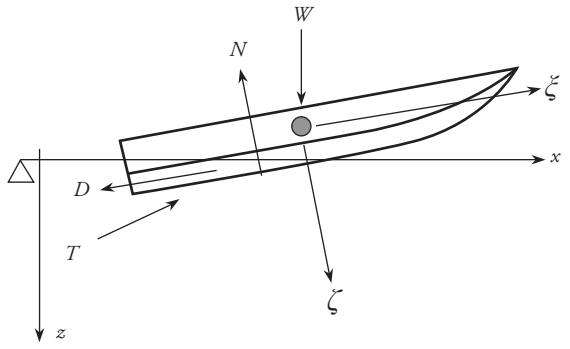

The equations of motion in the vertical plane are defined as,

$$M\frac{\partial^2 x_{cg}}{\partial t^2} = T_x - N\sin\theta - D\cos\theta \qquad (13a)$$

$$M\frac{\partial^2 z_{cg}}{\partial t^2} = T_z - N\cos\theta + D\sin\theta + W \qquad (13b)$$

and

$$I\ \frac{\partial^2 \theta}{\partial t^2} = Nx_c - Dx_d - Tx_p \qquad (13c)$$

The terms defined in Eq. (13) are given as,
M : vessel mass.
I : pitch moment of inertia.
T_x : thrust component in the x-direction.
T_z : thrust component in the z-direction.
x_c : moment arm of the normal force about the center of gravity.
x_d : moment arm of the drag force about the center of gravity.
x_p : moment arm of the propeller thrust about the center of gravity.

One of the most challenging terms to estimate in the equations of motion is the time varying hydrodynamic pressure. Integrating this pressure over the wetted hull surface at each instant in time provides, *N(t)*. Zarnick chose to use hydrodynamic impact theory of Wagner (1932) for the *N(t)* calculation, such that the vertical force per unit

length, at constant values of ξ is the body fixed system, can be defined as,

$$f = -\left\{ \frac{D}{Dt}(m_a V) + C_{D,c}\,\rho\, b\, V^2 \right\} \qquad (14)$$

where,
m_a :hull sectional, two-dimensional, added mass coefficient.
V :vertical velocity in the hull cross section plane.
$C_{D,c}$:cross-flow drag coefficient.
ρ :fluid mass density.
b :hull cross section local wetted half beam.
The added mass coefficient, following Wagner (1932), takes the following form,

$$m_a = k_a \frac{\pi}{2} \rho\, b^2 \qquad (15)$$

where k_a is an empirically determined coefficient ranging between 0 and 1. Expansion of the first term in Eq. (14) yields,

$$\frac{D}{Dt}(m_a V) = m_a \frac{\partial V}{\partial t} + \frac{\partial m_a}{\partial t} - \frac{\partial}{\partial \xi}(m_a V)\frac{\partial \xi}{\partial t} \qquad (16)$$

where the last term incorporates the ξ dependence in both m_a and V.

Fig. 6. Coordinate system used in seakeeping analysis.

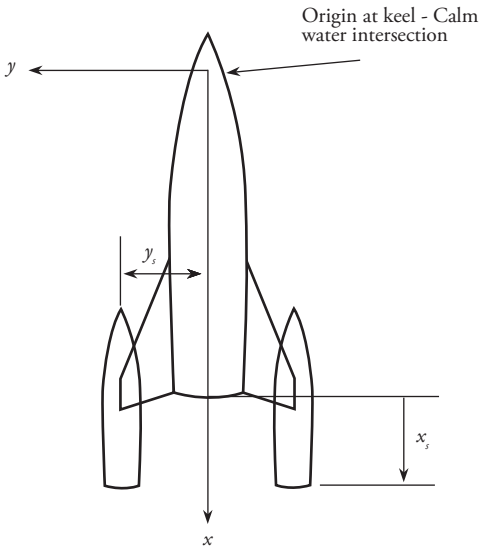

Center hull is air-transportable in a C17 and has performance specifications similar to existing monohull concepts. Wing-hulls are air-transportable in a C130 and can reach speeds of 82 knots.

The seakeeping method defined above was extended to the multihull case by allowing the three forces and three moments in the coordinate directions, (x,y,z), to be applied to the center hull. The equations of motion take the form,

$$M\frac{\partial^2 x_{cg}}{\partial t^2} = T_x - N\sin\theta - D\cos\theta + 2V_x \qquad (17a)$$

$$M\frac{\partial^2 z_{cg}}{\partial t^2} = T_z - N\cos\theta + D\sin\theta + W + 2V_z \qquad (17b)$$

and,

$$I\frac{\partial^2 \theta}{\partial t^2} = Nx_c - Dx_d + Tx_p + 2M_y \qquad (17c)$$

Note the horizontal and vertical shear forces, V_x and V_z, appear in Eq. (17). Further, the pitch moment created by each sidehull on the centerhull, M_y, is the additional term arising in the last equation of (17). The relative orientation of the sidehulls relative to the centerhull is provided in Figure 6. No hydrodynamic interaction is included in this formulation between the centerhull and sidehulls. All interaction is limited to rigid body motion modification due to force and moment transmission through the sidehull to centerhull joining structure.

Structural Design and Evaluation Methodology

Ship structures are influenced to varying levels by primary, secondary, and tertiary loading, as discussed in detail in Hughes (1988). However, loads imparted to planing hull structures are dominated by the localized dynamic loading which is associated with operation in a seaway. The localized loading causes the secondary and tertiary structural cases to drive the resulting structural design.

The general approach used in preliminary design of planing hulls is to repeatedly use strip beam theory in a static mode, as an approximation to the transient grillage - plate problem. Several papers have been authored on this topic at varying levels of rational mechanics rigor.

The dynamic load factor, *DLF*, concept requires,

$$ESL = DFL \times F_d(t) \tag{18}$$

where the dynamic load, $F_d(t)$, when multiplied by *DLF* yields the equivalent static load, *ESL*. The equivalent static load produces a static stress and strain value, $(\sigma_s, \varepsilon_d)$ such that,

$$\sigma_s = \sigma_d(t)$$
$$\varepsilon_s = \varepsilon_d(t) \tag{19}$$

where $(\sigma_d(t), \varepsilon_d(t))$ are the dynamic stresses and strains produced during transient loading. The strip beam concept utilizes one-dimensional beam elements to approximate the response of two-dimensional grillage plates via a high aspect ratio panel assumption.

This methodology of combining the dynamic load factor and strip beam theory was utilized and documented in detail in Heller and Jasper (1960). Several other authors have extended or developed similar approaches to planing hull structural design which include Allen and Jones (1977) and Spencer (1975).

Ultimately, in this study, the loading applied to the equivalent static strip beam model was approximated based upon estimation of the local acceleration and dynamic pressure magnitudes. The methods of Zarnick (1978), Zarnick (1979), and Akers et al (1999) were used to predict the vessel response and associated acceleration loading at locations of interest in the structure. The method of Heller and Jasper (1960) and Allen and Jones (1977) were used to make to the first estimate of the hull scantling plan. The resulting design was then checked against the 2001 Guide for Building and Classing High-Speed Craft published by the American Bureau of Shipping. The scantling plan was then adjusted such that ABS guide lines were met.

For this preliminary design study and ease of analysis, all hull material was assumed to be aluminum. Application of fiberglass and composite technology to this design may be very attractive from a strength to weight perspective and should be evaluated in future design work.

Multi-Hull Concept Selection

As mentioned in earlier sections, both trimaran and catamaran concepts were considered. The trimaran configuration was selected over a catamaran vessel for three primary reasons: air-transportability, modes of independent operation, and seakeeping performance.

The catamaran concept is based upon joining two 80 ft vessels with a common deckhouse structure that spans between the two hulls. Air-transport would be performed with a pair of C17 aircraft. The deckhouse structure would also have to be removable and packaged for air transport with the side hulls. Unlike the trimaran, the catamaran design does not readily allow each sidehull to operate in an independent mode. Once the sidehulls are joined together no convenient mode of independent operation exists unless the joining structure is completely jettisoned.

The trimaran concept, as shown in the sketch in Fig, 6, would use wing structures to join the 80 ft. center monohull to two 40 ft. wing units. The wing units are air-transportable in a C130 aircraft with the centerhull being transportable in a C17. The wing and center units are all capable of independent operations and missions. The centerhull can operate without the wing units and with the wing structures stored in a retracted mode.

C130 aircraft are more readily available to the SOF than C17 aircraft. As a result, the trimaran concept is more desirable from the air-transport perspective. The trimaran also exhibits advantages over the catamaran in that each of the trimaran component hulls are capable of independent modes of operation.

In addition to air-transportability and independent modes of operation of the component hulls, the trimaran offers the ability to increase the effective length of the craft by giving the wing units an aft longitudinal bias. This bias effectively increases

the length to beam ratio of the combined vessel, when compared to the center monohull alone, in a head sea condition. The net result is a vessel with improved seakeeping response over the monohull. The catamaran does not have this attribute.

Trimaran Concept Development

The design approach for the trimaran concept was to modify a monohull concept similar to the existing Mark V and incorporate two detachable wing hulls, as shown in Fig. 6. A main feature of the design is the aftward longitudinal location of the wing hulls relative to the center hull. This aftward movement of wing units results in an equivalent monohull with an increased length to beam ratio, *L/B*, when compared to only the centerhull (Fig. 7). An increase in the effective *L/B* ratio, when exposed to a head sea condition, results in improved dynamic response of the vessel.

The wing units are powered to have an independent top speed which is more than 50% greater than the top speed of the center hull. Hence, the wing units can be considered propulsion booster units that offer an increased speed capability compared to the sole center hull. With the added power, the trimaran high speed platform is designed to allow the SOF to travel faster and with less fatigue when compared with traditional 80 ft class monohull designs.

The trimaran design also emphasizes the integration of several vessels similar in characteristics to the current SOF fleet including, Mark V, HSAC, RHIB, CRRC, and PWC, into one common high speed platform. The detachable wing units shown in this figure, similar in size to the current HSAC, could be capable of both manned and unmanned modes of operation.

It is expected that unmanned platforms will become more in demand as the requirements for vessel operations in environments not limited by human exposure increase (e.g. Cooper and Norton (2002)). Sokel and Hansen (2001) cite Senator Warner of Virginia challenge to Congress in 2000-2001 to significantly increase plans for buying and developing unmanned systems. Further, Sokel and Hansen (2001) go on to quote the Director of Naval Operations and Strategic Studies group stating that within 50 years 75% of all ship sensors and weapons will be remote.

Trimaran Preliminary Concept Design Details

As mentioned previously when considering relative merits of trimaran's and catermarans, the aftward movement of side-hulls results in an equivalent monohull with an increased length to beam ratio, *L/B*, when compared to only a single center-hull (Fig. 7). Specifically, given a monohull of length overall, $L_{monohull}$, with two side-hulls attached such that the transom of the side-hull is x_s feet aft of the transom of the monohull, the effective length of the trimaran becomes,

$$L_S = L_{monohull} + x_S \tag{20}$$

In a head sea condition, the trimaran acts effectively as a lengthened monohull via,

$$\frac{L_e}{B} > \frac{L_{monohull}}{B} \tag{21}$$

also shown in Fig. 7. This effective increase in the length to beam ratio has favorable implications on seakeeping performance. The position of the side-hull relative to the center-hull is defined by the coordinates, (x_s, y_s), Fig 6. The effect of the side-hull position on the vertical acceleration experienced at the center of gravity, CG, and the bow of the craft is provided in Fig. 8.

Figure 8 shows that nearly a factor of two reduction in bow acceleration can be achieved by moving side-hull position from $x_s = 0ft$ to $x_s = 20ft$. The data provided corresponds to operation in sea state 3 at a speed of 50 knots for a 5 minute exposure period.

Bow and CG acceleration seakeeping results for a specific value of $x_s = 15ft$ and a range of sea states are also shown in Fig. 9. This figure also shows a significant improvement in seakeeping qualities of the trimaran over the monohull design from both a maximum perspective. All results shown in

Fig. 7. Conceptual illustration of how side-hulls in a trimaran concept produce an effective monohull with an increased length to beam ratio.

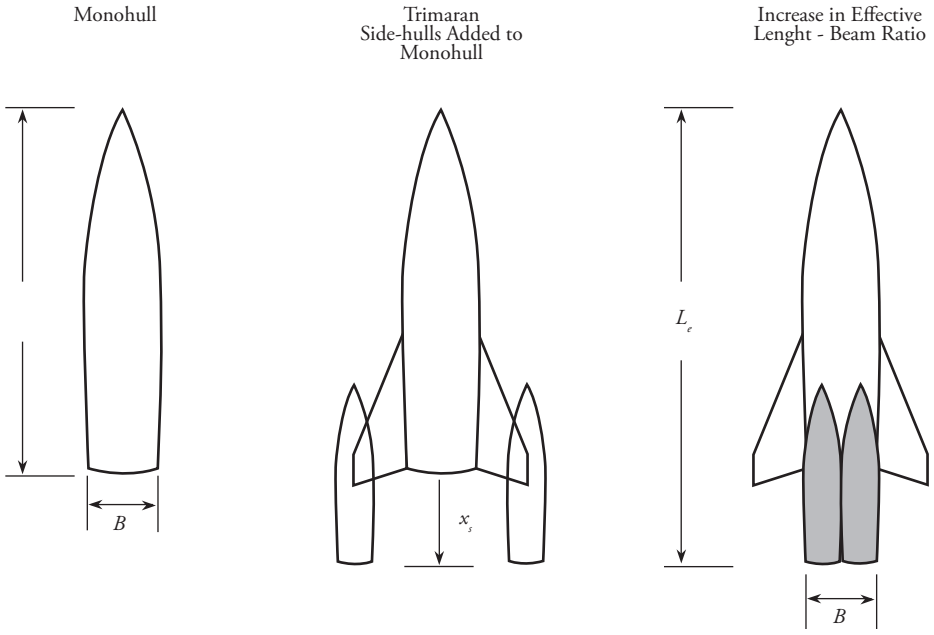

Fig. 8. Bow and CG acceleration response to variation in longitudinal position of side-hulls relative to center-hull. Exposure limit for the computation was 5 minutes. The speed was 50 knots and the sea conditions were sea state 3

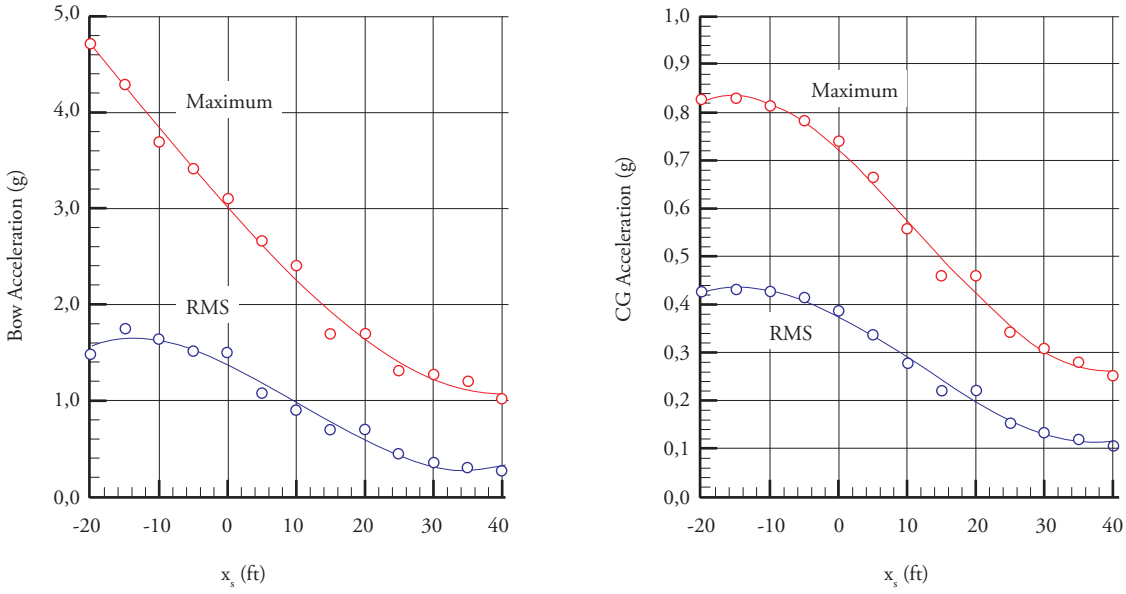

these two figures were for a 3-hour exposure while operating at 50 knots in sea state 3.

As a result of this preliminary seakeeping analysis, trimaran designs were developed with a side-hull position range defined by,

$$\begin{matrix} x_S \in (15,20)\, ft \\ y_S \in (15,25)\, ft \end{matrix} . \qquad (22)$$

The initial trimaran design was considered with the side-hull position of,

$$\begin{matrix} x_S = 20\, ft \\ y_S = 25\, ft \end{matrix} . \qquad (23)$$

This transverse spacing coupled with the large vertical load imparted by the side-hull at the end

Fig. 9. Bow and CG maximum acceleration response as a function of sea condi-tions. The side-hull transom was 15 feet aft of the center-hull transom, $x_s = 15ft$. All computations were based on a 3-hour exposure at a speed of 50 knots.

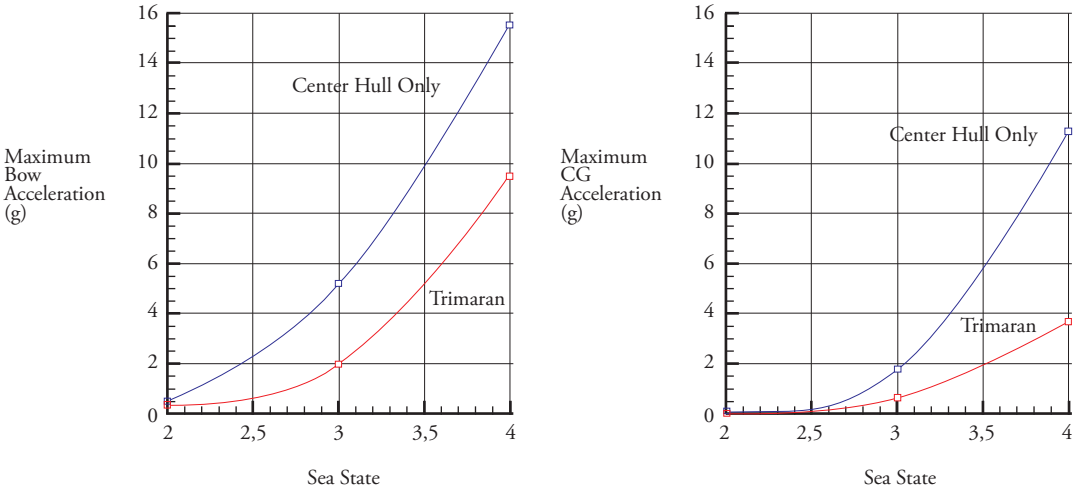

Fig. 10. Bow and CG RMS acceleration response as a function of sea conditions. The side-hull transom was 15 feet aft of the center-hull transom, $x_s = 15ft$. All computations were based upon a 3-hour exposure at a speed of 50 knots.

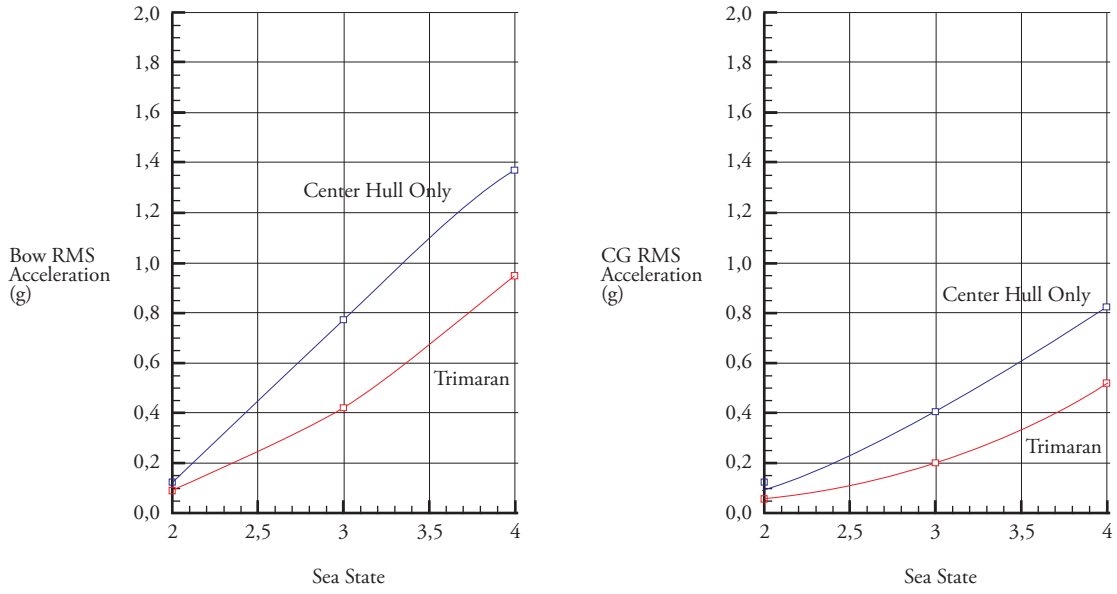

of the wing structure, proved to make this version of the design unfeasible. The structure needed to carry the load became too large with evaluated against weight constraints.

As a result, the position of the side-hulls was moved closer to the center-hull with,

$$\begin{matrix} x_S = 15\,ft \\ y_S = 18\,ft \end{matrix} \quad . \qquad (24)$$

as shown in Fig. 11. The total length and beam for the trimaran concept is 94 feet 3 inches and 46 feet 1 inch, respectively. The total displacement is approximated at 59 long tons. The top speed for this design is estimated to range between 56 to 62 knots. This represents a 4 to 10 knot increase in the top speed over an equivalent monohull concept.

The side-hull design consists of two craft approximately 40 feet in length with beams of 9

feet 3 inches. These craft have displacements of 13,000 lbs and top speeds of 82 knots.

Each vessel is powered by twin SeaTek 10.3 Endurance diesels each driving Arneson surfacing systems. A fuel capacity of 400 US gallons allows a range of 540 nautical miles at a cruise speed of 50 knots. The range at a maximum speed of 82 knots is reduced to 200 nautical miles. The hulls are expected to be constructed of a composite based fiberglass reinforced plastic (FRP).

The total concept range is calculated to be 600 nautical miles at a cruising speed of 40 knots. A range of 540 nautical miles is maintained at 50 knots, with the range dropping to 220 nautical miles for the top speed condition. The range is reduced at top speed due to the full power demand on the four SeaTek diesels located in the side-hulls at this operating point. The total fuel capacity is 4,400 US gallons representing the summation of 2,600 US gallons for the center-hull and 800 US gallons for the two side-hulls combined.

Fig.11. Trimaran concept showing modified wing structure. Position of side-hulls rela-tive to the center-hull has been reduced both transversely and longitudinally based upon transient structural analysis with operation at 50 knots in sea state 3. Center hull is air-transportable in a C17 and has performance specifications similar to existing monohull concepts. Wing-hulls are air-transportable in a C130 and can reach speeds of 82 knots.

LOA: 94 feet 3 inches
Beam: 46 feet 1 inch
Max. Speed: 56 - 62 kts
Cruise Speed: 40 kts
Payload: 8,400 lbs (approx.)
Range: 600 NM at 40 kts, 540 NM at 50 kts
Range at Max Speed: 220 NM

Engines: 4 x 1050 HP SeaTek 10.3
Endurance: 2 x 2285 HP MTU 12V4000
Drives: 4 x Arneson Surfacing Drives
KaMeWa K50s Watejets
Fuel: 4,400 US Gal
Hull Material: Aluminum & FRP
Displacement: 58.8 LT (approx.) 2 x

Trimaran Steady Hydrodynamic Analysis

The methods described in steady planing and seakeeping sections were used to design the hullform for the side-hull in the trimaran concept. The final side-hull craft is shown in Figures 11 and 12. Additionally, the analytical extension to Zarnick (1978) and Akers et al (1999), as defined in was also extended to compute the steady resistance and equilibrium position of the trimaran concept as a function of forward speed. This section of the report documents the design and performance of the independent side-hull hullforms and the trimaran concept.

The non-dimensional longitudinal coordinate of the hullform is given by,

$$\xi = \frac{x}{z_{ch}} \tag{25}$$

where z_{ch} is the maximum chine half beam. The deadrise at the transom is 20 degrees and is maintained to a value of ξ = 1,5 at which point the deadrise increases to a value of 55 degrees at the chine-keel intersection. The maximum chine

Fig. 12. Lines plan for the side-hull of the trimaran concept

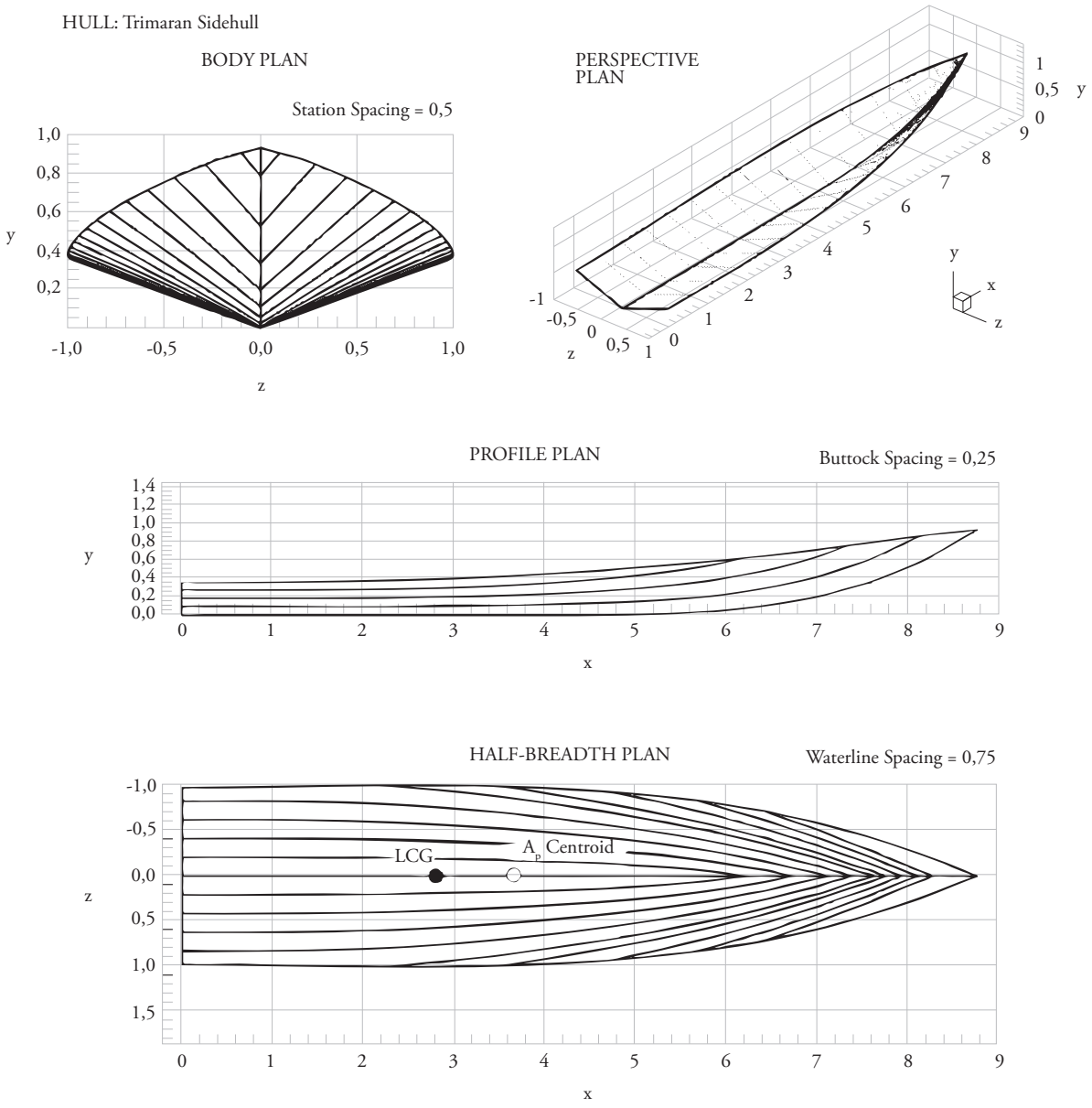

beam is located at ξ = 3,0 and is approximately maintained aft to the transom. The keel contour is flat from the transom to ξ = 5,0 where the keel elevation begins to increase to the maximum value of approximately,

$$\frac{y}{z_{ch}} = 1{,}0 \qquad (26)$$

at the chine-keel junction. The hullform planing surface is defined by the deadrise distribution, chine beam distribution, and keel elevation. The lines plan, consisting of the body, plan, and profile views is shown in Figure 12. The centroid of the planing area, A_p, is located,

$$\frac{x_{A_\gamma}}{z_{ch}} = 1{,}0 \qquad (27)$$

with the longitudinal center of gravity position being,

Fig. 13. Trimaran concept side-hull corresponding to F_∇= 4,0 (32.7 kts). Plots include a) total pressure coefficient, b) sectional dynamic and static lift coefficient, and c) velocity vector and streamline orientation. *(x,y,z)* coordinates are nondimensionalized by maximum chine half-beam, Z_{ch} . Note the extent of chines-wet flow.

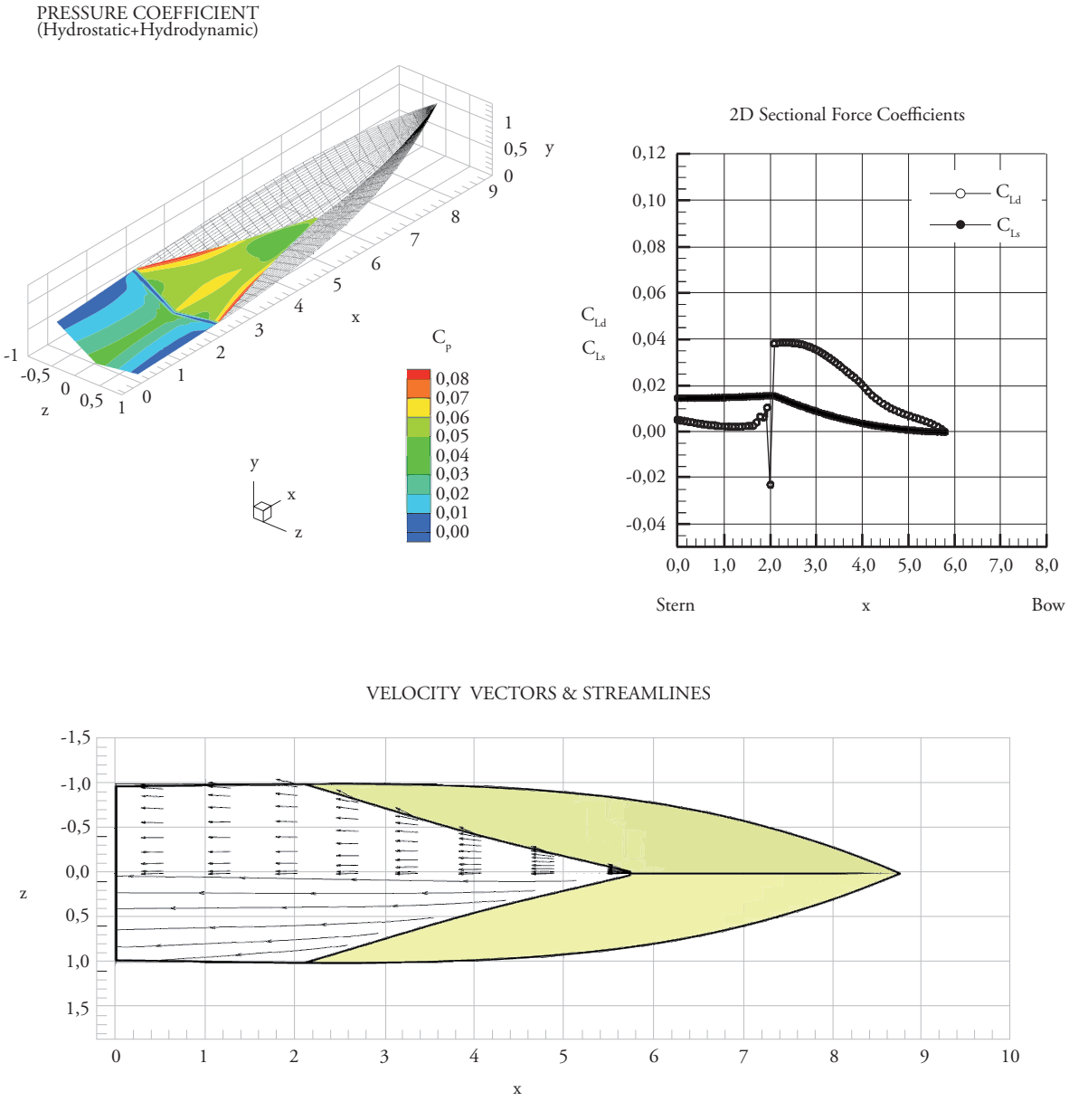

$$\frac{L_{cg}}{z_{ch}} = 2{,}75 \qquad (28)$$

forward of the transom. The length of the planing surface, L_p, is 35 feet. The centroid of the A_p is 41.7% forward of the transom with the L_{cg} located a distance of 10% of L_p aft of the A_p centroid.

Results of the steady hydrodynamic analysis for the side-hull hullform are provided in Figures (13) through (15). These figures correspond to a volumetric Froude number,

$$F_{\nabla} = \frac{U}{\sqrt{g\nabla^{1/3}}} \qquad (29)$$

ranging from 4.0 to 12.0. The associated speed ranges from 32.7 knots to 98.0 knots.

Fig. 14. Trimaran concept side-hull corresponding to F_{∇}= 10,0 (81.7 kts). Plots include a) total pressure coefficient, b) sectional dynamic and static lift coefficient, and c) velocity vector and streamline orientation. *(x,y,z)* coordinates are nondimensionalized by maximum chine half-beam, Z_{ch} . Note the extent of chines-wet flow.

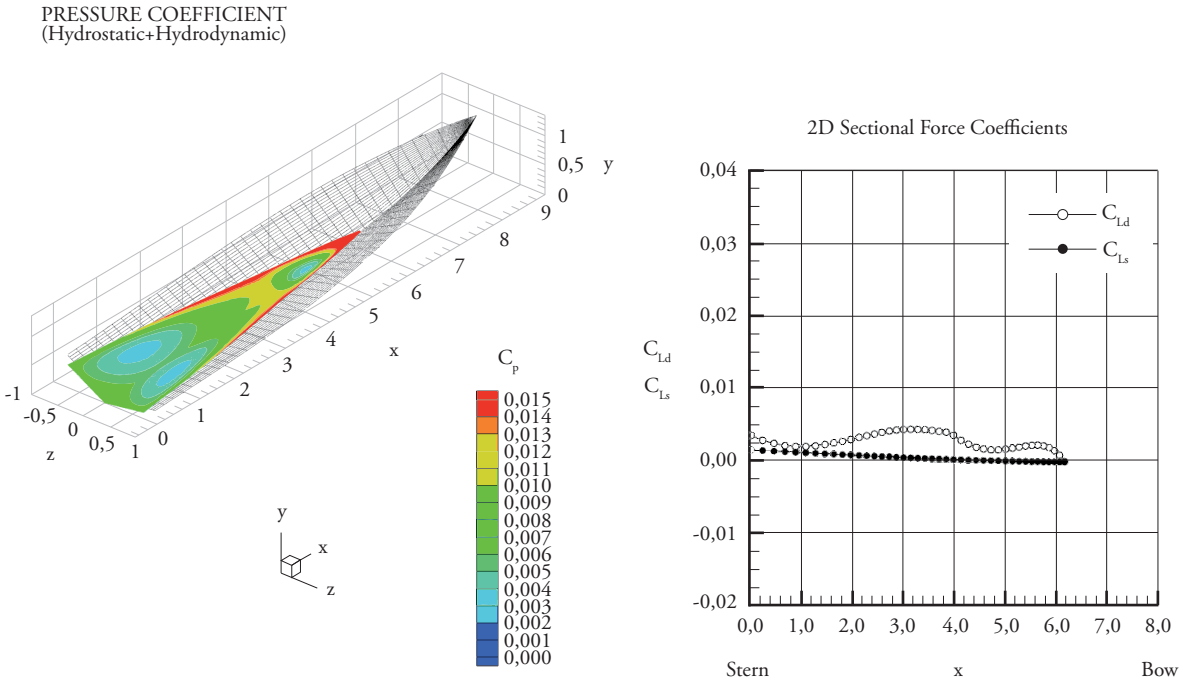

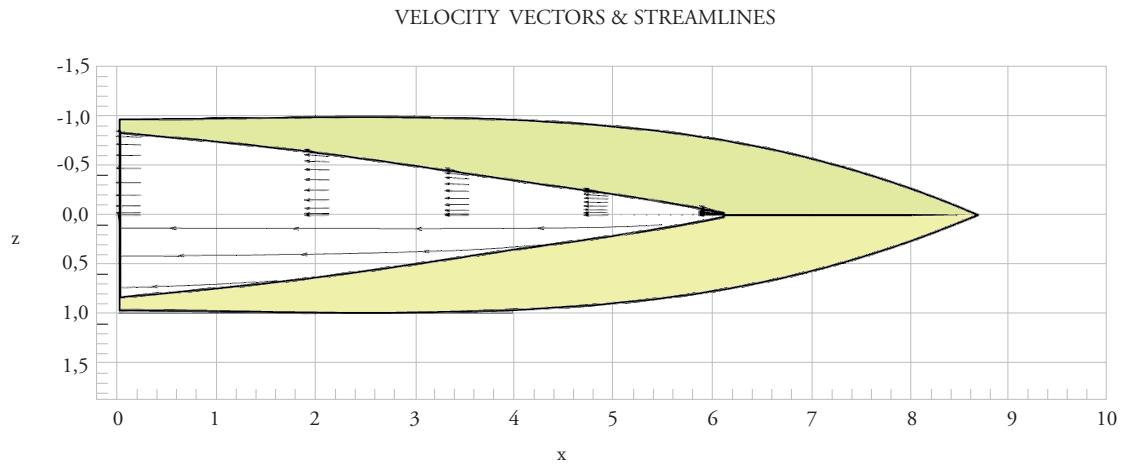

Fig. 15. Side-hull lift and drag coefficient as a function of F_∇

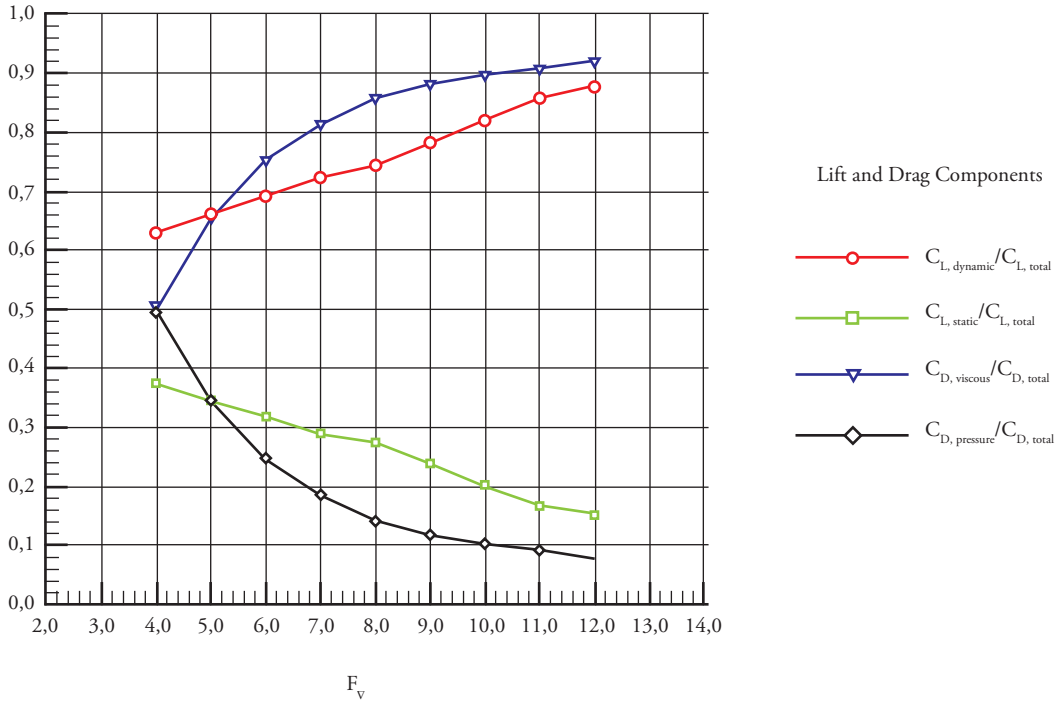

The total pressure coefficient is defined as,

$$C_p = \frac{P}{\frac{1}{2}\rho U^2} \tag{30}$$

with the sectional, two-dimensional, force coefficients given by,

$$C_{L_d} = \frac{P_d}{\frac{1}{2}\rho U^2 B} \qquad C_{L_s} = \frac{P_s}{\frac{1}{2}\rho U^2 B} \tag{31}$$

The hydrodynamic and hydrostatic lift force per unit length of the hull are L_d and L_s, respectively. The entire wetted planing surface is comprised of the chines-dry flow phase at a F_∇ = 8 or 65.3 knots. At this speed, no chines-wet phase is present.

Figure 15 shows the contribution of hydrodynamic and hydrostatic lift as a percentage of total lift for varying volumetric Froude number. Similarly, the percentage of viscous and pressure drag of the total drag is also shown in this figure. At a F_∇ = 4 (32.7 knots) the lift ratios are,

$$\frac{C_{L,\,dynamic}}{C_{L,\,total}} \cong 0{,}62, \tag{32a}$$

$$\frac{C_{L,\,static}}{C_{L,\,total}} \cong 0{,}38. \tag{32b}$$

and at F_∇ = 12 (98.0 knots) these ratios become,

$$\frac{C_{L,\,dynamic}}{C_{L,\,total}} \cong 0{,}86, \qquad \frac{C_{L,\,static}}{C_{L,\,total}} \cong 0{,}14. \tag{33}$$

At 32.7 knots the pressure and viscous drag components are nearly equivalent. However, at top speed of 98.0 knots, the viscous drag dominates the total drag as shown by,

$$\frac{C_{D,\,viscous}}{C_{D,\,total}} \cong 0{,}92, \qquad \frac{C_{D,\,pressure}}{C_{D,\,total}} \cong 0{,}08. \tag{34}$$

This illustrates how any method, such as bubble drag reduction or hull steps, can have a potentially large influence on the top speed of the craft in this Froude number range.

Figure 16 illustrates the contribution to lift and drag from the chines-dry and chines-wet flow

Fig. 16. Side-hull lift and drag contribution for chines-dry and chines wet flow phases as a function of F_∇

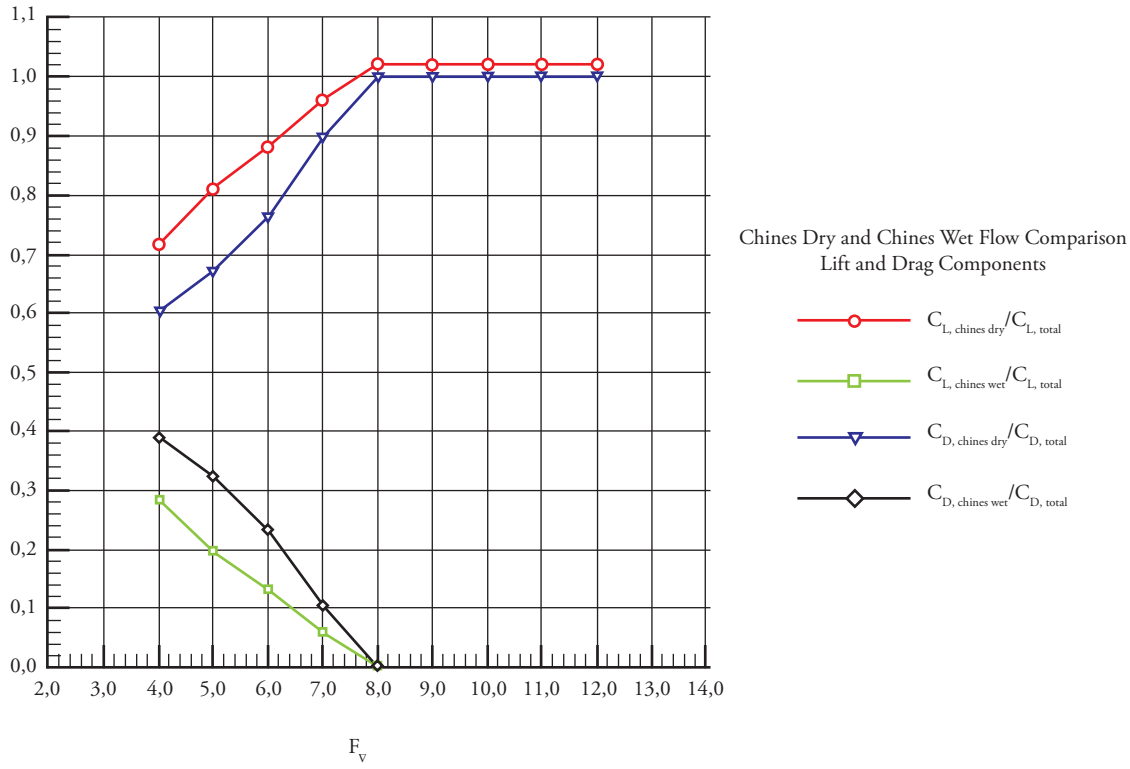

regimes as a function of F_∇. This figure shows that the CW flow phase is completely avoided at $F_\nabla = 8$ and how the majority of lift and drag is associated with the CD area.

The resistance to displacement ratio is defined as,

$$\frac{R_t}{\Delta} \tag{35}$$

The combined performance of the monohull and two side-hulls for the trimaran concept is shown in Figure 17. The monohull, trimaran, and trimaran (MOD1), are depicted in this figure. The monohull curve is the same curve shown in of the monohull hydrodynamics section. The trimaran curve (blue line) is the steady BHP required at each speed computed by satisfying the vertical plane equations, through, in the following modified form,

$$\begin{aligned} 0 &= T_x - N\sin\theta - D\cos\theta + 2V_x\,, \\ 0 &= T_z - N\cos\theta + D\sin\theta + W + 2V_z\,, \end{aligned} \tag{36}$$

and

$$0 = Nx_c - Dx_d + Tx_p + 2M_y\,.$$

The acceleration terms on the left hand-side of all equations is set to zero for the steady case. Figure (17) shows that the maximum speed for the monohull alone is 51.9 knots given a total BHP available of 4,570 hp. The total power available in the trimaran configuration from two MTU 12V4000 and four SeaTek 10.3 Endurance diesels is 8,770 hp. The trimaran curve (blue line) indicates that the top speed in the trimaran mode increases to 56 knots from 51.9 knots for the monohull case.

Aft positioning of the side-hulls with positive x_s values tends to cause a net reduction in operating trim angle when compared with independent monohull operation. This reduction in trim magnifies the viscous drag penalty. Hence, stepped planing hulls or drag reduction methods, have the potential to increase the attainable top speed for the trimaran. An estimate or upper bound for this speed increase can be approximated by adding the BHP requirement for the monohull and side-hull component when each hull is operating in an independent mode. Adding the BHP curves provided in Figure 17 yields the green curve

Fig. 17. Comparison of monohull and trimaran BHP requirements

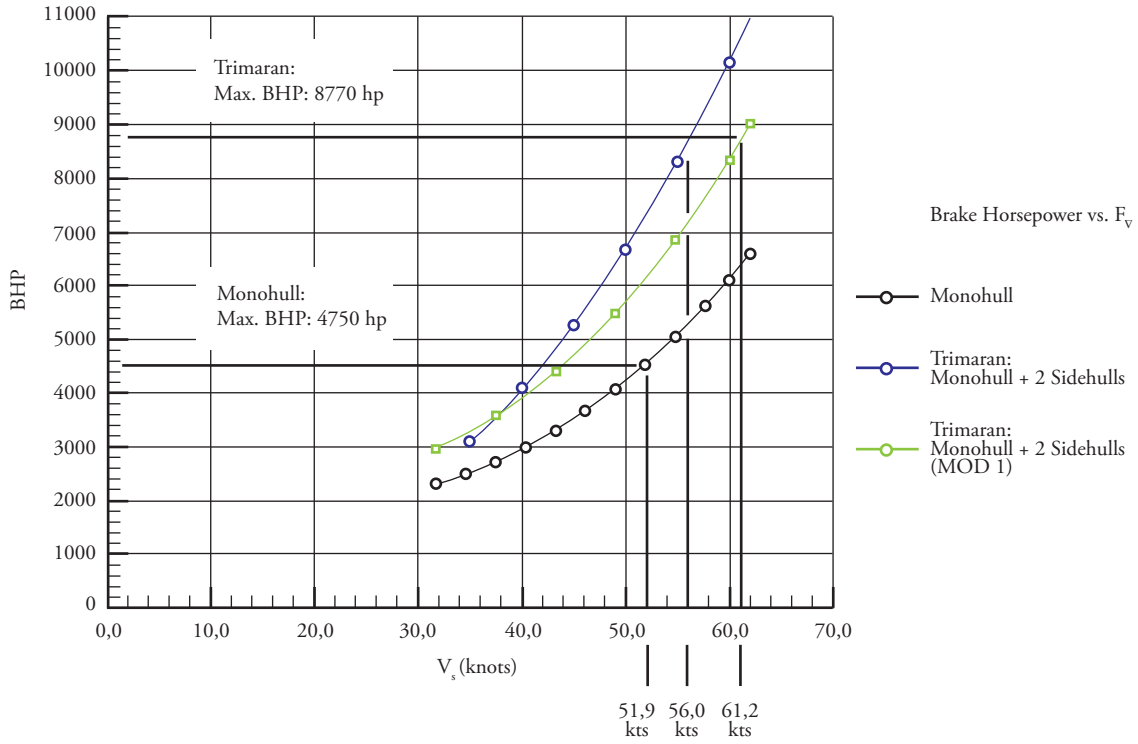

labeled "Trimaran: (MOD1)." This curve shows the top speed for the trimaran concept increasing to 61 knots and yielding a 9-knot increase when compared to the monohull case.

Hence, the trimaran concept provides a 4 to 9-knot potential increase in top speed when compared to operation of the monohull alone.

Trimaran Seakeeping Analysis

A seakeeping analysis is documented in this section for the trimaran concept. The concept consists of joining two side-hulls to a center-hull via a wing structure connection as is described in the concept development discussion. The methods defined by Zarnick (1978), Zarnick (1979), and Akers et al (1999) have been extended and generalized to allow for computation and analysis of planing multi-hull configurations.

Table 2 defines the combination of craft speeds and sea conditions analyzed in this study for the trimaran. All results shown reflect a 3-hour exposure period. Table 2 shows that no bow acceleration exceeds 2.5 g for the trimaran case at the speeds analyzed of 25, 50, and 60 knots, with operation in sea state 2 or 3. Further, for the trimaran, no CG acceleration exceeds 1 g while operating at 35, 50, or 60 knots in sea state 2 or 3. However, the monohull predictions show bow acceleration values of 4 to 5 g for these same cases. The maximum acceleration values for the CG and bow have also been plotted for both the trimaran and monohull for the 50 knot case in Figures 18 and 19.

Figures 18 and 19 show a comparison of trimaran and monohull response to the same wave elevation time history. These plots show a portion of a 3-hour simulation for the vessels operating at 50 knots in sea state 4. Sea state 4 has a significant wave height of 6.2 feet. The time histories plotted show the maximum value for the monohull operating without the side-hulls. The green lines show the response of the trimaran to this same wave elevation excitation. These results highlight the significant reduction in vertical acceleration experienced at both the CG and bow of the trimaran when compared with the monohull case. Specifically, a

Table 2. Trimaran Seakeeping Maxima Results for a 3-Hour Exposure Period

			Trimaran		Monohull	
Speed (kts)	**Sea State**	**Location**	**Max**	**RMS**	**Max**	**RMS**
35	2	Bow	**0.27**	0.0.71	0.38	0.123
35	2	CG	**0.08**	0.022	0.12	0.035
35	3	Bow	**1.64**	0.338	4.42	0.610
35	3	CG	**0.39**	0.135	1.63	0.272
35	4	Bow	**8.03**	0.687	14.75	1.135
35	4	CG	**2.49**	0.338	7.57	0.638
50	2	Bow	**0.36**	0.088	0.50	0.136
50	2	CG	**0.11**	0.031	0.18	0.045
50	3	Bow	**1.98**	0.417	5.17	0.773
50	3	CG	**0.71**	0.191	1.83	0.398
50	4	Bow	**9.49**	0.924	15.54	1.342
50	4	CG	**3.68**	0.516	11.37	0.837
60	2	Bow	**0.42**	0.099	0.51	0.146
60	2	CG	**0.14**	0.038	0.22	0.052
60	3	Bow	**2.53**	0.510	4.18	0.836
60	3	CG	**1.02**	0.250	1.77	0.459
60	4	Bow	**10.75**	1.086	- - -	- - -
60	4	CG	**4.7**	0.639	- - -	- - -

Fig. 18. Monohull and trimaran bow vertical acceleration time history comparison.
The maximum values for a 3-hour exposure operating at 50 knots in sea state 4 are shown

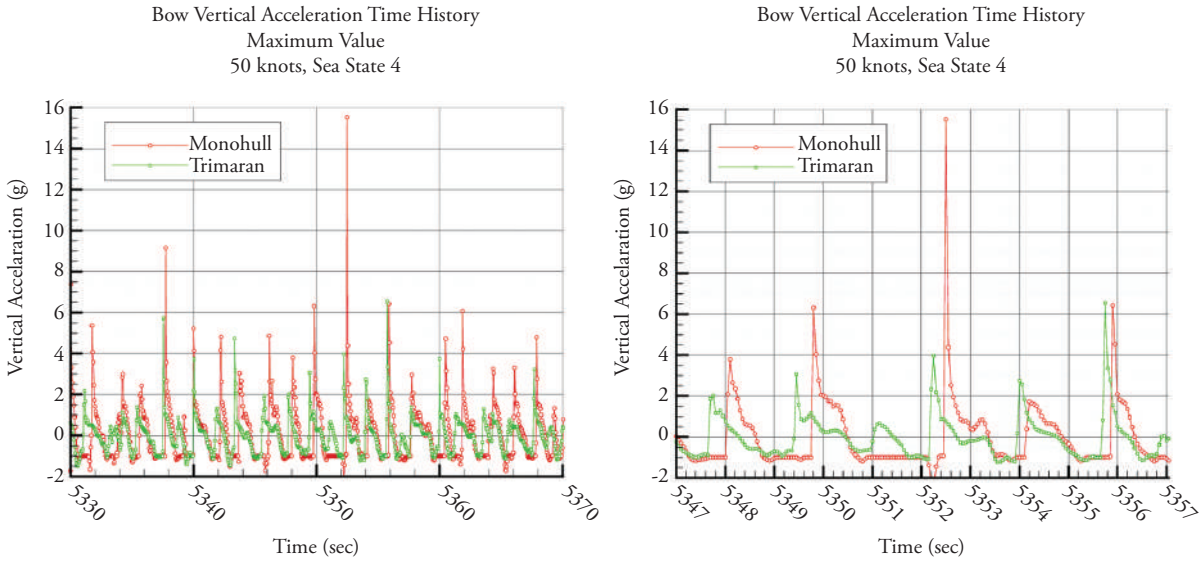

maximum bow acceleration of over 15 g is predicted for the monohull in these conditions. The trimaran bow acceleration is predicted to be only 4 g. The maximum CG acceleration computed is nearly 12 g for operation in sea state 4 at 50 knots for 3 hours for the monohull. The trimaran concept experiences a CG vertical acceleration of only 2 g in these same conditions.

Fig. 19. Monohull and trimaran CG vertical acceleration time history comparison.
The maximum values for a 3-hour exposure operating at 50 knots in sea state 4 are shown

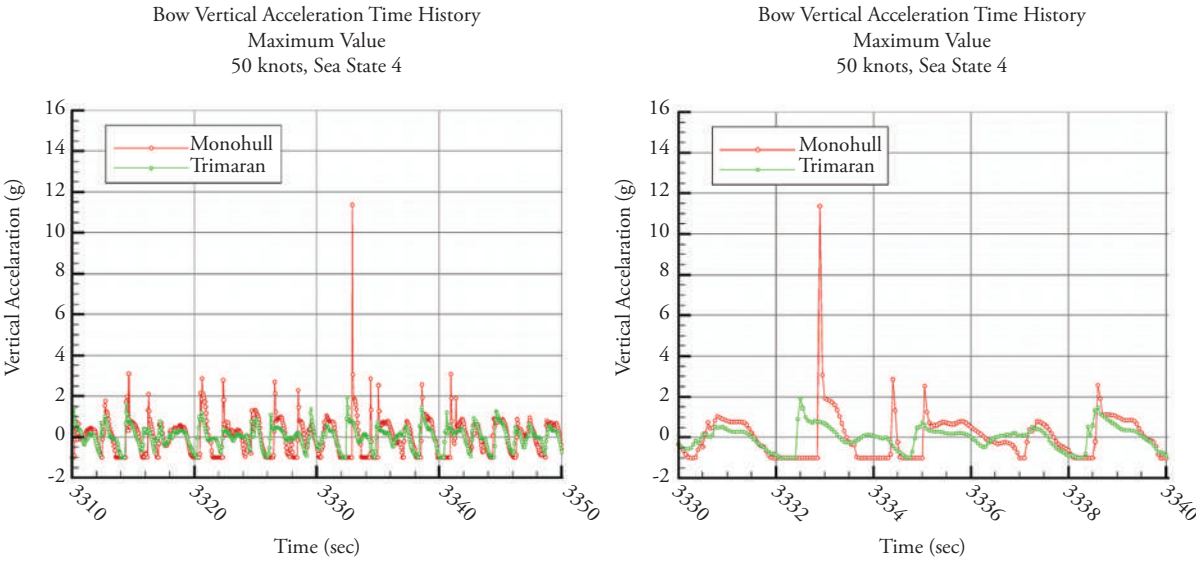

Fig. 20. Perspective view of space frame structure designed to carry side-hull loading.
Structural design is shown from transom to forward engine room bulkhead

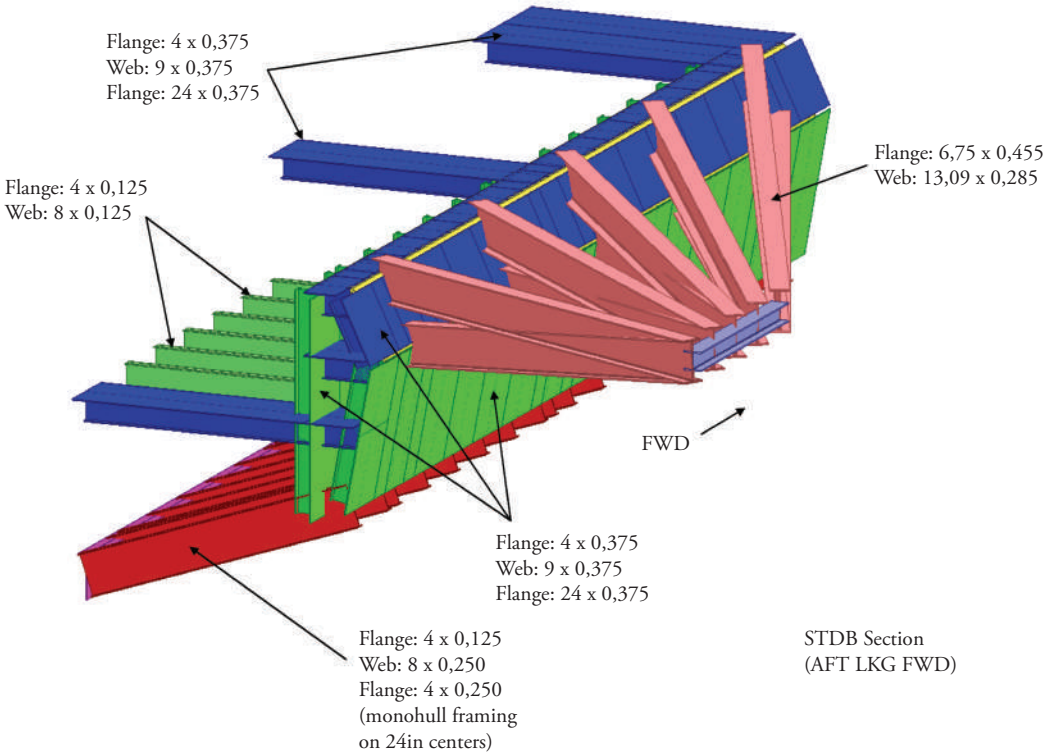

Trimaran Structural Design and Evaluation

One of the main challenges with the trimaran concept is the structural design. The structure must be able to withstand a transient loading environment generated by operating at high speed in a seaway. This environment imposes high levels of stress throughout the entire hull. Further, the transient nature of the seaway generated loads also causes the structure to endure several loading and unloading cycles. Hence, this can be considered both a high-stress and high-cycle structures problem.

The analysis contained in this section consists of designing a space frame structure for two load cases. The first load case is static suspension of the entire 13,000-pound side-hull from the center-hull. The second load case corresponds to the maximum vertical transient force generated by operation of the trimaran system at 50 knots in sea state 3 over a 3-hour duration period. This results in a maximum load pulse with an amplitude of 70,000 lbs and a pulse width of approximately 1,000 milliseconds (1.0 seconds).

The space frame structure designed to withstand this loading environment is provided in Figure 20. Due to the severity of the transient load case, the size of several of the monohull members had to be increased. Additionally, the transverse frame spacing was reduced aft of the engineroom bulkhead from 48 inches for the monohull case to 24 inches for the trimaran center-hull structure.

The aft cargo bay and engine room access have been maintained. The loading impulse utilized in this analysis is given by,

$$V_z(t) = A\sin^2\left(\frac{\pi t}{T}\right) \tag{37}$$

where $A = 70.000lbs$

Each of the members defined in Figure 20 were modeled as beam columns. The structural dynamics problem was solved using a transient finite element analysis (FEA) solver where both forces and moments are transferred at FEA joint locations. Zero displacement and zero slope boundary conditions are maintained along the centerline of the structure.

The increase in size of scantlings aft of the engine room bulkhead has been significant. The weight of the wing structure is 10,144 pounds. The weight aft of the engine room bulkhead for the center-hull becomes 20,288 pounds. The weight aft of the engine room bulkhead for the monohull design is only 6,210 pounds. Hence, the weight penalty added to convert the monohull concept into the center-hull of the trimaran concept is 14,078 pounds.

Table 3 shows the monohull weight estimate modified to include the additional wing structure. The total weight of the center-hull has increased from 98,974 pounds for the monohull to 113,052 pounds for the center-hull. This increase of 14,000 pounds in weight is significant. However, assuming that the loading coefficient of,

$$\frac{A_p}{\nabla^{2/3}} = 6.2 \tag{38}$$

is acceptable, as discussed in connection with formulas through, the total displacement of center-hull in a loading configuration similar to the current Mark V would be approximately 127,000 pounds. This displacement estimate for the center-hull still allows for a 14,000 pound contingency in the weight estimate.

The results of this section underscore the challenging nature of designing a structure to withstand the transient load environment encountered by high speed planing hulls operating in sea state 3 and above. The weight implications of the additional structure have been shown to be significant, but they may be within reasonable bounds from a loading coefficient perspective.

Summary

Design Summary

A design study has been completed for a mission configurable combatant craft. Several different

Table 3. Monohull preliminary weight estimate with wing structure

Description	Unit Weight	Qty	Total (lbs)
Aluminum Structure	13,801 lbs.	NA	13,801
Engines: MTU 12V 4000, with gears & fluids	16, 620 lbs	2	33,240
Waterjets: KaMeWA K50s	1,941 lbs	2	3,882
Diesel Fuel	8.5 lbs/US Gallon	2,600	22,100
Fresh Water	10.0 lbs/US Gallon	250	2,500
Gray Water	10.0 lbs/US Gallon	250	2,500
Outfitting: All systems.	75% of Alum. Struct. Weight.	NA	10,351
Crew:	350 lbs/crew	16	5,600
RHIB	2,500 lbs	2	5,000
Wing Structure	14,078 lbs	1	14,078
		Total:	**113,052**

concepts have been evaluated. Each concept was air-transportable and readily reconfigurable to meet a broad range of mission demands. Two design themes emerged in the process of completing this work. One centered around a technically conservative monohull concept which provided capabilities and performance similar to current SOF craft and the second centered around a multi-hull concept that exhibited significant technical risk, but offered significant operational and vessel performance enhancements.

Monohull: All design and analysis work for the monohull concept which included potential modifications to the current Mark V craft, centered around air-transportability in a C17 cargo plane. Modularity of the monohull concepts were not pursued since the C17 cargo volume is very similar to the dimensions required for an 80-foot, 50-knot planing hull. Hence, there was no need to subdivide into modules a new monohull design that had dimensional particulars similar to the current Mark V. However, the height of the Mark V was determined to be the main geometric constraint with air-transportation in a C17. Proposed modifications included to permanently lower the current hardtop deckhouse by lowering the main deck beams in way of the deckhouse or remove the current deckhouse hardtop and replace it with a collapsible canvas top and clear enclosure.
Drag reduction measures such as micro-bubble injection and stepped hulls were considered. The conceptual utility of stepped hulls was discussed in connection with maximizing the favorable chines-dry flow regime on a planing surface. The top speed of the monohull concept design was shown to potentially increase from 52 knots to 58 knots for the same delivered power using a stepped hull.

The final monohull concept developed had a length overall of 81 feet and a beam of 17 feet. The top speed of the vessel was 52 knots and the cruise speed was 40 knots. The range for this craft at cruise speed was 650 nautical miles. The vessel was designed to operate continuously at 50 knots in sea state 3. The vessel was also designed to be air-transportable in a C17 cargo plane with no assembly or disassembly required.

The monohull concept exhibited minimal technical risk and can be considered a re-design of the current Mark V for air-transportation in a C17 cargo plane.

Trimaran: The design approach used for the trimaran concept was to modify the monohull design to incorporate two detachable side-hulls. The side-hulls were sized to allow air-transport of each hull in a C130 aircraft while the center-hull was transportable in a C17. The connection mechanism between the wing-hulls and center-hull allowed for assembly of the trimaran platform

at a remote forward insertion point. Further, the connection mechanism was designed to incorporate a quick disconnect feature to facilitate side-hull detachment allowing the side-hulls to perform manned or unmanned missions independent of the center-hull.

The side-hulls had an independent top speed of 82 knots having been designed with propulsion booster units that offer an increased speed capability compared to the single center-hull. The top speed of the trimaran concept was estimated to range from 56 to 61 knots. This represented a 4 to 9-knot increase in top speed compared with the monohull. The seakeeping performance was shown to markedly improve with the trimaran concept when compared with the monohull. Hence, when assembled, the trimaran high speed platform was designed to allow the SOF to travel faster and with less fatigue when compared with 80-foot class monohull designs.

The trimaran design also emphasized the integration of several vessels similar in characteristics to the current SOF fleet including, Mark V, HSAC, RHIB, CRRC, and PWC, into one common high speed platform.

The trimaran design displayed several attractive attributes. However, the trimaran concept was identified as posing significant technical risk. This risk was found to be most pronounced when the structure was considered to withstand the highly transient loads generated by this system when operating at high speed in a seaway. Structural dynamic FEA analyses were performed on models representing all major scantlings aft of the engine room bulkhead. These analyses indicated that additional structure, weighing in total 14,000 pounds, must be added to the conventional monohull design. This weight penalty represented nearly a 15% increase in the total weight of the monohull.

Conclusions

In summary, the monohull concepts could be implemented with traditional small craft naval architecture methods. Planing hulls with similar design attributes have a long history of successful operation. The design conclusions for the monohull include,

The trimaran concept offers several attractive attributes which are coupled to significant technical challenges that must be overcome for successful implementation of the design.

Characteristics of the trimaran design include,

- Modularity is used to integrate several vessels, similar to craft in the current SOF fleet, into one high speed platform;
- Option for manned and unmanned operation of side-hulls and other vessels are used in the concept;
- Increased seakeeping performance when compared to the monohull design;
- Increased top speed capability when compared to the monohull design;
- Significant challenges associated with designing structure to attach side-hulls to the centerhull;
- Detachment and reattachment of the wing structure from the centerhull to allow air-transportation provides additional operational and structural challenges;
- Detachment and reattachment of the side-hulls from wing structure introduces further operational and structural challenges; and,
- Operation in quartering seas will introduce additional maneuvering, seakeeping, and structural issues that must be addressed.

Acknowledgments

The authors would like to thank Battelle Memorial Institute, Raytheon, and the United States Special Operations Command for the opportunity to work on this interesting and challenging project.

The efforts and contributions of Ms. Constance Savander, Maritime Research Associates, L.L.C., are also gratefully acknowledged.

References

AKERS, R.H., HOECKLEY, S.A., PETERSON, R.S., AND TROESCH, A.W. (1999) Predicted vs. Measured Vertical-Plane Dynamics of a Planing Boat. FAST 1999. Seattle, Washington, USA.

AMERICAN BUREAU OF SHIPPING (2001) Guide for Building and Classing: High Speed Craft. Houston.

ALLEN, R.G. AND JONES, R.R. (1977) Considerations on the Structural Design of High Performance Marine Vehicles. SNAME, New York and Metropolitan Section Meeting, January 13.

BLOUNT, D.L. AND HANKLEY, D.W. (1976) Full Scale Trials and Analysis of High Performance Planing Craft Data. Transactions, SNAME, Vol. 84.

CLARK, V. (2002) SeaPower 21 Series Part I: Projecting decisive joint capabilities. Naval Institute Proceedings, October.

COOPER, S. AND NORTON, M. (2002) New paradigms in boat design: An exploration into unmanned surface vehicles. Association for Unmanned Vehicle Systems International Symposium.

FRIDSMA, G. (1971) A Systematic Study of Rough-Water Performance of Planing Hulls (Irregular Waves - Part II), Stevens Institute of Technology, March.

GALE, P.A. (2003) The Ship Design Process. Chapter 5, Ship Design and Construction. The Society of Naval Architects and Marine Engineers (SNAME), Jersey City, New Jersey, pp. 5-1 to 5-40.

HELLER, S.R. AND JASPER, N.H. (1960) On the Structural Design of Planing Craft. Quarterly Transactions, RINA. July.

HUGHES, O.F. (1988) Ship Structural Design: A Rationally-Based, Computer-Aided, Optimization Approach. SNAME, Jersey City.

SAVANDER, B.R. (1997) Planing Hull Steady Hydrodynamics. Ph.D. Thesis, Department of Naval Architecture and Marine Engineering, The University of Michigan.

SAVANDER, B.R., SCORPIO, S.M., AND TAYLOR, R.K. (2002) Steady Hydrodynamic Analysis of Planing Surfaces. SNAME, Journal of Ship Research, Vol. 46, No. 4.

SAVITSKY, D. AND BROWN, P.W. (1976) Procedures for Hydrodynamic Evaluation of Planing Hulls in Smooth and Rough Water. Marine Technology, SNAME, October 1976.

SOKOL, W. AND HANSEN, E. (2001) Unmanned vehicles: A technology whose time has come. July 2001 Excerpt. www.dt.navy.mil.

SPENCER, J.S. (1975) Sructural Design of Aluminum Crewboats. Marine Technology, SNAME, New York, July.

TULIN, M. P. (1957) The theory of slender planing surfaces at high speed. Schiffstechnik, 4, 1225-133.

VORUS, W.S. (1996) A flat cylinder impact theory for analysis of vessel impact loading and steady planing resistance. Journal of Ship Research, Vol. 40, No. 2, pp. 89-106.

WAGNER, H. (1932) Uberstross-und gleitvorgange an der oberflache von flussigkeiten. ZAMM, 12 pp. 193-215.

ZARNICK, E.E. (1978) A Nonlinear Mathematical Model of Motions of a Planing Boat in Regular Waves. David W. Taylor Naval Ship Research and Development Center. Report Number DTNSRDC-78/032.

ZARNICK, E.E. (1979) A Nonlinear Mathematical Model of Motions of a Planing Boat in Irregular Waves. David W. Taylor Naval Ship Research and Development Center. Report Number DTNSRDC/SPD-0867-01.

Designing for Damage Stability and Survivability – Contemporary Developments and Implementation

Diseño para Estabilidad en Avería y Supervivencia – Desarrollos Recientes y Puesta en Práctica

Dracos Vassalos,[a]
Luis Guarín[b]

Abstract

With the new harmonised regulations for damage stability, SOLAS 2009, now in place (since January 2009), a number of ship owners and consequentially yards and classification societies are venturing to exploit the new degrees of freedom afforded by the probabilistic concept of ship subdivision. In this process, designers are finding it rather difficult to move away from the prescriptive mindset that has been deeply ingrained in their way of conceptualising, creating and completing a ship design. Total freedom it appears is hard to cope with and a helping hand is needed to guide them in crossing the line from prescriptive to goal-setting design. This will be facilitated considerably with improved understanding of what this concept entails and of its limitations and range of applicability. This paper represents an attempt in this direction, based on the collective knowledge and experience of the authors, deriving from many years of research on damage stability and survivability and a string of new concept designs for the passenger ship industry.

Key words: Probabilistic rules, damage stability and survivability, risk-based ship design

Resumen

Con la nueva normativa para estabilidad en avería SOLAS 2009, en vigor desde enero de 2009, algunos propietarios de buques y en consecuencia los astilleros y sociedades de clasificación se están aventurando a explotar los nuevos grados de libertad que ofrece el concepto probabilístico de compartimentación del buque. En este proceso, a los diseñadores les cuesta superar la forma tradicional de conceptualizar, crear y terminar el diseño de un buque. Aparentemente, enfrentar la libertad total es difícil y requieren ayuda para atreverse a cruzar la línea entre el diseño tradicional y el diseño por objetivos. Esa labor sería facilitada con una mejor comprensión de lo que implica este enfoque de diseño y cuáles son sus limitaciones y rango de aplicación. Este trabajo es un esfuerzo en este sentido, con base en el conocimiento y experiencia de los autores, obtenidos en muchos años de investigación sobre la estabilidad en avería y supervivencia, y una serie de nuevos diseños conceptuales para la industria de buques de pasajeros.

Palabras claves: Normas probabilísticas, estabilidad en avería, supervivencia, diseño de buques basado en riesgo

[a] The Ship Stability Research Centre (SSRC), Department of Naval Architecture and Marine Engineering, Universities of Glasgow and Strathclyde, UK

[b] Safety at Sea Ltd, Glasgow, UK
e-mail: l.guarin@safety-at-sea.co.uk

Introduction

From a ship stability viewpoint, the most fundamental goal to be achieved is for a ship to remain *afloat* and *upright*, especially so after an accident involving water ingress and flooding. Regulations to address the former are targeting subdivision and the latter damage stability. More recent instruments in the regulatory process tend to cater for both issues whilst contemporary developments have adopted a more holistic approach to safety that encompasses considerations of all principal hazards over the life-cycle of the vessel.

Notably, the first Merchant Shipping Act of 1854 is the first known legal requirement addressing safety at sea concerning watertight bulkheads, leading eventually and after heavy loss of life to the adoption of the first internationally agreed system of subdivision in SOLAS 1929.

The first damage stability requirements, on the other hand, were introduced following the 1948 SOLAS Convention and the first specific criterion on residual stability standards at the 1960 SOLAS Convention with the requirement for a minimum residual GM of 0.05m. This represented an attempt to introduce a margin to compensate for the upsetting environmental forces. "Additionally, in cases where the Administration considered the range of stability in the damaged condition to be doubtful, it could request further investigation to their satisfaction". Although this was a very vague statement, it is representative of the first attempts to legislate on the range of stability in the damaged condition. It is interesting to mention that a new regulation on "Watertight Integrity above the Margin Line" was also introduced reflecting the general desire to do all that was reasonably practical to ensure survival after severe collision damage by taking all necessary measures to limit the entry and spread of water above the bulkhead deck.

The first probabilistic damage stability rules for passenger vessels, deriving from the work of Kurt Wendel on “Subdivision of Ships”, [1] were introduced in the late sixties as an alternative to the deterministic requirements of SOLAS ‘60. Subsequently and at about the same time as the 1974 SOLAS Convention was introduced, the International Maritime Organisation (IMO), published Resolution A.265 (VIII). The next major step in the development of stability standards came in 1992 with the introduction of SOLAS part B-1 (Chapter II-1), containing a probabilistic standard for cargo vessels, using the same principles embodied in the 1974 regulations. The same principle was used in launching at IMO the regulatory development of “Harmonisation of Damage Stability Provisions in SOLAS, based on the Probabilistic Concept of Survival” in the belief that this represented a more rational approach to addressing damage stability safety.

Evidence, however, of “common sense” driving rule making is very scarce; with accidents providing the main motivation for rule making, emphasis has primarily been placed on reducing consequences, i.e., on cure rather than prevention. Against this background, it is widely believed that the prevailing situation could be drastically improved through understanding of the underlying mechanisms leading to vessel loss and to identification of governing design and operation parameters to target risk reduction cost-effectively. This in turn necessitates the development of appropriate methods, tools and techniques capable of meaningfully addressing the physical phenomena involved.

Having said this, it was not until the early 90s when **dynamic** stability pertaining to ships in a **damage** condition, was addressed by simplified numerical models, such as the numerical model of damaged Ro-Ro vessel dynamic stability and survivability [2]. The subject of dynamic ship stability in waves with the hull breached received much attention following the tragic accident of Estonia, to the extent that lead to a step change in the way damage stability is being addressed, namely by assessing the performance of a vessel in a given environment and loading condition on the basis of first principles. In parallel, motivated by the compelling need to understand the impact of the then imminent introduction of probabilistic damage stability regulations on the design of cargo and passenger ships and the growing appreciation

of deeply embedded problems in both the rules and the harmonisation process itself, an indepth evaluation and re-engineering of the whole probabilistic framework was launched through the EC-funded €4.5M, 3-year project HARDER [3]. The overriding goal of the HARDER project was to develop a rational procedure for probabilistic damage stability assessment, addressing from first principles all relevant aspects and underlying physical phenomena for all types of ships and damage scenarios. In this respect, HARDER became an IMO vehicle carrying a major load of the rule development process and fostering international collaboration at its best – a major factor contributing to the eventual success in achieving harmonisation and in proposing a workable framework for damage stability calculations in IMO SLF 47.

Deriving from developments at fundamental and applied levels in project HARDER as well as other EU projects such as NEREUS, ROROPROB and SAFEVSHIP and other international collaborative efforts (e.g., work at ITTC), a clearer understanding of damage stability started to emerge together with a confidence in the available knowledge and tools to address the subject effectively. All these efforts provided the inspiration and the foundation for SAFEDOR (2004–Design/Operation/Regulation for Safety), a 20- million Euro EU FP6 Integrated Project of 4 years duration, which provided the opportunity for consolidating contemporary developments on damage survivability, thus rendering implementation possible even at design concept level. The knowledge gained can now be used to address critically all available regulatory instruments and to foster new and better methodologies to safeguard against known design deficiencies in the first instance, until safer designs evolve to reflect this knowledge, [4], [5], [6]. At this point in time, it is known for example that damaged ships in waves may capsize in one of the following modes (the first three after the final equilibrium condition is reached post-damage):

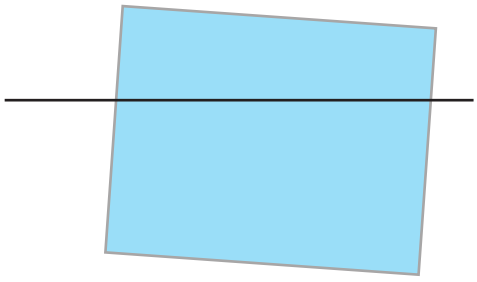

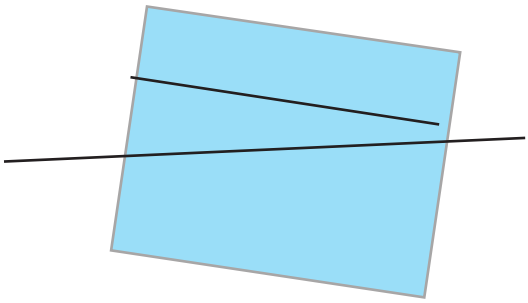

High freeboard ships: *Provided there is some minimal positive righting lever and range of stability the ship will not capsize in moderate waves. Wave impacts on the side of the ship will induce some rolling in marginally stable cases, which could result in capsize at the larger sea states. Often ships are more vulnerable with the damage to leeward, since the GZ levers are typically less in the damaged direction and the induced dynamic roll is typically somewhat greater leeward.*

Low freeboard Ro-Ro ships: *This is the typical mechanism of capsize for Ro-Ro ships. The wave action gradually pumps water up onto the vehicle deck. The height of the water gradually increases until either a reasonably stable equilibrium level is reached where inflow is approximately equal to outflow for ships with sufficient reserve stability, or if stability is inadequate, the heeling moment of the water will cause a capsize to windward. In some rare cases Ro-Ro vessels may heel to leeward after the first few wave encounters with an insufficient freeboard on the weather side to prevent further water accumulation and the ship will continue to take water on the vehicle deck until a capsize results.*

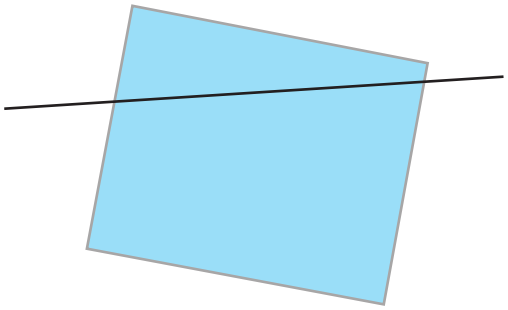

Low freeboard conventional ships: *This is the typical mechanism of capsize for non-Ro-Ro ships. The highest waves will form boarding seas and will pile-up on the windward side of the deck, inducing roll and capsize, usually to windward. The weather deck tends to drain quickly if there is no capsize, and there is no build-up or accumulation of water as seem with enclosed Ro-Ro decks. One or two high waves in close succession are often sufficient to cause capsize.*

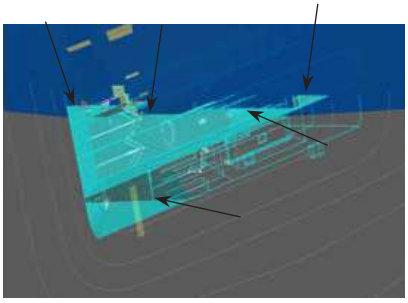

Multi-Free-Surface Effect: *This mechanism of capsize is relevant to ships with complex watertight subdivision such as cruise ships. As the hull is breached, water rushes through various compartments at different levels, substantially reducing stability even when the floodwater amount is relatively small. As a result the ship can heel to large angles, even for small damage openings, letting water into the upper decks that spreads rapidly through these spaces and may lead to rapid capsize at any stage of the flooding.*

The aforementioned mechanisms of vessel capsize help to judging how relevant or effective available regulatory instruments are, in being able to prevent or mitigate disasters, as indicated in the following for the instruments currently in use or due to be enforced:

- SOLAS 74: 1-compartment standard (prevent ship from sinking if one compartment is breached; resistance to capsize in waves unknown)
- SOLAS 90: 2-compartment standard (prevent ship from sinking if any two compartments are breached; resist capsize of 2-compartment worst damage in sea states with Hs approximately 3m – Ro-Ro vessels)
- Stockholm Agreement (as above but with a pre-defined level of water on deck depending on freeboard and in operational sea states of up to 4m Hs), [7]
- Harmonised SOLAS Chapter II-1(SOLAS 2009 – equivalent to SOLAS 90.

Concerning the latter, a stage has now been reached where the draft text of the major revision to the subdivision and damage stability sections of SOLAS Chapter II-1 based on a probabilistic approach has been completed following final amendments in January 2005 to Regulation 7-1 involving calculation of the "p" factor. The revised regulations were adopted in May 2005 at the IMO MSC and entered into force for new vessels with keels laid on or after 1st January 2009. The new regulations represent a step change away from the current deterministic methods of assessing subdivision and damage stability. Old concepts such as floodable length, criterion numeral, margin line, 1 and 2 compartment standards and the B/5 line will be disappearing.

With this in mind there appears to be a gap in that, whilst development of the probabilistic regulations included extensive calculations on existing ships which had been designed to meet the current SOLAS regulations, little or no effort has been expended into designing new ships from scratch using the proposed regulations. This gap has been addressed to a large extent in [4]. This paper builds on that by examining this (now) statutory requirement alongside other contemporary developments.

Contemporary Developments

Contemporary regulatory developments are already a step ahead, necessitating concerted effort at global level to ensure safe transition from deterministic to goal-based safety. More specifically, in May 2000, the IMO Secretary- General called for a critical review of the safety of large passenger ships noting that "what merits due consideration is whether SOLAS requirements, several of which were drafted before some of these large ships were built, duly address all the safety aspects of their operation – in particular, in emergency situations". This visionary prompt led IMO Maritime Safety Committee (MSC) to adopt a new "philosophy" and a working approach for developing safety standards for passenger ships. In this approach, illustrated in Fig. 1 (SLF 47/48), modern safety expectations are expressed as a set of specific safety goals and objectives, addressing design (prevention), operation (mitigation) and decision making in emergency situations with an overarching safety goal, commensurate with no loss of human life due to ship related accidents. The term "Safe Return to Port" has been widely adopted in discussing this framework, which addresses all the basic elements pre-requisite to quantifying the safety level (life-cycle risk) of a ship at sea.

Fig. 1. The IMO Framework – Passenger Ship Safety

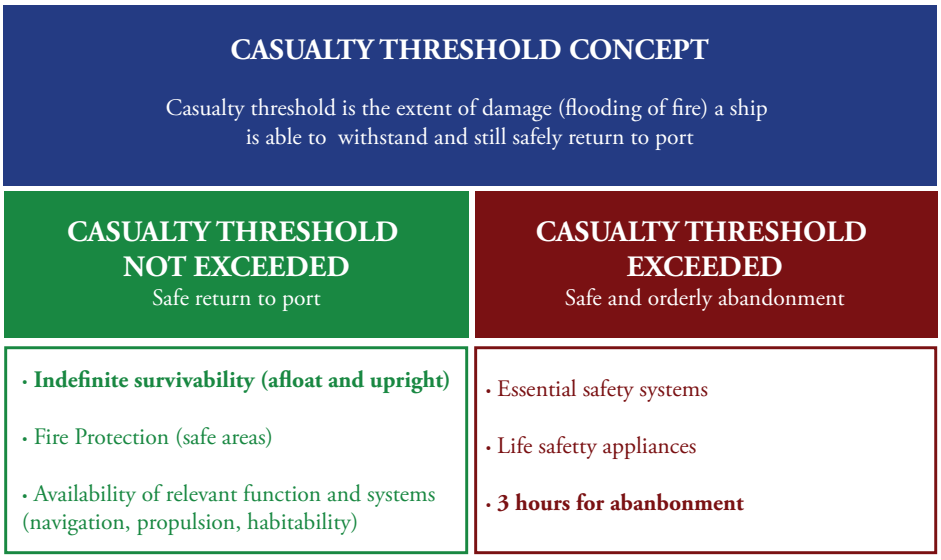

More specifically the following elements are explicitly addressed:

1. Prevention/Protection: Emphasis must be placed on preventing the casualty from happening in the first place as well as on safeguards (in-built safety) to limit consequences.

2. Timeline Development: The focus is clearly on the timeline development of different events. For the first time in the history of rule-making, it is not only important to know whether a vessel will survive a given casualty in a given loading condition and operating environment but also the time the vessel will remain habitable, the time it takes for safe and orderly abandonment and for recovery of the people onboard.

3. Casualty Threshold: This advocates the fact that the ship should be designed for improved survivability so that, in the event of a casualty, persons can stay safely on board as the ship proceeds to port. In this respect and for design purposes (only), a casualty threshold needs to be defined whereby a ship suffering a casualty below the defined threshold is expected to stay upright and afloat and be habitable for as long as necessary [5 days recommended] in order to return to port under its own power or wait for assistance.

4. Emergency Systems Availability / Evacuation and Rescue: Should a casualty threshold be exceeded the ship must remain stable and afloat for sufficiently long time to allow safe [3 hours recommended] and orderly evacuation (assembly, disembarkation and abandoning) of passengers and crew. Emergency systems availability to perform all requisite functions in any of the scenarios considered is, therefore, implicit in the framework. In addition, the ship should be crewed, equipped and have arrangements in place to ensure the health, safety, medical care and security of persons onboard in the area of operation, taking into account climatic conditions and the availability of SAR functions and until more specialised assistance is available.

Considering the above, it is worth emphasising that none of the questions arising (survival time?; functional availability post-casualty?; time needed for abandonment?) can be addressed in terms of rule compliance. Nonetheless, achievement of these goals in the proposed holistic, goal-based and proactive approach would ensure safety of human life commensurate with the safety expectations of today, by implicitly addressing all key elements of risk, for total risk (Safety Level) estimation and for direct use in Risk-Based Design, as explained in [8]. An evaluation framework, already being applied in the design of cruise/RoPax ships, is shown in Fig. 2 next.

Fig. 2. Risk-Based Design Implementation (Safety Level)

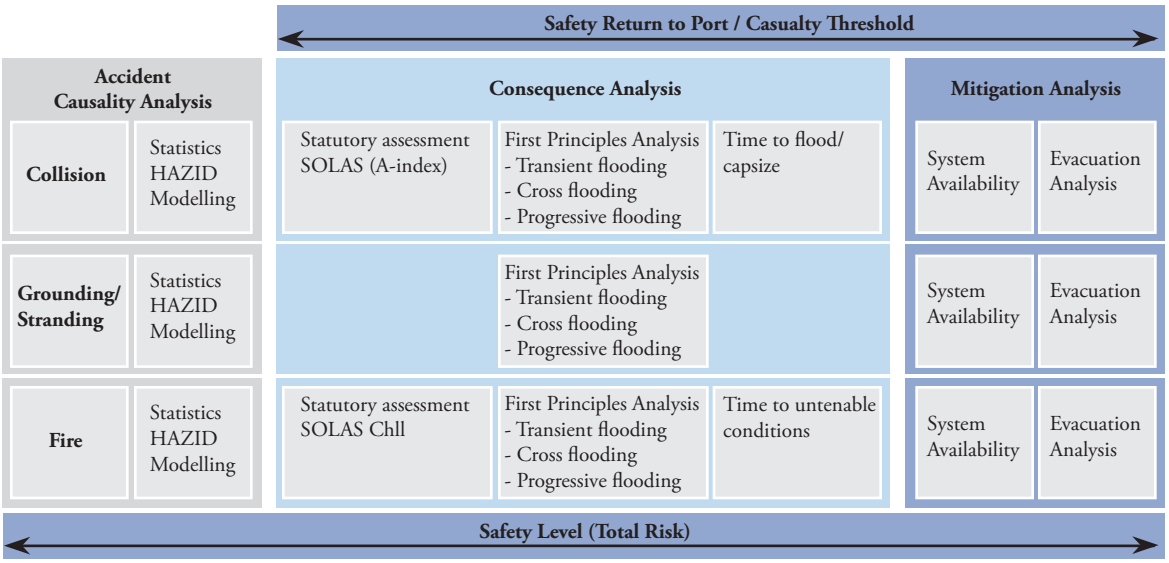

The focuses in this paper is on the flooding survivability analysis though describing and discussing some early implementation results.

Early Implementation Results

In this section, some early results will be presented aiming to provide answers and clarity to concepts deriving from contemporary developments in damage survivability. To this end, a hypothetical cruise ship is used with the following particulars: (See Table 1). The subdivision layout is shown in Figure 3.

Table 1. Principal particulars of example cruise vessel

Length	270 m
Breadth	35.5 m
Draught	8.3 m
Displacement	56,500 tonnes
Metacentric Height	2.35 m
Number of passengers	2,300
Attained Index of Subdivision, A	0.8
Required Index of Subdivision, R	0.8

Fig. 3. Largely "Unguided" Subdivision (Probabilistic Rules)

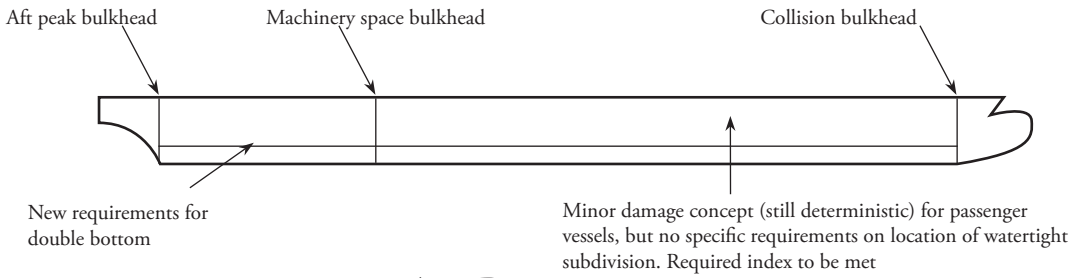

Flooding Survivability Analysis

Flooding survivability analysis normally entails the following, the first three of which are addressed here at various levels of detail.

- Statutory Assessment
  – Compliance with SOLAS 2009 (probabilistic rules)
  – Optimisation of watertight subdivision
- Transient-, cross- and progressive-flooding assessment
  – Static vs. dynamic stability
  – Time to flood
- Time to Capsize
  – Probabilistic approach for selection of damage (collision and grounding) cases
  – Vulnerability approach for survivability assessment
- Systems availability for each flooding scenario
  – Geometrical and topological evaluation of main ship systems
- Evacuability assessment
  – Assembly and evacuation performance
  – Assessment of time to capsize against total evacuation time
- Evaluation of casualty threshold / return to port capability
  – Probabilistic approach; link to system availability post-casualty

Statutory assessment

Acknowledging that emphasis on preventing a casualty from occurring in the first instance must take priority, focus on risk reduction by passive means (in-built safety) must come next and this must start at the beginning. To this end, the dilemma of prescriptive SOLAS-minded designers, illustrated in Fig. 3, in the simplest of levels, must be overcome. It is obvious that internal subdivision arrangement is a key issue affecting ship performance, functionality and safety, all of which have to date been catered for through the provision of rules and regulations that reflect, in essence, codification of best practice. Throwing this away and leaving on the table a blank sheet, makes ship subdivision a very difficult problem indeed. This was essentially the problem addressed in the EU project ROROPROB, [9].

Building on the understanding of Index A as outlined [4] – [6], affords a straightforward way of determining the relative (collision damage) risk profile of a vessel at an early design stage and hence devise an effective means of risk reduction by focusing primarily on the high risk scenarios.

The fully automated optimisation process typically produces several hundred design alternatives depending on the complexity of the ship's layout and the number of variables. Typical variables of the optimisation problem include: type of subdivision, number, location and height of watertight bulkheads, deck heights, tank arrangement, casings, double hull, and position of staircases, lifts and escapes.

Using the Attained Subdivision Index, payload capacity, steel weight and other regulatory requirements as typical objectives/constraints, the optimisation problem outcome typically includes: reduced number of bulkheads, reduced deck heights, reduced void volume, reduced number of escape ways and required staircases, reduced steel weight, reduced complexity in tank arrangements, increased crew and service areas, improved functionality and, if required, improved Attained

Subdivision Index. In order to make the process effective, participation by all decisionmakers (designer, owner and yard) is essential to properly define the optimisation variables, objectives and constraints as early as possible in the design stage. Using this approach, known as platform optimisation, high survivability internal ship layouts can be developed, without deviating much from the current SOLAS practice, this making it easier for ship designers to relate to the proposed procedure. The actual process for platform optimisation as it is currently being applied to newbuildings design is illustrated in Fig. 4. In order to make the process effective, the participation of all decision-makers (the designer, the owner, the yard) is essential to properly define the optimisation variables, objectives and constraints. Using this approach, high survivability internal ship layouts have been developed, without deviating much from the current SOLAS practice, this making it easy for ship designers to relate to the proposed practice. A sample of the optimisation problem outcome is presented in Fig. 5.

Fig. 4. Platform Optimisation Process

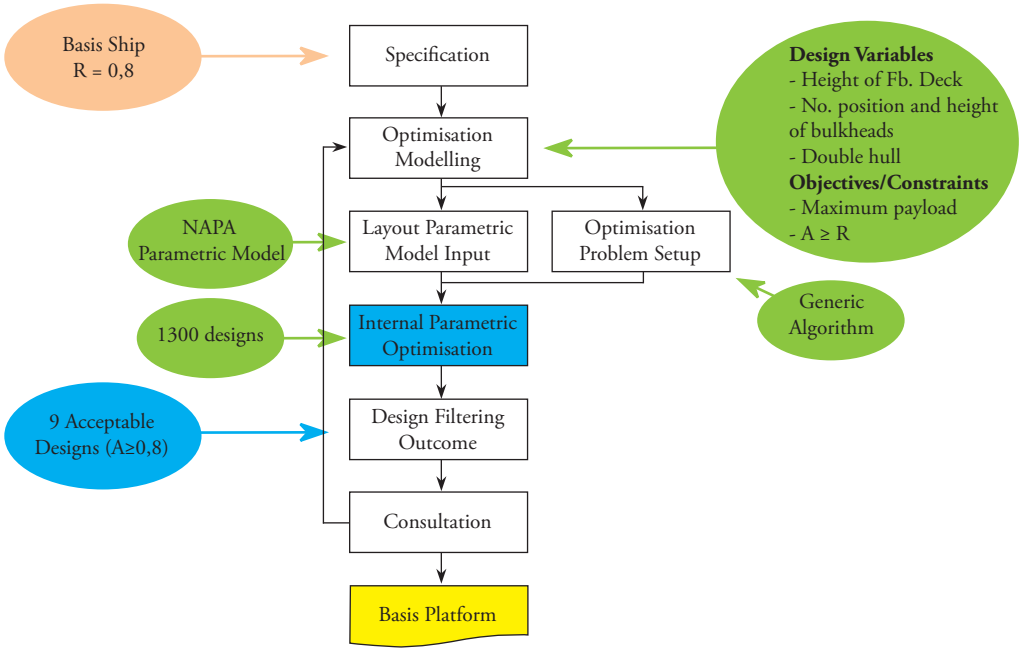

Fig. 5. Platform Optimisation Process – Concept Designs

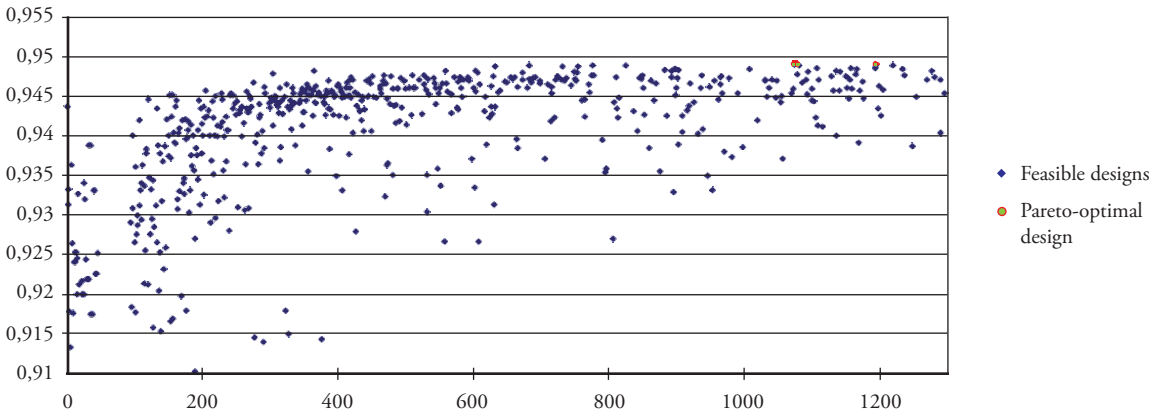

Using Table 1 particulars and Fig. 6 (Version 1) as a basis, Version 5 (Fig. 7) is produced using the process utilised above with A=0.92.

Taking additional measures from the available array of current best SOLAS practice, it was possible to further increase the attained AIndex to 0.985, without sacrificing any of the vessel's functionality. Time domain simulations with PROTEUS3, [10], have shown that such a vessel survives all probable damages up to 4-compartment damage for all sea states up to 4 m Hs.

Fig. 6. Hypothetical cruise vessel subdivision, Ver 1

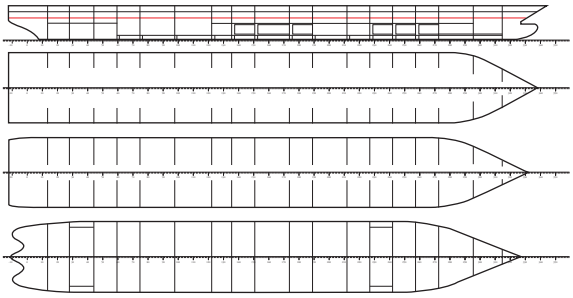

Flooding Vulnerability Assessment

The risk profile of Version 1 ship is illustrated in Fig. 8 for all the statistically possible damage

Fig. 7. Hypothetical cruise vessel subdivision, Ver 5

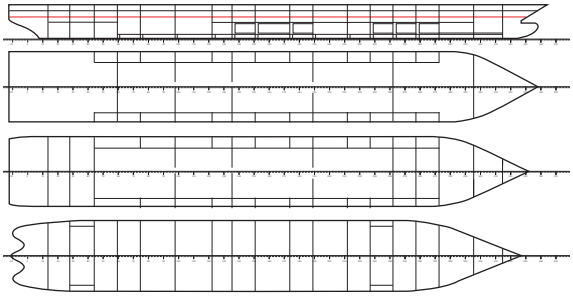

scenarios deriving from the probabilistic rules (Hs, loading condition, collision and grounding – the latter in addition to the current set of scenarios, which relate only to collision damage statistics).

These scenarios could be supplemented by using relevant experiential knowledge judiciously and through HAZID/brainstorming sessions with designer/yard/owner participating, aiming to identify any design vulnerability. Numerical simulations can then be used in calm water and in waves (as required) to establish the exact flooding mechanism and identify cost-effective changes for the local watertight arrangement using, for example, the PROTEUS3 software suite. The results are analysed in terms of occurrence of potentially dangerous behaviour or attitudes by addressing the

Fig. 8. Distribution of Relative Contribution to Risk per Damage Case, Ver 1

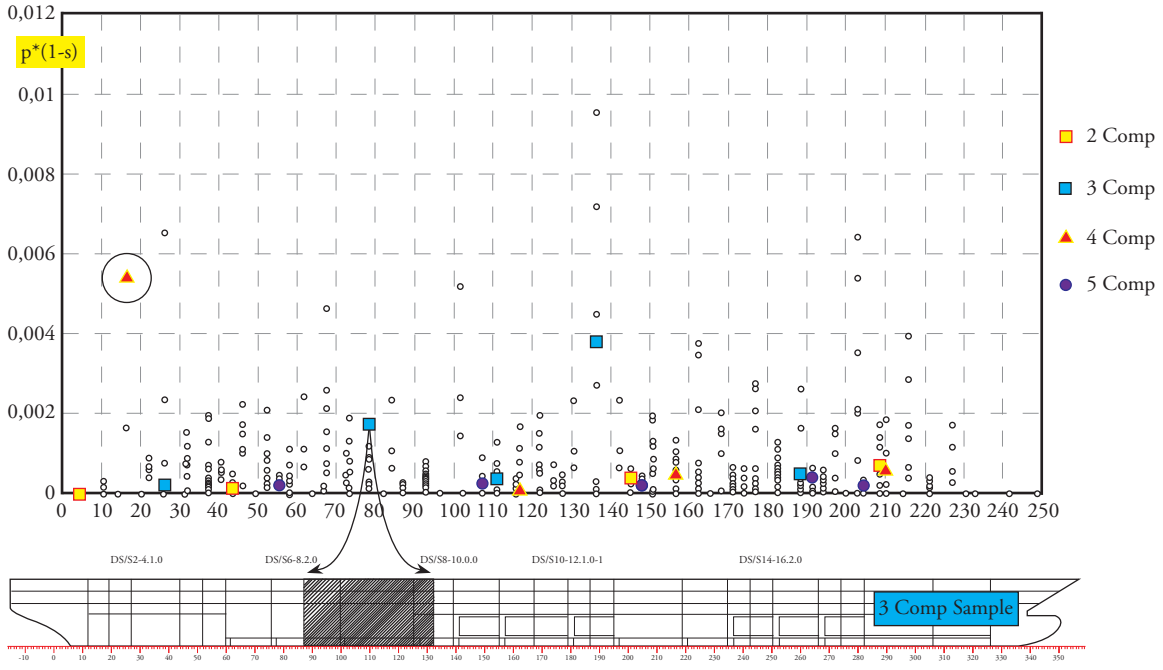

following three modes of flooding explicitly, on a case by case basis and using a much more complex (in terms of number of compartments and number of openings) and a more complete model (up to 5 decks are being modelled – see Fig. 9):
(i) Initial (transient) Flooding
(ii) Cross-Flooding
(iii) Progressive Flooding

Fig. 9. Typical Model used for Flooding Survivability Analysis

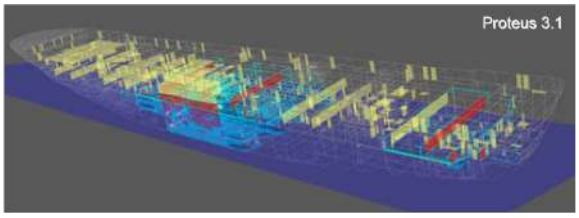

Transient and Intermediate Flooding

Having to deal with such a complex geometry, explicit dynamic flooding simulation of a damaged ship in waves is a must. Static analysis simply will not do. Moreover, in some cases where cross-flooding through intricate connection arrangements becomes a problem in terms of long cross-flooding times, results from simplified time-domain simulation codes need to be supported using CFD as the only viable option for a proper treatment of such a problem. The fact that industry appears to be pre-ordained to use static analysis when addressing damage survivability could at best affect adversely the design process and at worst severely undermine safety. Figs 10 and 11 (see fig.11 in page 67) demonstrate two such cases. In Fig. 10, the sfactor results in zero, because the angle of inclination exceeds the statutory range, which does not reflect what actually happens.

Conversely, Fig. 11 shows a damage case where the s-factor is non-zero based on the SOLAS 2009 formulation whilst numerical simulation results indicate progressive flooding, likely to result in capsize/sinking.

Multi-free Surface Effect

Fig. 12 demonstrates the result described in the introductory section.

Fig. 12. Multi-Free Surface Effect during Intermediate Stages of Flooding

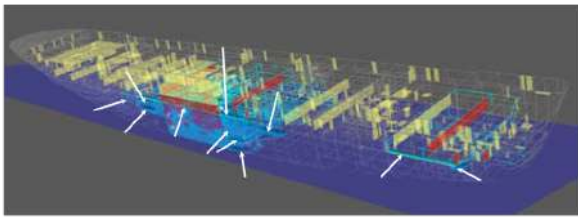

Bulkhead Deck Submergence and Progressive Flooding (Ducting, Piping, Doors, Windows, Shafts, etc)

Scenarios of this nature demonstrate the need for explicit knowledge on how the flooding process evolves, as in many cases it proves to be rather

Fig. 10. Numerical Simulation of Transient Flooding behaviour (calculated s=0)

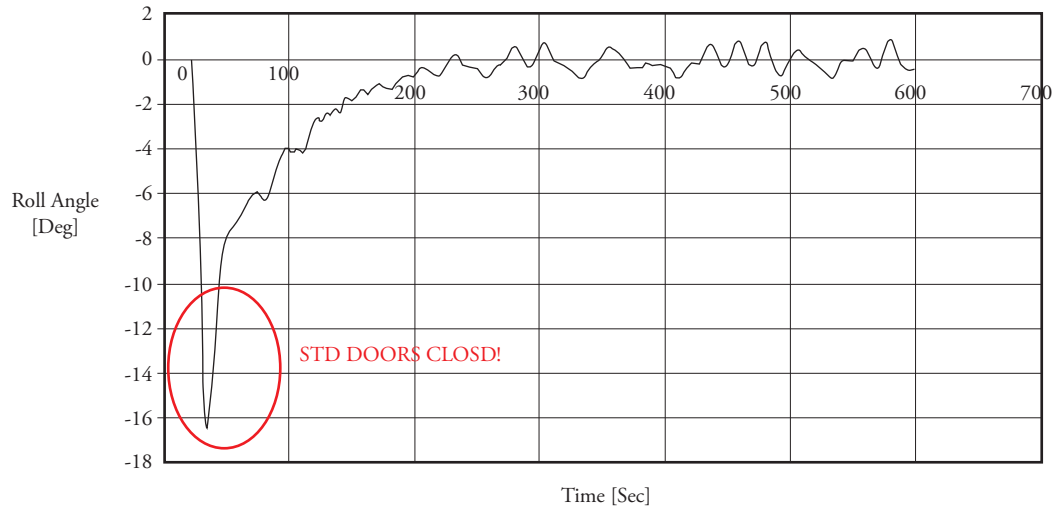

Fig. 11. Numerical Simulation of Transient Flooding behaviour (calculated s=1)

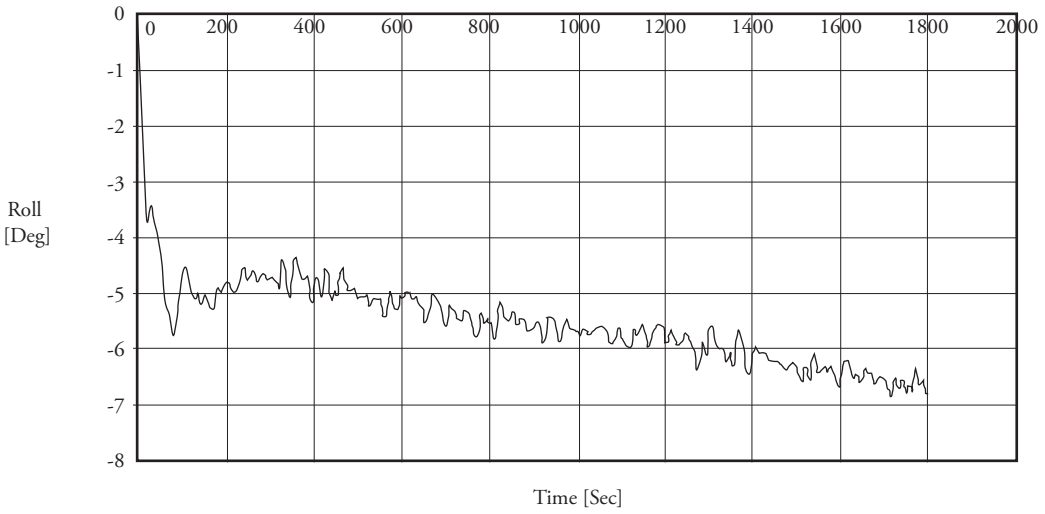

straightforward to impede the evolution of flooding with easy and very costeffective measures. Figs 13 and 14 show the post-processing that modern tools afford in this quest.

Fig. 13. Time-Domain Simulation of the Flooding Process (windows and SWT doors)

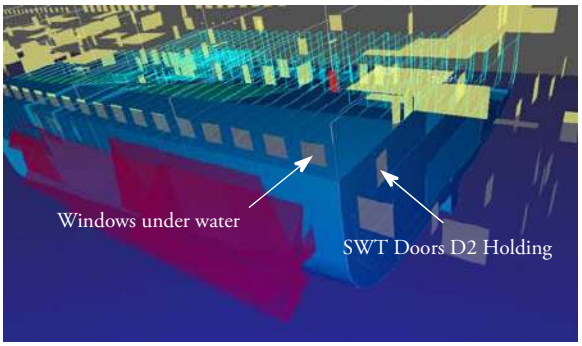

Fig. 14. Time-Domain Simulation of the Flooding Process (various openings)

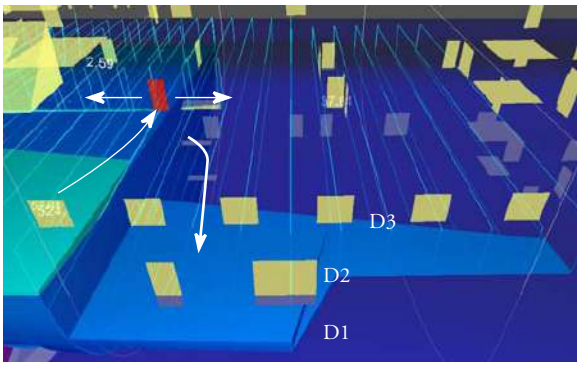

Time to Capsize

The results of the foregoing investigation is analysed in terms of the distribution for the time it takes the vessel to capsize/sink, one of the key parameters in flooding risk estimation.

Accounting only for the damage case scenarios implicit in the new harmonised rules for damage stability (normally over 1,000) and considering the 3 loading conditions, also implicit in the rules, and some 10 sea states per damage case, it becomes readily obvious that brute-force time-domain simulations is not the "route to salvation". In view of this, two lines of action are being followed: the first entails automation of the process using Monte Carlo simulation and performance-based assessment; the second relates to the development of a simpler (inference) model for estimating the time to capsize for any given collision damage scenario. For the example cruise vessel, results using the simpler model are displayed in Fig. 15.

A close examination of Fig. 15 reveals that a 15% increase in Index-A from version 1 to version 5 of the hypothetical cruise ship, results in a 60% reduction in the probability to capsize within 3 hours. Knowledge of the probability of survival beyond [3] hours in all relevant flooding scenarios would provide the basis for ascertaining safe return

Fig. 15. Cumulative probability distribution for time to capsize within a given time for two ship layouts shown in Figs. 6 and 7

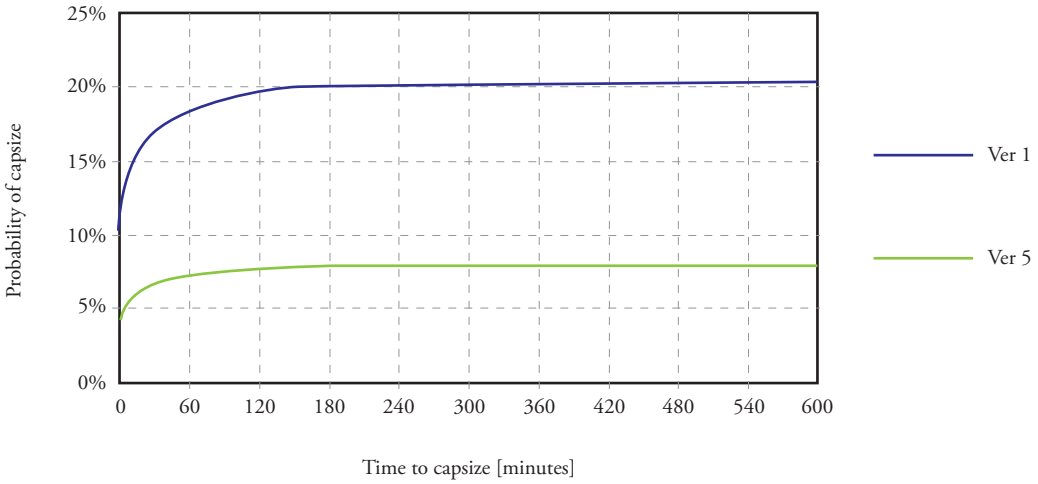

to port capability.

Moreover, an introspective look into the results of the example cruise ship, shown below in Fig. 16, reveals that with Index-A of 0.8 the risk contribution of 2-compartment damages is just over 2%, reducing to zero for Version 5 (A=0.92). In the latter, even for 3-compartment damages the risk contribution falls below 2%. Hence, with little judiciously expended effort, the damage survivability standard of passenger ships could be increased well beyond current levels without any adverse defect on ship functionality and earning potential.

Fig. 16. Defining a Damage Threshold

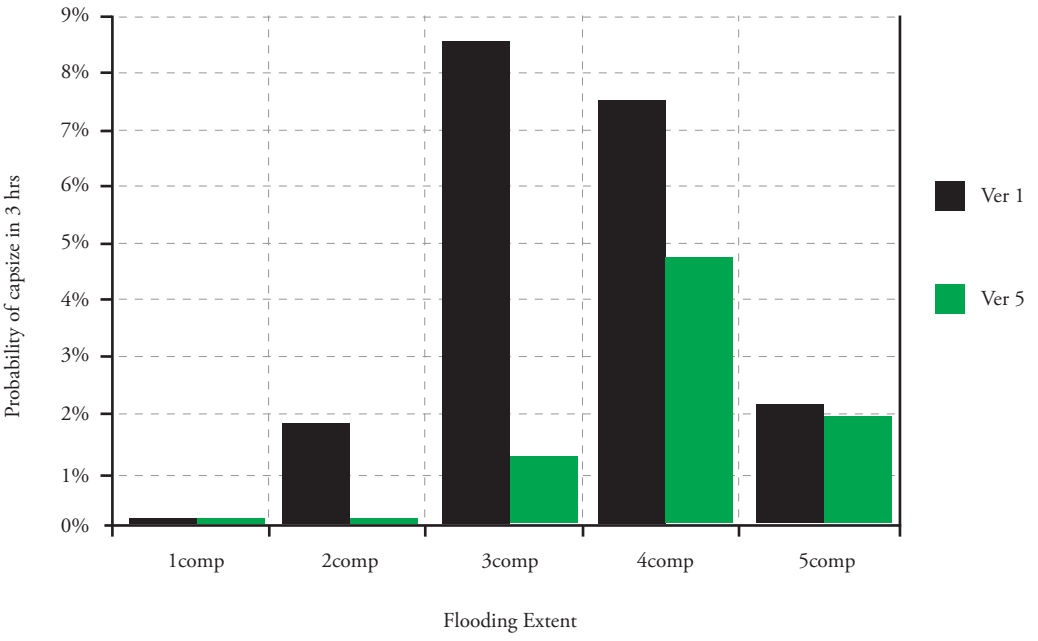

Concluding Remarks

Based on the work presented in the foregoing, the following concluding remarks may be drawn:

- With a clear trend towards probabilistic and risk-based frameworks to addressing ship safety in a holistic manner, it is important to base

such developments on clear understanding of the underlying principles and of the intention of the ensuing rules and regulations and/or criteria.

- The need to inculcate all major stakeholders in these new developments must remain a priority and clear targets set to facilitate the transition from prescriptive to goal-setting regulations.
- The probabilistic framework of the new harmonised rules for damage stability calculations offer flexibility and added degrees of freedom for designers to enhance safety cost-effectively both in targeting statutory compliance as well as pursuing specific safety objectives in the strife of the maritime industry to embrace innovation as a means of ginning and sustaining competitive advantage.

Acknowledgments

The support received over the years by the European Commission in undertaking part of the research work presented here is gratefully acknowledged. The authors would also like to express their appreciation and sincere thanks to the UK Maritime and Coastguard Agency for their continuing support in undertaking safetyrelated research.

References

[1] WENDEL, K, "Subdivision of Ships", Diamond Jubilee International Meeting, New York, June 1968, pp 12-1 to 12-21.

[2] VASSALOS, D. AND TURAN, O., "Development of Survival Criteria for Ro-Ro Passenger Ships - A Theoretical Approach". Final Report on the S0T Ro-Ro Damage Stability Programme, University of Strathclyde, December 1992.

[3] "Harmonisation of Rules and Design Rationale – HARDER", U Contact No. GDRB-CT-1998-00028, Final Technical Report, 31 July 2003

[4] VASSALOS, D, YORK, A, JASIONOWSKI, A, KANERVA, M AND SCOTT, A: "Design Implications of the New Harmonised Damage Stability Regulations", STAB 2006, Rio de Janeiro, Brazil. September 2006.

[5] VASSALOS, D AND JASIONOWSKI, A: "SOLAS 2009 – Raising the Alarm", 9th International Stability Workshop, Hamburg, Germany, August 2007.

[6] VASSALOS, D, JASIONOWSKI, A, YORK, A AND TSAKALAKIS, N: "SOLAS '90, Stockholm Agreement, SOLAS 2009 – The False Theory of Oranges and Lemons", 10th International Stability Workshop, Daejeon, Korea, March 2008.

[7] IMO Resolution 14, "Regional Agreements on Specific Stability Requirements for Ro-Ro Passenger Ships" – (Annex: Stability Requirements Pertaining to the Agreement), adopted on 29 November 1995.

[8] VASSALOS, D, JASIONOWSKI, A AND GUARIN, L: "Risk-Based Design: A Bridge too far?", OC 2008 Seakeeping and Stability, Osaka, Japan, March 2008.

[9] ROROPROB – "Probabilistic Rules- Based Optimal Design for Ro-Ro Passenger Ships", EU FP5 RTD Project G3RD-CT-2000-00030, 1999-2002.

[10] JASIONOWSKI, A. (2001): "An Integrated Approach to Damage Ship Survivability Assessment", PhD Thesis, SSRC, University of Strathclyde, February 2001, Glasgow.

Stability and dynamical effects of water on deck on the survivability of small fishing vessels

Estabilidad y efectos dinámicos del agua sobre cubierta en la supervivencia de barcos pesqueros pequeños

Alberto Francescutto[a]
Gabriele Bulian[a]
Manuel Urcia Larios[b]
Maximiliano Arroyo Ulloa[b]

Abstract

Starting from the analysis of casualties at sea involving small fishing vessels (Lbp<24 m), the paper presents the results of an experimental study on the capsizing resistance in beam or following steep or high waves of scale models in the towing tank of University of Trieste. The physical mechanisms leading to capsizing are highlighted and the experimental result are compared with existing theoretical approaches. The results stress the importance of deck wetness and of the presence of fishing nets as wave trappers on the probability of capsizing. The importance of complying with the existing regulations for dimensioning the freeing ports, although only voluntary, appears also an element of paramount importance.

Key words: Fishing vessels, Stability, Water on deck, Sloshing, Capsizing, Roll motion

Resumen

En la Universidad de Trieste se ha desarrollado un plan de investigación en seguridad y estabilidad del buque. La investigación se dirige principalmente a mejorar el conocimiento de los movimientos de grande amplitud del buque, con particular atención al movimiento de balanceo en diversas condiciones de la ola, y al efecto del chapoteo del agua a bordo.
La importancia del agua en la cubierta con la capacidad de volcar pequeños pesqueros, de puntal bajo y francobordo, cubierta grande, en olas de grande altura y/o inclinación, se ha confirmado en base de los experimentos conducidos después de accidentes en el mar. Particularmente, la degradación posible de la estabilidad, debida al agua atrapada en las redes, es relevante a los estudios de la seguridad del buque. Finalmente, la altura de ola crítica propuesta por Dahle y otros, se confirma para los buques muy pequeños en olas de través. Sería interesante extender en el caso de olas de popa, considerando que actualmente el criterio más acreditado de la estabilidad refiere a un mecanismo que vuelca en viento y mar de través…

Palabras claves: Barcos pesqueros, estabilidad, agua sobre cubierta, chapoteo, volcamiento, rolido

[a] Dipartimento di Ingegneria Navale, del Mare e per l'Ambiente, Università degli Studi di Trieste
e-mail: Gabriele Bulian (gbulian@units.it); Alberto Francescutto (francesc@units.it)

[b] Universidad Católica del Santo Toribio de Mogrovejo
e-mail: Manuel Urcia Larios (murcia@usat.edu.pe); Maximiliano Arroyo Ulloa (marroyo@usat.edu.pe)

Introduction

A long term research plan is currently run at University of Trieste on Ship Safety and Stability. The research is principally aimed at improving the knowledge of large amplitude ship motions with particular regard to rolling motion in different wave conditions and to the effect of sloshing of water on board.

In particular, the behavior in waves of two fishing vessels was studied from an experimental point of view and some conclusions are drawn regarding large amplitude roll motion modeling and the effect of green water on deck [1-5]. Due to the reduced size, this low built type of fishing vessels, which is quite common in the Mediterranean, presents high difficulties in motion computation and at the same time it is very sensitive to meteomarine environment. In both cases the research was originated by court trials following the capsizing of the original vessels with loss of life and was conducted on an experimental basis. The intact ship case was investigated with the aim of clarifying the capsizing mechanisms in beam or following waves and the effect of low freeboard, relatively large deck well, small efficiency of freeing ports and the possible deterioration of stability connected with water trapped in the nets on the stern side of the deck.

The safety of fishing vessels and the Torremolinos Convention

From a comparison between the occupational fatality statistics it appears that fishing industry is one of the most dangerous. The occupational safety and health branch of the International Labor Organization (ILO) estimates that fishing has an index of fatality of 80 per 100,000 workers, or approximately 24,000 lives per year as a consequence of 25 million non fatal accidents per year [6]. In the same period the general average of occupational fatalities was only 14.5 per 100,000, fishing excluded.

The International Torremolinos Convention for fishing vessels was established in 1977 [7] to set a safety regime for the fishing vessels of 24 m in length and upwards.

The Convention contains detailed rules concerning the standards of construction, including all safety equipment, that will be essentially applied to new ships. Being considered too strict, in the following years the Convention was not ratified by the number of administrations necessary for its entering into force.

The deficiency of ratifications, together with the need to update some technical aspects, led to a new Convention, held again in Torremolinos, in 1993. This Convention issued a Protocol to the 1977 Convention. The Protocol included provisions concerning the construction, structure, subdivision and stability, machinery and electrical installations, the fire protection, fire detection and fire extinction, the protection of the crew, the life-saving appliances and arrangements, the radio-communications and the safety of navigation.

The Torremolinos Protocol will enter into force one year after having been ratified by at least 15 Administrations, representing an aggregated fleet of 14,000 fishing vessels (approximately 50% of the world fleet of fishing vessels with length 24 m or more). On February 2nd 1999 it was ratified by 5 countries only; in 2007 by 13 countries with an aggregated fleet just exceeding 3.000 vessels.

The lack of ratification of these important provisions for the improvement of safety in this delicate sector was recently discussed at the International Maritime Organization (IMO) who solicited a study to identify the actions the Organization could undertake to promote the application of Torremolinos Protocol.

We have to note, on the other hand, that most provisions of the Convention concern vessels with length of 45 m and upwards, whereas the adoption of the provisions for vessels in the range 24 m – 45 m are left to regional agreements. This was effectively done, for instance by the European Community who, under European Directive 97/70 established a harmonised safety regime for fishing vessels of 24 metres in length and over [8].

Recently, however, IMO drafted voluntary guidelines for fishing vessels in the range 12 m – 24 m [9], whereas provisions for smaller units are under discussion [10]. Following recent statistics 93 per cent of workers are on vessels below 100 GRT (roughly 90 per cent of the workers work in vessels less than 24 meters in length)…

Relevant rules from the Draft text of the revised FAO/ILO/ IMO Voluntary Guidelines for the Design, Construction and Equipment of Small Fishing Vessels

Application. Unless otherwise stated, the provisions of these guidelines are intended to apply to new decked fishing vessels of 12 m in length and over, but less than 24 m in length. Nevertheless, even where not otherwise stated, the competent authority should as far as reasonable and practical give consideration to the application of these provisions to existing decked fishing vessels.

Freeing ports (§2.14). Where bulwarks on weather parts of the working deck form wells, the minimum freeing port area (A) in m^2, on each side of the vessel for each well on the working deck should be determined in relation to the length (l) and height of bulwark in this well as follows:

- $A = K \bullet l$, where: K = 0.07 for vessels of 24 m in length and K = 0.05 for vessels of 12 m in length; for intermediate lengths the value of K should be obtained by linear interpolation (l need not be taken as greater than 70% of the length of a vessel).
- Where the bulwark is more than 1.2 m in average height, the required (A) should be increased by 0.004 m^2 per metre of length of well for each 100 mm difference in height.
- Where the bulwark is less than 900 mm in average height, the required area may be decreased by 0.004 m^2 per metre of length of well for each 100 mm difference in height.

1. Subject to the approval of the competent authority the minimum freeing port area for each well on the superstructure deck should be not less than one half the area (A), given above, except that where the superstructure deck forms a working deck for fishing operations the minimum area each side should be not less than 75% of the area (A).
2. Freeing ports should be so arranged along the length of bulwarks as to provide the most rapid and effective freeing of the deck from water. Lower edges of freeing ports should be as near the deck as practicable. Two thirds of the total freeing port area per side should be provided in the half of the well nearest the lower point of the sheer curve, and some freeing port area should be placed as near the ends of the well as practicable.
3. Poundboards and means for stowage and working the fishing gear should be arranged so that the effectiveness of the freeing ports will not be impaired or water trapped on deck and prevented from easily reaching the freeing ports. Poundboards should be so constructed that they can be locked in position when in use and will not hamper the discharge of shipped water.
4. Freeing ports over 300 mm in depth should be fitted with bars spaced not more than 230 mm nor less than 150 mm apart or provided with other suitable protective arrangements. Freeing port covers, if fitted, should be of approved construction. It should not be possible to lock freeing ports, but they may be fitted with external top-hinged flaps/shutter and internal gratings. Such arrange ments may, however, not lead to a considerable reduction of the effective freeing port area. Any shutter or external rubber flaps in freeing ports should be fastened with hinges in the upper edge. The shutter should fit freely so that they cannot get stuck. The hinges should be made of materials that are not susceptible to corrosion. There should not be any arrangements for the locking of freeing port shutters.
5. In vessels intended to operate in areas subject to icing, covers and protective arrangements from freeing ports should be capable of being easily removed to restrict ice accumulation. The size

of opening and means provided for removal of these protective arrangements should be to the satisfaction of the competent authority.

6. Where wells or cockpits are fitted in the working deck or superstructure deck with their bottoms above the deepest operating waterline, efficient non-return means of drainage overboard should be provided. Where bottoms of such wells or cockpits are below the deepest operating waterline, drainage to the bilges should be provided.
7. Alternatively, the drainage of the wells could be by pumps to the satisfaction of the competent authority.

Stability criteria (§3.2). The following minimum stability criteria should be met unless the competent authority is satisfied that operating experience justifies departure therefrom:

- the area under the righting lever curve (GZ curve) should not be less than 0.055 m-rad up to 30° angle of heel and not less than 0.090 m-rad up to 40° or the angle of flooding ϕ_f if this angle is less than 40°. Additionally, the area under the righting lever curve between the angles of heel of 30° and 40° or between 30° and ϕ_f, if this angle is less than 40° should not be less than 0.030 m-rad. ϕ_f is the angle of heel at which openings in the hull, superstructures or deckhouses which cannot rapidly be closed watertight commence to immerse. In applying this criterion, small openings through which progressive flooding cannot take place need not be considered as open;
- the righting lever GZ should be at least 200 mm at an angle of heel equal to or greater than 30°. The righting lever GZ may be reduced to the satisfaction of the competent authority but in no case by more than 2•(24-L)%, with L in m;
- the maximum righting lever GZmax should occur at an angle of heel preferably exceeding 30° but not less than 25°; and
- the initial metacentric height GM_0 should not be less than 350 mm for single deck vessels. In vessels with complete superstructure the metacentric height may be reduced to the satisfaction of the competent authority but in no case should be less than 150 mm. It should be ensured that stability characteristics of the vessel will not produce acceleration forces which could be prejudicial to the safety of the vessel and crew;
- for decked vessels for which, by reason of insufficient stability data, the provisions above cannot be applied, an approximate formula for the minimum metacentric height GM_{min} for all operating conditions should be used as the criterion.

It is to be noted that similar provisions are included in the regulations for smaller vessels under discussion [10]. The Weather Criterion is on the contrary recommended for larger fishing vessels (45 m in length and over), although the Voluntary Guidelines seem to indicate that it should be applied also in the range 12 m – 24 m as a replacement of another provision for assessment of stability in severe weather conditions [7].

Mechanisms that can lead to total ship stability failure (Capsizing)

The mechanisms that can lead to ship capsize have been the subject of a large number of studies culminated in the recent adoption at IMO of a framework and a plan of action for the development of a new generation of intact stability criteria based on the actual ship performances at sea [11, 12]. Modern terminology, developed at IMO in the frame of the discussion of the new generation intact stability criteria distinguishes the stability failures in partial and total (ship loss). The case of fishing vessels has also been studied in some detail, leading to the conclusion that the greatest danger in intact condition for beam sea is constituted by steep and high waves and the subsequent inclining moments and green water on deck [11, 12]. In longitudinal/quartering waves, on the other hand, the mechanisms of loss of stability in waves, surf-riding and broaching, and parametric rolling have been identified [5, 13-15]. These can be connected with steep waves and/or with resonance mechanisms, like parametric rolling.

It is worth noting that, in spite of the great progress of the knowledge in this field, the intact stability criteria did not progress in parallel. Today we still have the general criterion established in the '60 as consequence of the study of Rahola of 1939 and the weather criterion established in the '80 mostly as a consequence of studies conducted by Japanese in the '50. Paradoxically, these criteria are considered too strict by shipowners and oversimplified by scientists…

As a consequence, they are still at the level of recommendations since none of them is yet mandatory at international level for the fishing vessels.

In the following, we report and discuss some of the results obtained recently concerning the safety from capsizing of fishing vessels. In this paper the attention is devoted to approaches based on the dynamic stability as reserve of energy against capsizing, mostly using the results of ad-hoc experiments connected with the analysis of casualties.

Beam sea

The results of the experiments done by several researchers were used by Dahle et al. [11-12] to obtain the height of a "critical" wave Hc, i.e. a steep wave capsizing the vessel, as a function of the "potential energy" E:

$$E = \Delta \int_0^{\phi_v} \overline{GZ}(\phi)\, d\phi \qquad t_f \cdot m \cdot deg \qquad (1)$$

connected with the classical dynamical stability up to the vanishing static stability angle ϕ_v or to the angle of progressive flooding ϕ_f. This led to the diagram reported in Fig. 1 where the critical wave for ships with bulwark and for ships with rail are indicated. Starting from this result, the statistical distribution of steep waves height can be used to evaluate the risk of capsizing of the vessel.

The following conclusions were reached during the study:

- with corresponding $\overline{GZ}$ curves, a loaded vessel is safer that one in ballast;
- the area below the $\overline{GZ}$ curve is important, and may be provided by enclosed superstructures, by low $\overline{KG}$ or both;
- for large angle of vanishing static stability and reasonable Δ and $\overline{GZ}$ values, capsize is very unlikely;
- models with positive $\overline{GZ}$ values extending beyond 90 degrees never capsized in waves up to 10 m height.

Fig. 1. Critical wave height for capsizing in beam steep and high waves [11-12]. Solid line refers to fishing vessels with bulwark, while dashed one to fishing vessels with rail. The points represent the results of the experiments conducted at the University of Trieste:
◆ ■ represent tests with capsize;
◇ □ represent tests with water on deck but not capsize.

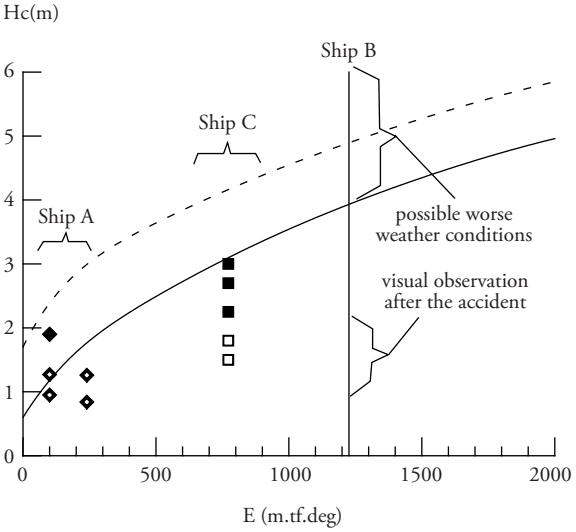

The vertical line represents the E value of the ship C in the loading conditions at the time of capsize.

Fig. 2. Relative deck wells volume for fishing vessels [13]

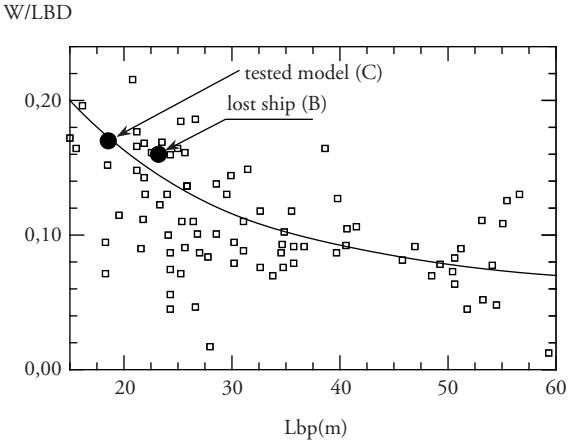

Quartering waves: The difference between quartering, following and beam waves was brought to the attention of the scientists by the paper of Grochowalsky [13] who stressed the fact that new phenomena can appear in quartering waves, so that this case cannot be simply discussed as a superposition of the other two.

The new phenomenon can be created when the bulwark and part of the deck become submerged during the dynamic motions of a ship in quartering breaking waves and can lead to the capsize of a ship otherwise considered safe. There is, indeed a strong difference in the hydrodynamics of water on deck with respect to that of bulwark/deck in water.

Among the many conclusions of these studies, the following are relevant to this paper:

- the light loading condition was more responsive to the wave, with greater tendency to riding, broaching and capsizing than the full load;
- the influence of forward speed is different in the two typical loading conditions. In light loading the increase of the forward speed facilitates surf riding, broaching and capsizing, whereas in full loading the increase of forward speed reduces the probability of water on deck and capsizing.

The examined casualties

Model "A". Ship "A" is a very small (12.4 L_{bp}) fishing vessel (Table. 1 and Fig. 3). The research, connected with a full scale capsizing with loss of a life while the vessel was reaching sheltered waters to escape a storm in the delta of river Po, was conducted in high waves on a 1:10 scale model equipped with instrumentation to measure roll motion. Several different loading conditions (Table. 2 and Figs 4-5), almost within the same displacement, realising centre of gravity values in the interval between the different IMO Intact Stability requests were tested in regular beam waves with steepness ranging from 1/30 to 1/10.

Fig. 3. Schematic view of the fishing vessel A

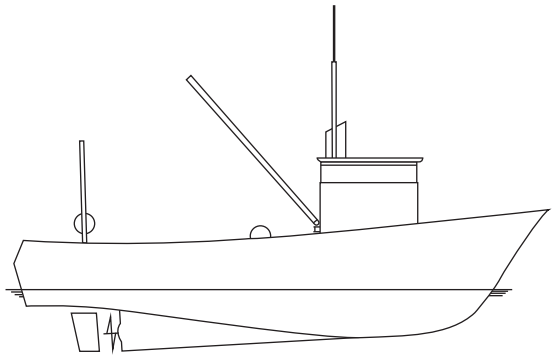

Fig. 4. Assumed metacentric height values for fishing vessel A. For comparison, the values satisfying the different requirements of Intact Stability are reported (numbering follows old Registro Italiano Navale rules):
- 4.4.5: General Stability Criterion;
- 4.4.9: Attenuation of previous for ships with less than 20 m in length;
- 4.5.2: Weather Criterion.

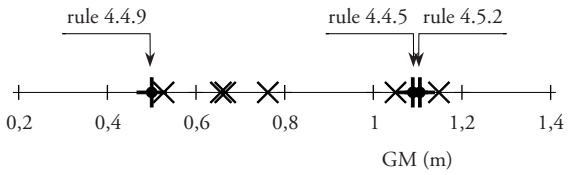

Fig. 5. Righting arm curves of the selected loading conditions for fishing vessel A. For comparison, the curves satisfying the different requirements of Intact Stability are reported (numbering follows Registro Italiano Navale rules).

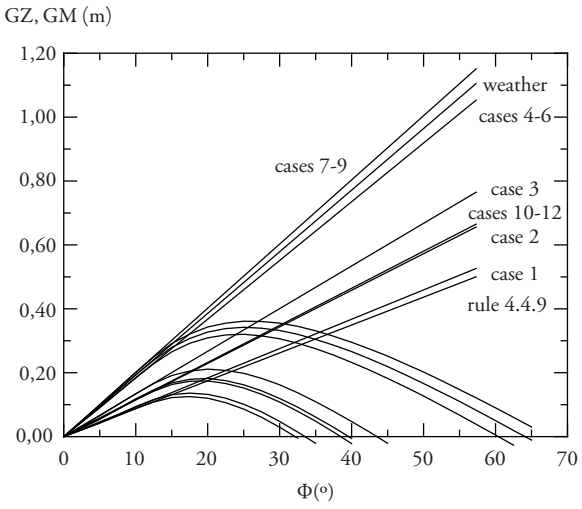

Table. 1. Principal dimensions of ship "A"

L_{BP}	12.400 m
B	4.200 m
D	2.600 m
T	1.600 m
L_{OA}	13.220 m

Table. 2. Tested loading conditions of ship "A"

Serie	Δ (t_f)	$\overline{GM}$(m)
1	24.194	0.527
2	23.764	0.656
3	23.689	0.762
4-5-6	23.689	1.050
7-8-8/1-9	23.689	1.148
10-11-12	24.530	0.666

The results of the experiments indicate that:

- the maximum roll amplitude is not very sensitive to the metacentric height. An explanation of the substantial independence of roll peak amplitude on initial stability was given [3] in terms of the mechanics of ship rolling by means of the analysis of a non-linear mathematical model with coefficients based on a least square fitting to the experimental results. The results indicated that the effective wave slope coefficient (coefficient "r") is largely overestimated in the original IMO formulation.
- on the contrary, water accumulation on deck is more sensitive to metacentric height and extension of positive stability range (Fig. 6). In several cases, water on deck resulted from the test. In particular, in the worse case, with some water on deck from a previous test, a capsizing by water accumulation was observed and recorded [1-3]. The relevant parameters of these cases were computed and reported in the diagram of critical wave height for surviving in beam waves. A good agreement with the threshold curve has been obtained.

Fig. 6. Maximum roll amplitude, maximum roll excursion and angle of vanishing static stability as a function of metacentric height for fishing vessel A.

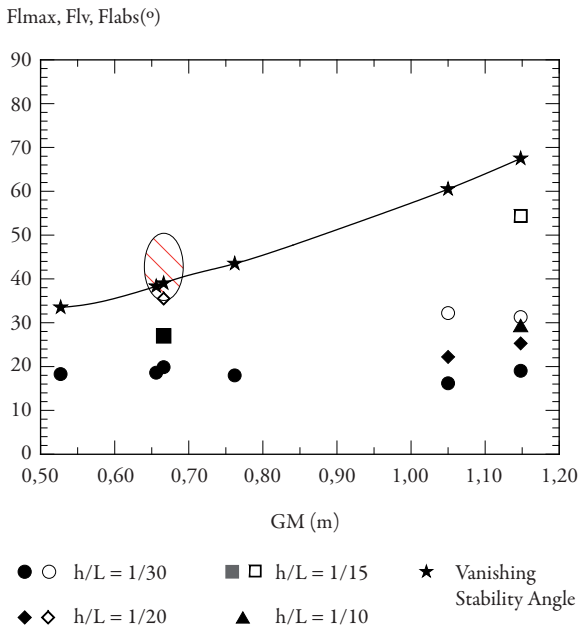

The vessel "B" and the model "C": The second ship (Ship "B", see Table.3 and Fig. 7) is a 23.2 m Lbp fishing vessel which was lost in the gulf of Napoli in very steep quartering waves also during the return to sheltered waters as a consequence of rapidly deteriorating weather conditions.

The presence of a witness allowed to reconstruct the casualty history in terms of roll motion and stability deterioration, trim and sinkage due to water on deck (and possible progressive flooding from the deck). The ship was in full load condition. From the description of the survivors, it results that the forward speed in breaking quartering waves was voluntarily reduced to a few knots due to bad weather. The sea condition during the sinking was described by a survivor as corresponding to sea state 3-4 with some exceptional waves. The official weather reports mention a sudden deterioration of weather and a maximum seastate 6-7.

Fig. 7. The fishing vessel "B"

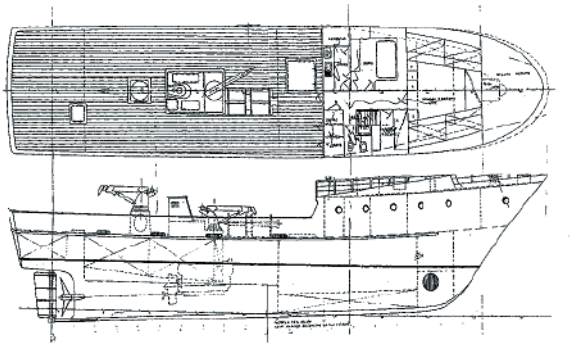

Table. 3. Main dimensions and loading conditions of vessel "B"

$\mathbf{L_{BP}}$	23.200 m
B	6.400 m
D	3.360 m
T	2.340 m
$\mathbf{L_{OA}}$	27.680
Δ	174.9 tf
GM	0.982 m

Although the capsizing happened in following/quartering conditions, in Fig. 1 the value of E corresponding to the loading condition is reported. An $H_C \approx 4$ m would have been sufficient to capsize the ship in beam waves. This wave height is not in contrast with the reports from the casualty, although in sheltered waters this probably could have been the characteristic of few exceptional breaking waves of a growing sea more than the property of a regular train of waves.

It was decided to obtain a better understanding of the possible mechanism of capsizing and of the role of breaking and less high waves by doing a series of experiments in towing tank. A 1:15 scale model (model "C" - Table. 4) of a vessel of similar typology already existing in the Towing Tank of the University of Trieste was ballasted to the required loading conditions and a bulwark was fitted to the deck edge. In the tested condition both the freeboard and the bulwark height above deck at stern were 0.900 m full scale. With this arrangement, the fishing vessel had a relative deck well as indicated in Fig. 2. The static effect of water on deck, as indicated in Fig. 8, computed in agreement with the indication of the Torremolinos Convention, clearly stress the risks connected with the overtopping of the bulwark by high waves.

Fig. 8. Application of the guidance on a method of calculation of the effect of water on deck for fishing vessel C [7, Regulation 32].

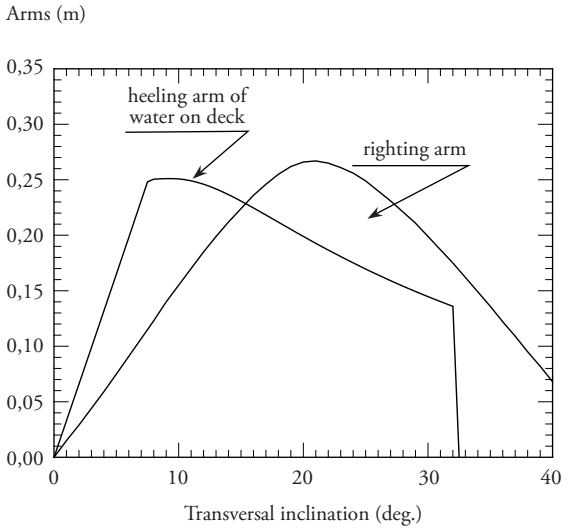

Several wavelengths and wave heights were tried in the following wave condition with the model completely free.

Table. 4 Main dimensions and loading conditions of vessel "C"

$\mathbf{L_{BP}}$	18.550 m
B	6.650 m
D	3.126 m
T	2.100
$\mathbf{L_{OA}}$	20.320
D	130.2 tf
GM	0.839 m

Apart from the model without anything on deck, three other configurations were tested:

- configuration with the nets on the aft part of the deck. The nets were simulated by folded fabric;
- configuration with some water pre-existing on deck. To simulate the effect

of a previous breaking wave some water (roughly 5-8% of the displacement or 12-20% of the deck well) was added on the stern part of the deck in coincidence with the first wave impact. This amount of water in the absence of waves produced a few degrees transversal inclination without immersing the deck edge;

- a combination of the two.

In most cases there was some water on deck, but in no case, in the range of the possible wave heights of this towing tank (3m full scale), the model capsized simply by wave action or due to the presence of the nets. On the contrary, in several cases it capsized in the configuration with water on deck and with water trapped in the nets, this last leading to a more sudden and frequent capsizing. The analysis allowed to identify the threshold in terms of the wave height for the capsizing. As is evident from Fig. 1 this mechanism identifies a strongly reduced resistance to waves once a breaking/high one has partly flooded the deck. It can explain also the disagreement between visual observations of wave height.

Several capsizing cases were observed as a consequence of bad manual steering of the model to avoid it grounding on the wave absorbing beach of the towing tank after the end of the useful train of waves. The model exhibited indeed a strong tendency to sail downwave at a full scale speed of about 4-5 kn. As a result of attempts to drive it, the model went readily with deck in water or transversal to the waves and capsized.

Conclusions

The importance of water on deck in capsizing of small, low built, large deck well, vessels in steep/high waves has been confirmed on the basis of experiments conducted following casualties at sea. All the experiments leading to capsize needed some water on deck pre-existent, at least in the range of wave heights/steepnesses tested. In particular, the possible stability degradation connected with water trapped on the nets appears relevant to the studies of ship safety. It appears also that some conclusions obtained in previous research, like the effect of forward speed on the probability of capsizing in different loading conditions should be brought to the attention of the masters, since casualty to ship B could also be connected with voluntary speed reduction. Finally, the critical wave height proposed by Dahle et al. [14] is confirmed for very small vessels in beam waves. It would be interesting to extend the present analysis to investigate the reliability of this limiting value, in higher waves than those tested in this paper, for the case of following/quartering waves. We have not to forget that the presently existing stability criterion for this ship typology and size is still based on statistics of casualties, while the most accredited stability criterion based on physical modeling, not applicable to fishing vessels of the investigated size, refers to a capsizing mechanism in beam wind and waves...

A final consideration concerns the freeing ports. This seems to be the major weakness of ordinary fishing vessel constructions: small ports to avoid fish leakage and often definitely locked by thick layers of painting.

References

[1] FRANCESCUTTO, A., CONTENTO, G., "Dynamic Effects of Sloshing of Water on Board a Fishing Vessel", Proceedings of the International Workshop on Fishing Vessel Technology (Umeda, N., Editor), Publ. Nat. Res. Inst. of Fish. Eng. Hasaki, Japan, 1997, N. 6, pp. 58-71.

[2] FRANCESCUTTO, A., CONTENTO, G., "A Case Study of the Stability of a Small Fishing Vessel in Waves", Proc. 2nd International Conference on Marine Industry MARIND'98, P. A. Bogdanov Ed., Varna, Bulgaria, Vol. 1, pp. 127-132, 1998.

[3] D'ESTE, F., FRANCESCUTTO, A., "Experimental Study of the Dynamic Stability of a Small Fishing Vessel", Proceedings 1st International European Inland Waterway Navigation Conference - EWIN'99,

Balatonfured, Hungary, 9-11 June, 1999, pp. 106-114.

[4] BOCCADAMO, G., FRANCESCUTTO, A., RUSSO KRAUSS, G., SCAMARDELLA, A., "An Accident Investigation: Lessons Learning for Enhancing Safety of Fishing Vessels", Proceedings 1st International Congress on Maritime Transport, Barcelona, November 2001, pp. 687-698.

[5] BULIAN, G., FRANCESCUTTO, A., "Safety and Operability of Fishing Vessels in Beam and Longitudinal Waves", International Journal of Small Craft Technology (Trans. Royal Institution Naval Architects Vol. 148, Part B2), 2006, pp. 1-15.

[6] Tripartite Meeting on Safety and Health in Fishing Industry, Note on the Proceedings, International Labour Organization, Geneva, 1999.

[7] 1993 Torremolinos Protocol and Torremolinos International Convention for the Safety of Fishing Vessels, Consolidated Edition 1995, IMO, London.

[8] European Directive 97/70/CE setting up a harmonised safety regime for fishing vessels of 24 metres in length and over, 11 December 1997.

[9] "Revised FAO/ILO/IMO Code of Safety for Fishermen and Fishing Vessels, Part B", IMO document MSC 79/23/Add.3. See also "Voluntary Guidelines for the Design, Construction and Equipment of Small Fishing Vessels", 2005, IMO Document MSC 79/23/Add.2, 2004.

[10] "Safety of Small Fishing Vessels - Consolidated text of the draft Safety recommendations for decked fishing vessels of less than 12 meters in length and undecked fishing vessels", Submitted by the Secretariat, IMO Document SLF 51/5, 2007.

[11] SEVASTIANOV, N. B., "Practical and Scientific Aspects of the Stability Problem for Small Fishing Vessels", Proc. RINA Int. Conf. on Design Considerations for Small Craft, London, 1984.

[12] DAHLE, E. A., MYRHAUG, D., DAHL, S.J., "Probability of Capsizing in Steep and High Waves from the Side in Open Sea and Coastal Waters", Ocean Engng., Vol. 15, 1988, pp. 139-151.

[13] GROCHOWALSKI, S., "Investigation into the Physics of Ship Capsizing by Combined Captive and Free-Running Model Tests", Transactions SNAME, Vol. 97, 1989, pp. 169-212.

[14] UMEDA, N., RENILSON, M. R., "Broaching of a Fishing Vessel in Following and Quartering Seas", Proceedings of the 5th International Conference on Stability of Ships and Ocean Vehicles, 1994, Vol.3, pp. 115-132.

[15] NEVES, M.A.S., PÉREZ, N.A. AND VALERIO, L. "Stability of small fishing vessels in longitudinal waves", Ocean Engineering, Vol. 26 1999, pp. 1389–1419.

Integrating topology and shape optimization: a way to reduce weight in structural ship design

Metodología para Optimización Topológica y de Forma de Elementos Estructurales

Germán A. Méndez Algarra,[a]
Andrés Tovar Pérez, Ph.D.[b]

Abstract

The Hybrid Cellular Automaton (HCA) algorithm is a methodology developed to simulate the process of functional adaptation in bones. The HCA algorithm combines elements of the cellular automaton (CA) paradigm with finite element analysis. This methodology has proved to be computationally efficient to solve topology optimization problems. In this paper, the HCA algorithm is integrated with a shape optimization algorithm that uses sequential quadratic programming. The geometry of the topologically optimized structure is converted into a two-dimensional solid model using an edge detection algorithm and parametric B-splines. An example problem of a Michell structure is presented. Also shown is the application of the shape optimization algorithm in the redesign of the lightening holes in the transverse floors of a riverine patrol vessel designed by COTECMAR. In both cases an appreciable weight reduction was obtained.

Key words: Computational structural design, Topology optimization, Shape optimization

Resumen

El método de los Autómatas Celulares Híbridos (HCA) para optimización topológica simula el proceso de adaptación funcional en estructuras óseas. El método HCA combina la técnica de los elementos finitos para análisis estructural con el paradigma de los Autómatas celulares (CA) para el diseño y ha demostrado ser una técnica efectiva para optimización topológica en estructuras continuas. En este trabajo se integra el método HCA con un algoritmo de optimización de forma que utiliza programación cuadrática secuencial. La geometría optimizada topológicamente es utilizada para construir un modelo bidimensional sólido aplicando un algoritmo de detección de bordes en imágenes y esplines paramétricos. Un ejemplo de una estructura Michell es presentado. También es presentada la aplicación de un algoritmo de optimización de forma en el diseño de unos aligeramientos en las varengas de un buque patrullero fluvial diseñado por COTECMAR. En ambos casos una apreciable reducción del peso fue obtenida.

Palabras claves: Diseño de estructuras, optimización topológica, optimización de forma

[a] Department of Mechanical and Mechatronic Engineering,
National University of Colombia
e-mail: gamendeza@unal.edu.co

[b] Department of Mechanical and Mechatronic Engineering,
National University of Colombia
e-mail: atovarp@unal.edu.co

Introduction

Optimization techniques applied to the structural design can provide the maximum benefit from the available resources. Adopting optimal design procedures converts the process of design into a sequence of rational decisions, while the indirect design is based in experience, creativity and random ideas of the design team. Two of the main fields of application for the structural optimization are the topology and the shape optimization techniques. Several works have been published, showing applications of these methods in different engineering fields [8, 13, 14, 18].

The goal of topology optimization is to find the optimal distribution of material in a finite volume. This maximizes a determined measure of mechanical performance under determined constraints [17]. The topology optimization algorithm selectively removes and relocates the material until optimal performance is reached [22]. However, this approach to structural optimization has some disadvantages. The resultant structure tends to present non-smooth edges, due to the design domain discretization [16]. Furthermore, it is common to find zones with relatively high stress in the resulting edges, with the potential to be improved [19].

In shape optimization the goal is to find the optimum profile for the structure components, while maximizing the performance under a given set of mechanical constraints [5]. This kind of optimization problems is very common in several fields of engineering; like electromagnetism, biomechanics, structural design and fluid-structure interaction applications [7, 11, 12]. There are different approaches to deal with a structural shape optimization problem. For the structural evaluation of the designs, the finite element and the boundary element methods are very popular. Nevertheless, there are proposals that intend to exceed the performance of these traditional methods [24]. The most employed approaches for the solution of the shape optimization problem are the basis vector and the shape perturbation methods [21].
This work intends to present a rational design methodology which integrates the Hybrid Cellular Automata method for topology optimization, (HCA) [20], with a shape optimization algorithm based on the shape perturbation approach, which applies the finite element method and uses Sequential Quadratic Programming (SQP) to solve the optimization problem.

To integrate effectively the topology and the shape optimization methods, an edge detection algorithm is used in conjuction with parametric B-splines modelling on the topologically optimized structure [3]. The resulting solid model is used as the initial design for the shape optimization algorithm.

Topology optimization using the Hybrid Cellular Automaton method

The Hybrid Cellular Automaton (HCA) method is intended to solve complex structural optimization problems in engineering. The premise of the HCA method is that complex static and dynamic problems can be decomposed into a set of simple local rules that operate over a large number of cellular automata (CAs) that only know local conditions [22]. The cellular automaton neighborhood has no size or location restraints, except for its being defined in the same way for all of the CAs. This is an idealization of a physical system in which space and time are discrete. Therefore, the computation of the local evolutionary rules can benefit from parallel computing capacity [20].

In the HCA method, the design variables for the algorithm correspond to the relative densities of each automata. The elastic modulus of an element E_i is expressed as a function of the relative density x_i as

$$\rho_i = x_i \cdot \rho_0 \quad (1)$$

$$E_i = x_i^p \cdot E_0 \quad (2)$$

where E_0 and ρ_0 are the elastic modulus and density of the solid material, respectively, r_i is a variable density. The power p is used as a penalization for intermediate relative densities, accordingly, helping to make the resultant design a black and white structure.

Along with the design variables, the state of each CA is determined by state variables y_i. This variables are expressed as

$$y_i = \frac{u_i}{x_i} \tag{3}$$

where u_i is the contribution of each element to the strain energy of the structure. The values of the state variables are determined using the Finite Element Method on each iteration of the algorithm.

The HCA algorithm solves a constrained optimization problem given by

$$\begin{aligned} \min_{\vec{x}} \quad & \omega \frac{U(\vec{x})}{U_0} + (1-\omega)\frac{M(\vec{x})}{M_0} \\ s.t. \quad & M/M_0 < m_f \\ & u_{\max} < u^* \\ & \sigma_{\max} < \sigma_Y \\ & 0 \le \vec{x} \le 1 \end{aligned} \tag{4}$$

where $U(\vec{x})$ is the total strain energy, $M(\vec{x})$ is the mass of the structure and ω is a weight coefficient. The first constraint specifies the available mass to be used in the design. The second and third constraints impose limits on the resulting structural displacements and stresses. Finally, the design variables fluctuate between the boundaries 0 and 1. Actually, the lower limit is not 0 but a small positive value, to avoid the singularity in the stiffness matrix during the finite element analisys.

The HCA topology optimization algorithm, as shown in Fig. 1, can be described as follows. First, the design domain is defined, along with the physical properties of the material, load conditions and initial design. The analysis of stresses and displacements using the finite element method determines the values of the state variables. The value for the design variables is updated according to the local evolution rule $\vec{x}_{(t+1)}=R(\vec{x}_{(t)},\vec{y}_{(t)})$. Then, the algorithm returns to the second step for the evaluation of the state variables. The convergence criterion is satisfied when there is no variation in the design variables, or when the maximum number of iterations is reached.

Fig. 1. HCA algorithm flow chart

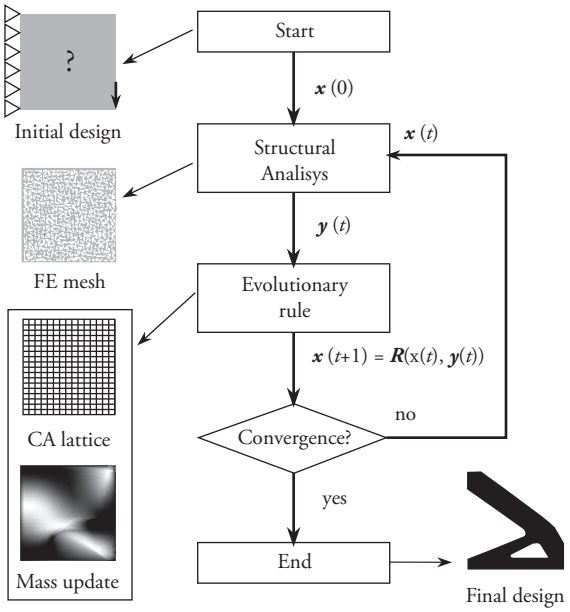

Shape optimization

Shape optimization for structural design aims to find the optimal profile or boundaries of a structure that minimizes certain objective function under specified mechanical constraints. The basis vector method and the shape perturbation method are the most common approaches to solve shape optimization problems [21].

In the basis vector approach, the shape of the structure is described by a combination of different trial designs called 'basis vectors'. The design variables are the weighting parameters that define the participation of each basis vector in the design process.

On the other hand, the shape perturbation approach requires the definition of perturbation vectors. These vectors deform the boundary of the initial design domain. The design variables are constituted by the components of the perturbation vectors, which determine the amount of perturbation during the optimization process [9].

This work makes use of the grid perturbation approach. Therefore, since this work focuses on two

dimensional domains, the design variables vector is composed by two perturbation values associated with each node in the model [1].

The shape optimization problem with nonlinear constraints can be expressed as

$$\begin{aligned} \min_{\vec{x}} \quad & F(\vec{x}) \\ s.t. \quad & g_1(\vec{x}) = \vec{d}_N \leq \vec{d} \\ & g_2(\vec{x}) = \sigma_{VM} \leq \sigma_Y \end{aligned} \tag{5}$$

where $\vec{x}$ is the design variables vector, $\vec{d}_N$ is the vector with the magnitude of the displacement for each node, and σ_{VM} is the maximum value of von Mises stress in the model. To solve this optimization problem the sequential quadratic programming (SQP) approach is employed.

Design variables

The horizontal and vertical coordinates that define the location of the *i*th node of the model, u_i and v_i respectively, are defined by

$$\begin{aligned} u_i &= u_{0i} + du_i \\ v_i &= v_{0i} + dv_i \end{aligned} \tag{6}$$

where u_{0i} and v_{0i} are the coordinates of the ith node on the initial design, and du_i and dv_i are, respectively, the horizontal and vertical perturbation on the same node. The design variables vector can be written as

$$\vec{x} = \begin{bmatrix} x_1 & x_2 & \cdots & x_{2n-1} & x_{2n} \end{bmatrix} \tag{7}$$

where $x_{2i-1}=du_i$, and $x_{2i}=dv_i$, for $i=1,2,\ldots, n$; with n being equal to the number of non-restrained nodes in the model. It follows that during the construction of the design variables vector it is necessary to define an adequate objective for the final shape.

Objective function

In order to obtain the desired complement between the topology optimization and the shape optimization algorithms, it is necessary an adequate definition of the objective for the last one. The shape optimization method developed for this work uses the weight of the structure as objective function. In the two-dimensional domain this function can be expressed as

$$F(\vec{x}) = \int_\Omega \rho \, dV = \rho \cdot t \cdot \int_\Omega dA \tag{8}$$

where t is the thickness of the element and ρ is the material's density.

The objective function requires the calculation of the area contained by each contour, then, the values for the interior loops are subtracted from the exterior contour. Thus, the objective function takes the form of

$$F(\vec{x}) = \rho \cdot t \cdot \left[\int_{\Omega ext} dA - \sum \left(\int_{\Omega \text{ int}} dA \right) \right] \tag{9}$$

Displacement constraint

The displacement constraint is imposed in order to maintain the geometric validity of the model. This constraint can be expressed as

$$d_i(\vec{x}) > \sqrt{x_{2i-1}^2 + x_{2i}^2}, \tag{10}$$

where

$$d_i(\vec{x}) = \min \left(\sqrt{(u_i - u_j)^2 + (v_i - v_j)^2} \right), \quad j \neq i, \tag{11}$$

and u_i and v_i are, respectively, the horizontal and vertical coordinates of the i^{th} node. The application of this constraint can significantly affect the performance of the optimization algorithm if a high number of nodes are used to describe the design boundaries.

Stress constraint

In order to maintain the required consistency between the topology and the shape optimization method, a stress constraint is imposed. This guarantees that the design is stiff enough to endure the load. The failure criterion used in this case is von Mises, due to its conservative results

and simplicity of implementation. The von Mises criterion for ductile materials undergoing a general state of stress is defined as

$$(\sigma_a - \sigma_b)^2 + (\sigma_b - \sigma_c)^2 + (\sigma_c - \sigma_a)^2 < 2\sigma_Y^2 . \quad (12)$$

This can be seen as the volume contained in a cylinder with radius $\sqrt{2/3}\sigma_y$ with a symmetry axe forming equal angles with the principal stress axes. This expression, for materials under plane stress, is reduced to

$$\sigma_a^2 - \sigma_a\sigma_b + \sigma_b^2 < \sigma_Y^2 \quad (13)$$

which represents the area of a rotated ellipse Fig. 2. The evaluation of this constraint requires a finite element analysis of the plane stress model on each iteration. The maximum Von Mises stress found in the model is compared with the permissible stress established for the problem. The allowable stress can be the yield stress for the material or can include a design safety factor.

Fig. 2. Von Mises criterion for two dimensions

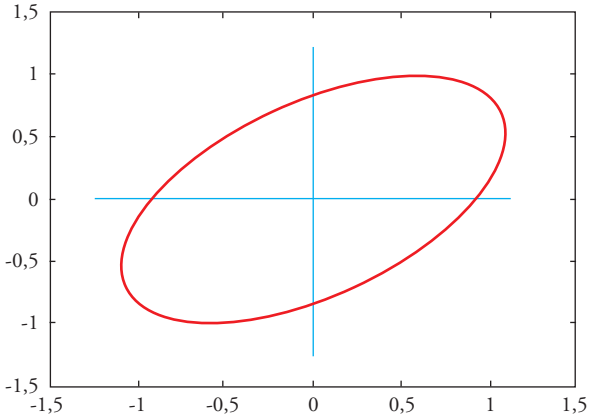

Integration of topology and shape optimization

In order to achieve the integration of the topology (TO) and shape optimization (SO) algorithms, it is necessary to apply an intermediate processing. The idea is to convert the result of the TO into a valid model usable as the initial design for the SO [23].

The result of the execution of the topology optimization algorithm is a matrix with the values of the relative densities of the cellular automata. A grayscale image that describes the shape of the structure can be obtained by using the design variables results as intensity values. Ideally a black-and-white image will be obtained; however, it is common to obtain some automata with intermediate relative density values.

In this image, one pixel corresponds to one cellular automaton. In consequence, the resolution of the image depends on the number of automata selected for the topology optimization algorithm. Therefore, the smoothness of the contours varies according to the discretization of the design domain, as shown in Fig. 3.

Fig. 3. Topology optimization results for a design domain of (a) 44x22 and (b) 80x40 cellular automata

Fig. 3a

Fig. 3b

An edge detection algorithm is applied to the image obtained using the topology optimization. The Canny method for edge detection, considered the optimal method for edge detection on digital images [6], is used.

The edge detection process reduces the information contained in the image, preserving the main structural properties [10]. The application of the Canny method to the image shown in Fig. 3a results in the image of the edges as seen in the Fig. 4.

Fig. 4. Canny's edge detection results

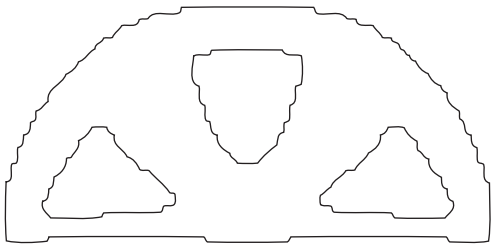

The next step to obtain the initial design for the shape optimization algorithm is to create a b-spline model for each contour in the image. By means of this, the contours of the model are smoothed [3].

At this point, the density of control points for the b-spline modeling is established . This parameter for the node density, K_F, sets the percentage of points on the edge image preserved as a node for the b-splines, and is expressed as

$$K_F = \frac{N_n}{P_d}, \qquad (14)$$

where N_n is the number of nodes in the b-spline model and P_d is the quantity of black pixels in the image obtained with the edge detector.

Since every node has two perturbation values associated as design variables in the grid perturbation method used in the shape optimization algorithm, this parameter directly determines the number of design variables for the shape optimization problem. Moreover, the density of control points is important in the definition of the displacement constraints and, consequently, an inadequate value can affect the performance of the algorithm.

Once the contours are modeled as b-splines, a solid model is generated by the subtraction of the interior portions from the exterior part. At this point the geometric model of the initial design is complete. The remaining step is to translate the boundary conditions of the problem (loads and restraints) to the corresponding nodes in this geometric model.

Application example

To illustrate the performance of the integrated methodology, the design of a two-dimensional Michell-type structure is considered [15]. The design domain has an area of 800 · 400 mm^2 with a thickness of 20 mm. The displacement of the left lower corner is restrained in both directions and the displacement of the opposite lower corner is constrained in the vertical direction. The design domain is discretized into 80 · 40 identical cellular automata. The properties of A-36 steel are used, and a vertical load of 5000 N is applied in the middle of the lower border, Fig. 5.

Defining the mass constraint limit to $M/M_0<0.40$, the HCA algorithm converges in 24 iterations to the result displayed in the Fig. 6.

Fig. 5. Design domain for a Michell-type structure

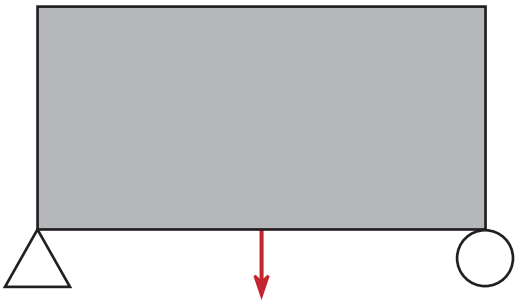

Fig. 6. Topology optimized structure with $M/M_0<0.4$

The application of the method to construct the shape optimization initial design, given the node density parameter a value of $K=0.04$, produces the model shown in Fig. 7. After the shape optimization process, a 4.47% reduction in weight is achieved. The algorithm converged, after 13 iterations, to the shapes presented in Fig. 8.

Fig. 7. Initial design for the shape optimization process

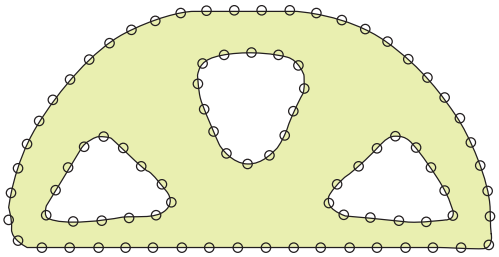

Fig. 8. Optimized shape of the Michell-type structure

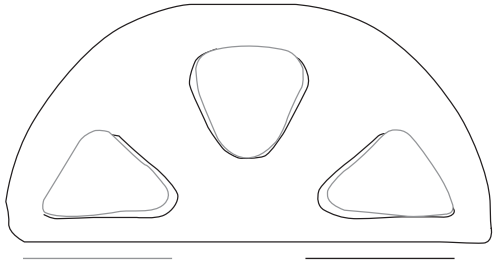

Shape optimization of structural floors in the PAFL

As an application of the shape optimization algorithm developed for this work, the reshape of the transverse floors in the parallel body of the riverine patrol vessel (PAFL for its Spanish acronym), designed by COTECMAR, the Science and Technology Corporation for the Naval, Maritime and Riverine Industries, is considered (see Fig. 9).

Initially, these elements were designed following the ABS Rules for building steel vessels for service on rivers [2]. As the operational profile of the ship requires a very low draft, the structural weight minimization is a primary objective for the next unit. The use of a documented direct calculus method, like the shape optimization presented here, enables the design to exceed the limits of the Classification Society rules.

The initial design for the shape optimization problem is extracted from the arrangement obtained applying the ABS Rules. The load condition includes the buoyancy pressure on the hull and, on the upper edge, the pressure from the maximum liquid column in case of damage to the compartment immediately above, as shown in the Fig. 10. The material used for the element is naval steel ASTM A131 [4].

Fig. 9. Riverine patrol vessel PAFL hull structure

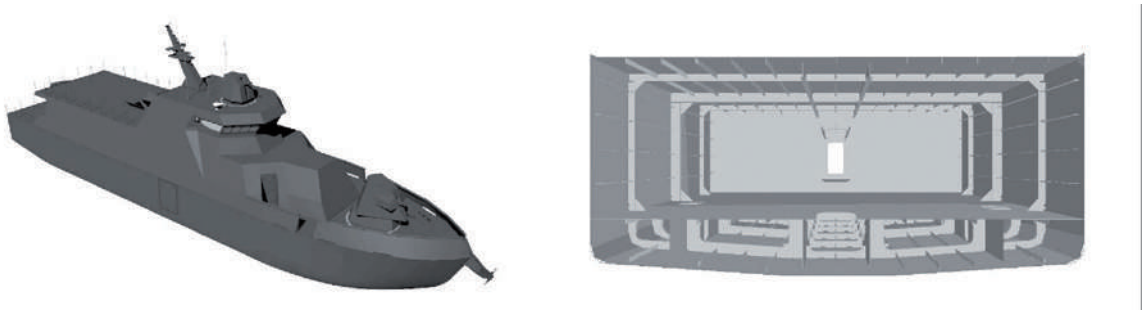

Fig. 10. Free body diagram of the structural floor

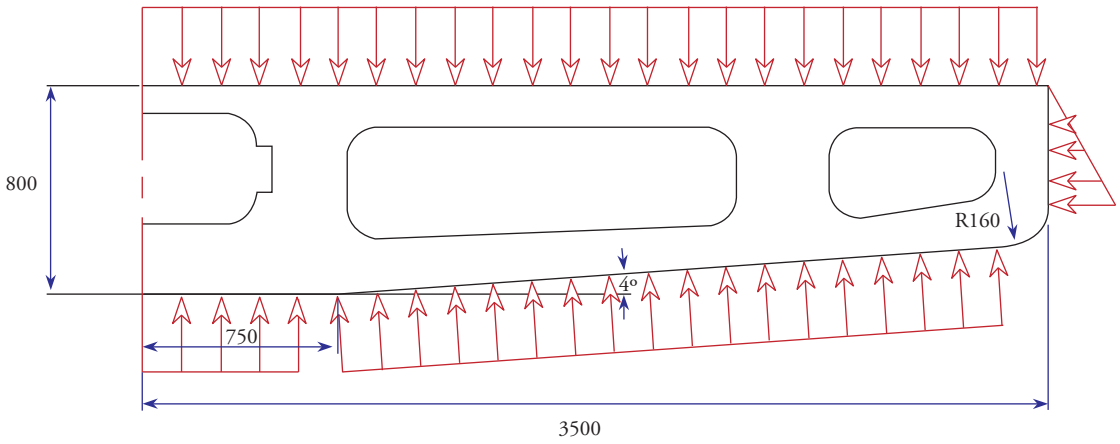

Fig. 11. Initial design for the shape optimization of the lightening holes

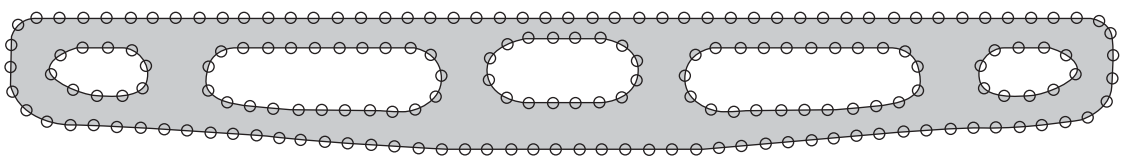

Fig. 11 shows the b-spline model of the initial design. Since the hull and inner bottom forms cannot be altered, the perturbation of the shape is only possible in the interior boundaries. The load condition is introduced as nodal loads in the bottom and tank top edges. The displacements for the extreme nodes in the inner bottom are restrained.

Table 1 shows the shape optimization problem parameters used for the reshape of the transverse floors.

The convergence criterion for this problem is satisfied when no change occurs in the objective function, which means that

$$\Delta F_t(\vec{x}) = F_t(\vec{x}) - F_{t-1}(\vec{x}) \approx 0 . \qquad (14)$$

Table 1. Shape optimization parameters

Shape optimization parameters		
Parameter	**Symbol**	**Value**
Number of nodes	n	187
Design variables	nv	164
Elasticity modulus	E	210 GPa.
Poisson's ratio	n_0	0,3

After 24 iterations, convergence is obtained to an objective function value of 15947 mm^2, equivalent to a 4.21 % reduction in weight of the structure. The objective function values and the final shape are shown in the Fig. 12.

Figure 12. Objective function vs. iteration number.

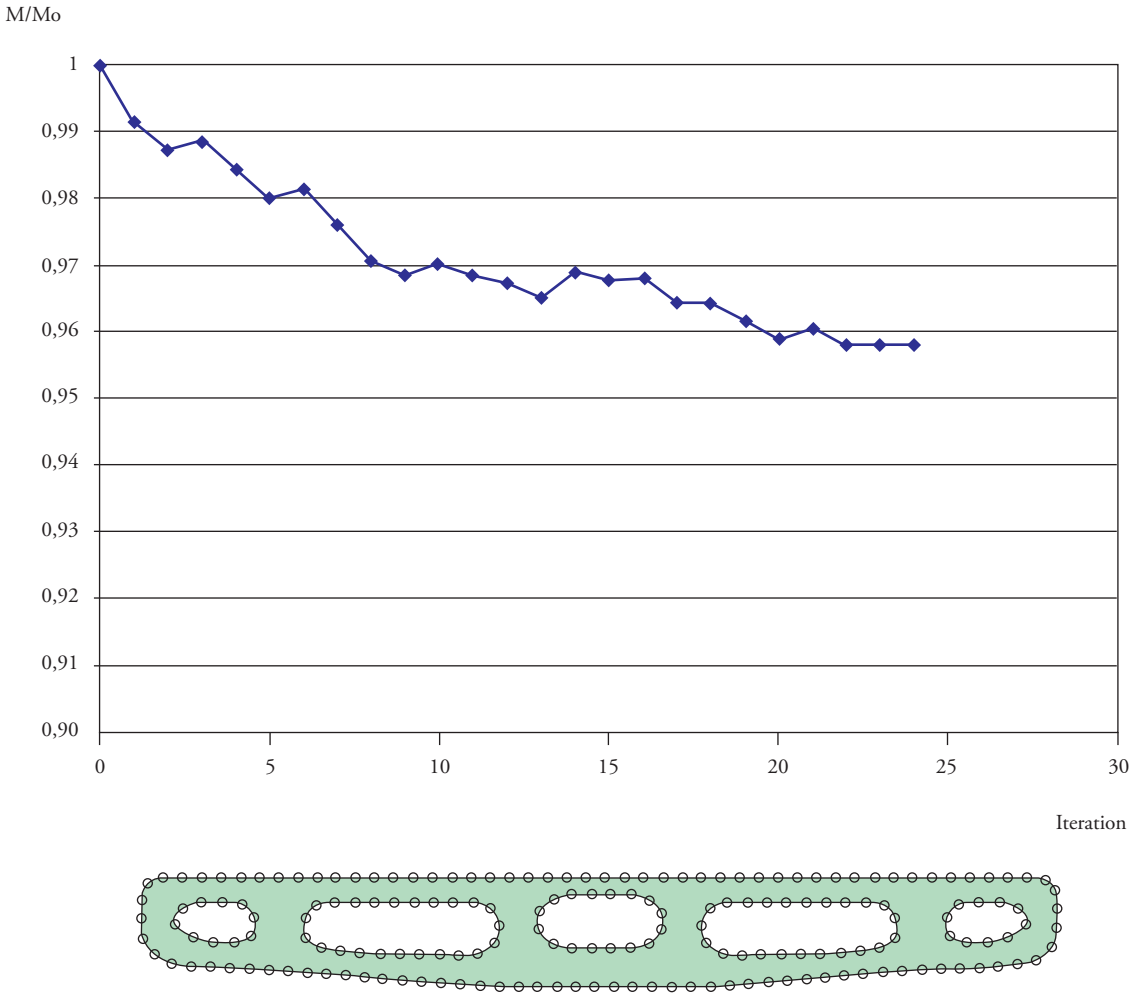

Conclusions

This first attempt for the integration of the Hybrid Cellular Automata method with a shape optimization algorithm constitutes a tool for structural design with applications in several fields of engineering. The design tool is particularly useful in applications where the reduction of weight is an upmost objective. The addition of the shape optimization algorithm, in conjunction with the edge smoothing, improves the weight reduction.

The use of this methodology in early stages of the design process of river vessels, where reduced draft is of primary importance, enables an appreciable reduction in the weight in some of the main structural components. Current work focuses in the refinement of the shape optimization algorithm and the exploration of other types of approaches, like evolutionary methods.

For each design case, the node density in the construction of the initial design for the shape optimization method must be selected with caution. The compromise between the desired level of detail and the computational cost must be considered and the sensibility of the results to the variation of this parameter is a subject of current analysis.

Further work will include the extension of the topology optimization to the design of plate structural members of ships, like the transverse floor shown in the example. This will include the constraints in the design domain that take account of the hull shape.

Acknowledgements

The authors would like to thank the Science and Technology Corporation for the Naval, Maritime and Riverine Industries, COTECMAR, for the support and assistance in this project. We also thank the anonymous referee for the detailed review of our paper and the important comments provided.

References

[1] ALLAIRE, G. *Shape Optimization By the Homogenization Method*. Springer, 2001.

[2] AMERICAN BUREAU OF SHIPPING,. *Rules for building and classing. Steel vessels for service on rivers and intracoastal waterways*. ABS, 2007.

[3] ANNICCHIARICO, W., AND CERROLAZA, M. Finite elements, genetic algorithms and beta-splines: a combined technique for shape optimization. *Finite Elements in Analysis and Design 33* (1999), 125–141.

[4] ASTM STANDARD A 131/A 131M 2004,. *Standard Specification for Structural Steel for Ships*. ASTM, DOI: 10.1520/A0131_A0131M-04, www.astm.org, 2004.

[5] BENDSOE, M. P. Optimal shape design as a material distribution problem. *Structural and Multidisciplinary Optimization 1* (1989), 193–202.

[6] CANNY, J. A computational approach to edge detection. PAMI 8 (1986), 679–698.

[7] CEA, J., GARREAU, S., GUILLAURME, P., AND MASMOUDI, M. The shape and topological optimizations connection. *Computer Methods in Applied Mechanics and Engineering 188* (2000), 713–726.

[8] CHIANDUSSI, G., GAVIGLIO, I., AND IBBA, A. Topology optimization of an automotive component without final volume constraint specification. *Advances in Engineering Software 35* (2004), 609–617.

[9] GIVOLI, D., AND DEMCHENKO, T. A boundary-perturbation finite element approach for shape optimization. *International Journal for Numerical Methods in Engineering 47* (2000), 801–819.

[10] GONZALEZ, R., AND WOODS, R. *Digital Image Processing*. Prentice Hall, 2002.

[11] HÄUßLER, P. Topology and shape optimization methods for cfd problems. In *CADFEM Users' Meeting*, Fellbach (2006).

[12] KEGL, M., AND BRANK, B. Shape optimization of truss-stiffened shell structures with variable thickness. *Computer Methods in Applied Mechanics and Engineering 195* (2006), 2611–2634.

[13] MACHADO, G., AND TRABUCHO, L. Some results in topology optimization applied biomechanics. *Computers & Structures 82* (2004), 1389–1397.

[14] MACKERLE, J. Topology and shape optimization of structures using fem and bem. a bibliography (1999 - 2001). *Finite Elements in Analysis and Design 39* (2003), 243–253.

[15] MICHELL, A. The limits of economy of material in frame-structures. *Philosophical Magazine 8* (1904), 589–597.

[16] PEREIRA, J., FANCELLO, E., AND BARCELLOS, C. Topology optimization of continuum structures with material failure constraints. *Structural and Multidisciplinary Optimization 26* (2004), 50–66.

[17] ROZVANY, G. Aims, scope, methods, history and unified terminology of computer aided topology optimization in structural mechanics. *Structural and Multidisciplinary Optimization 21* (2001), 90–108.

[18] SIGMUND, O., AND TORQUATO, S. Design of materials with extreme thermal expansion using a three-phase topology optimization method. *Journal of the Mechanics and Physics of Solids 45* (1997), 1037–1067.

[19] TANG, P., AND CHANG, K. Integration of topology and shape optimization for design of structural components. *Structural and Multidisciplinary Optimization 22* (2001), 65–82.

[20] TOVAR, A. Optimización topológica con la técnica de los autómatas celulares híbridos. *Rev Int Mét Num Cálc Dis Ing 21* (2005), 365–383.

[21] TOVAR, A., GANO, S., MASON, J., AND RENAUD, J. Optimum design of an interbody implant for lumbar spine fixation. *Advances in Engineering Software 36* (2005), 634–642.

[22] TOVAR, A., PATEL, N., NIEBUR, G., SEN, M., AND RENAUD, J. Topology optimization using a hybrid cellular automaton method with local control rules. *Journal of Mechanical Design 128* (2006), 1205–1216.

[23] YILDIZ, A., ÖZTÜRK, N., KAYA, N., AND ÖZTÜRK, F. Integrated optimal topology design and shape optimization using neural networks. *Structural and Multidisciplinary Optimization 25* (2003), 251–260.

[24] ZHANG, X., RAYASAM, M., AND SUBBARAYAN, G. A meshless, compositional approach to shape optimal design. *Computer Methods in Applied Mechanics and Engineering 196* (2007), 2130–2146.

Disposal and Recycling of HSC Materials

Manejo y reciclaje de materiales HSC

Henning Gramann[a],
Reinhard Krapp,
Volker Bertram

Abstract

The introduction gives an overview of current IMO activities concerning the disposal of ships at the end of their life-cycle and an overview of composite materials applications in ships. After a brief discussion of relatively unproblematic aluminum alloys, the article focuses on problems for composite materials. There is little experience for end of life treatment of composites in general and in the shipbuilding industry in particular. New legislation might regulate handling and disposal of these materials even further. The article identifies existing solutions as well as open questions.

Key words: Environment, recycling, composite, high-speed craft

Resumen

La introducción presenta un panorama de las actividades de la IMO relacionadas con el manejo de buques al final de su vida útil y de las aplicaciones de materiales compuestos en embarcaciones. Tras una breve discusión acerca de las aleaciones de aluminio que no presenta gran problema, el trabajo se enfoca en los problemas que presentan los materiales compuestos. Existe poca experiencia con el manejo de materiales compuestos al término de su vida útil en general y en la industria naval en particular. El manejo y eliminación de estos materiales podría ser regulado aún más por nuevas normas. Este artículo identifica las soluciones existentes así como preguntas actualmente sin respuesta.

Palabras claves: Medio ambiente, reciclaje, materiales compuestos, embarcaciones de alta velocidad

[a] Germanischer Lloyd, Hamburg/Germany,

e-mail: Henning Gramann (henning.gramann@gl-group.com); Reinhard Krapp (reinhard.krapp@gl-group.com);
Volker Bertram (volker.bertram@gl-group.com)

Introduction

Relevant IMO activities

The future IMO Convention on Ship Recycling focuses on safe and environmentally sound ship recycling, without compromising the operational safety and efficiency of ships. The whole life-cycle of ships is addressed, including dismantling and recycling or disposal of ships taking into account all materials contained. The convention requires for all ships above 500 GT a compendium of detailed information related to installed materials, which must be kept up-to-date during the entire operating life of a ship. In addition to this, the proper handling (including occupational health and safety, as well as environmental protection measures during dismantling of the materials at the ship recycling facilities) is a key issue of the convention and therefore will have to undergo a comprehensive certification process as well.

The core of the above mentioned convention affecting building and operation of ships will be the Part 1 of the "inventory of hazardous materials" (IHM), which is analogous to a Hazardous Materials blueprint. With this IHM, the location of hazardous materials contained in equipment and structure of the ship shall be easily determined. The basis for the IHM is the so called "Single List", which is a summary of materials which are considered to be potentially hazardous. The Single List consists of four tables, of which Table A and Table B are relevant for the IHM in the building and operational phase of the ship, see Table I.

For preparation of the IHM, all necessary information should be requested during the design and construction phase of a ship by the building yard, and during new installation of components on board existing ships by the owner or yard, depending on contractual arrangements. Manufacturers and suppliers must check all used components, equipment and coating systems against these two tables and provide this information to the shipyard. The shipyard collects this information and summarizes it in the ship specific IHM, which after delivery has to be kept up-to-date permanently. This will become part of shipboard tasks throughout the operating life of the ship. The updated IHM will be reviewed during inspections and prior to delivery to a recycling facility. Existing ships will also have to comply, but the IHM will be prepared by experts and cover materials of Table A only.

The transition to this future ship recycling and disposal management involves several challenges. *Gramann et al.* (2007) focus on 'administrative' aspects, namely the necessary IT (information technology) support for creating and maintaining data bases with inventories of materials on board ships. We will focus here on the special challenges that high-speed craft (HSC) pose due to the different nature of the material mix usually found in these vessels.

Relevant ISO activities

ISO is developing its 30.000 series for "ship recycling management systems", which will set up international requirements for certain aspects related to ship recycling. In particular these standards will define "safe and environmentally sound ship recycling facilities", best practice for ship recycling facilities, guidelines for selection of ship recyclers including a pro form contract; set out the requirements for bodies providing audit and certification, and the standard on information control for hazardous materials in the manufacturing chain of shipbuilding and ship operations. It has not been decided whether the ISO 30.000 will also include guidelines on surveying of ships for hazardous materials, minimum amount or content of hazardous materials to be reported, or on methods for removal of asbestos.

An industry standard like the ISO 30.000 series shall positively affect the strategies for the interim period until the IMO convention enters into force, providing a common voluntary standard outside of legally binding regime. ISO 30.000 may contribute also to successful implementation and compliance with the future IMO convention. It may provide unified standards and more guidance to all stakeholders involved than any legal instrument can provide. The main focus is on shipbuilding and the recycling preparations and processes. The standard

Table 1. Tables A and B of the Single List of IMO

No.	Materials		Legislation	Threshold Level	Proposed Threshold Level
A-1	Asbestos		SOLAS	Not Provided	0 ppm
A-2	Polychlorinated Biphenyls (PCBs)		Stockholm Convention	50 ppm	50 ppm
A-3	Ozone Depleting Substances	CFCs	MARPOL, Montreal Protocol	Not Provided	0 ppm
		Halons			
		Other fully halogenated CFCs-			
		Carbon Tetrachloride			
		1.1.1- Trichloroethane (Methylchloroform)			
		Hydrochlorofluorocarbons			
		Hydrobromofluorocarbons			
		Methylbromide			
		Bromochloromethane			
A-4	Organotin compouds	Tributyl Tins	AFS Convention	2500 ppm	2500 ppm
		Triphenyl Tins			
		Tributyl Tin Oxide (TBTO)			

No.	Materials	Legislation	Threshold Level	Proposed Threshold Level
B-1	Cadmium and Cadmium Compounds	RoHS (2002/95/EC), ELV (2000/53/EC)	100 ppm	100 ppm
B-2	Hexavalent Chromium Compounds		1000 ppm	1000 ppm
B-3	Lead and Lead Compounds		1000 ppm	1000 ppm
B-4	Mercury and Mercury Compounds		1000 ppm	1000 ppm
B-5	Polybrominated Biphenyl (PBBs)	RoHS (2002/95/EC)	1000 mg/kg	1000 mg/kg
B-6	Polybrominated Dephenyl Ethers (PBDEs)		1000 mg/kg	1000 mg/kg
B-7	Polychloronaphthalanes (more than 3 chlorine atoms)	Japanese Law	Not provided	0 ppm
B-8	Radioactive Substances	96/29 EURA TOM	Becquerel	No threshold
B-9	Certain Shortchain Chlorinated Paraffins (Alkanes, C10-C13, chloro)	AFS Convention	1,00%	1%

can be applied to all ships and all facilities, without any size limits and independently from the recycling countries ratification. Therefore more facilities can fall under a unified standard than what is possible under the future IMO convention. However, the basis for the ongoing development is that nothing will contradict the IMO requirements.

HSC materials

Lightweight construction is essential for HSC, having a decisive influence on displacement, draft and thus power consumption for given speed. Lightweight construction is also frequently chosen for superstructures of other ships (like passenger ships or naval vessels) due to stability constraints. Frequently, aluminum and composite materials (like fiber-reinforced plastics (FRP)) are chosen as materials to reduce weight in critical structures, *Fach and Rothe (2000), Fach (2002)*.

Aluminum alloys of the 5000 series (AlMg alloys) and the 6000 series (AlMgSi alloys) are commonly used for fast lightweight ships, Fig.1 and Fig.2. The 5000 series alloys are more corrosion resistant in the marine environment and therefore primarily employed for plates of the shell, decks and built-up girders. The 6000 series alloys are easier to extrude and therefore frequently used for extruded sections, but being less resistant to corrosion they are generally restricted to internal structures, *Bryce (2005)*. Both series alloys feature good weldability.

Fig.1. Aluminum catamaran

Fig. 2. Aluminum funnel block

FRP and other composites are used in assorted applications, Figs.3 to 6:

- For hulls in short vessels (pleasure craft, small navy craft, life boats, etc.)
- In naval vessels, for integrated masts, hangars, etc. for stealth and weight reasons, *Beauchamps and Bertram (2006)*.
- In propulsion: propeller shafts, propellers, rudders, etc.
- In equipment and outfitting: boat davits, furniture, deck gratings, deckhouses, insulation

Composites have been proposed also for ship repair. Plastics are found in a variety of small structures on board ships (cables, fixings, etc.).

There is a variety of different FRP materials, due to assorted combinations of reinforcement material (fibers), laminating resins and core material:

- For reinforcement, generally glass, carbon and aramide fibers are used. More recently, natural fibers have been advocated, also within the context of recycling properties, *Umair (2006)*. Carbon and aramide fibers have high tensile strength. The fibers are available in the form of rovings, mats, fabrics and non-woven fabrics and combinations of these. These materials allow tailor-made non-isotropic strength properties (depending on fiber orientation), but also quasi-isotropic behavior achieved by the respective laminate construction.
- The main laminating resins used are polyester, vinyl-ester and epoxy resins. Vinyl-ester and epoxy resins are highly resistant to hydrolysis, i.e. they absorb insignificant amounts of water and the risk of osmosis is practically excluded.

Sandwich structures are more or less complex mixtures of materials. These structures consist of a face material and a core, bonded together by a putty or adhesive bond (typically polyester). The faces mainly support the tensile and compressive stresses of the sandwich in bending, and the core material mainly supports the shear stresses. Face materials may be metal or composites like carbon fiber composites. Core materials available for sandwich

Fig. 3. FRP in superstructure of 33 m HSC yacht

Fig.4. Composite louver

Source: www.ebertcomposites.com

Fig.5. Carbon-fiber laminate propeller shafts

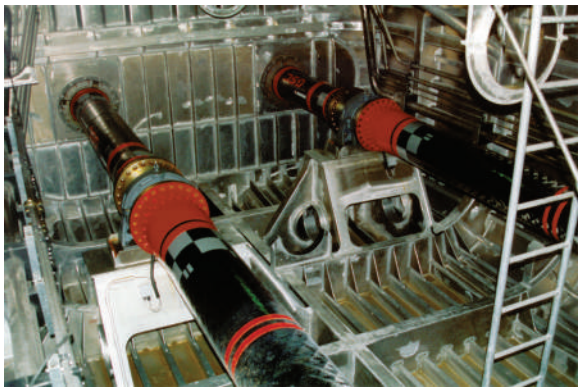

Fig.6: Contur® propeller of AIR Fertigung-Technologie GmbH

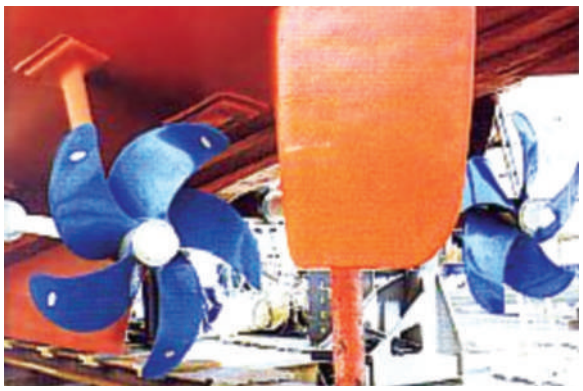

laminates are generally PVC foams, polyurethane (PUR) foams, polymethacryl (PMI) foams, balsa wood and honeycombs (thin aluminum or stainless steel plate honeycombs) as well as aramide paper (Nomex honeycomb). PUR foams are rarely used, *Müller (1990)*. See also *Umair (2006)* for a more detailed review of composites used in engineering particularly in shipbuilding. *Hedlund-Aström et al. (2005)* give composite mass data for the Swedish Visby class corvette. The ship contains 50 t carbon fibers, 40 t vinylester as matrix filler, 40 t of core material in sandwich structures (mixture of PVC and polymer of poly-urea/polyamid), 20 t of putty material (mainly polyester).

Sandwich structures in ships may contain assorted metallic inserts and embedded equipment. They may also contain hazardous materials. For example, the Visby class corvette sandwich structures contain 9 t of chlorine and 0.4 t of lead in the core material, in addition copper oxide in the bottom color and copper in the embedded electrical devices, *Hedlund-Aström et al. (2005)*. When chlorine is heated (e.g. during cutting operations), hydrochloric acid and dioxin is formed. Lead and copper affect health when consumed in food or drinks.

Recycling facilities specialize mainly in metal recovery. However, ships contain a multitude of materials, including composites. Composite materials are relatively young compared to the traditional metallic structural materials. Consequently, there is little experience in the industry on disposal and recycling techniques for these materials. However, increasing environmental demands from customers (navies) and authorities will force the industry to face this issue. While hazardous materials are at present the first priority problem to be solved, composite recycling and disposal will definitely be an issue for IMO regulations in the future.

In addition, recycling of FRP boats is an issue. These boats are not subject to IMO regulations and usually also outside direct class supervision. *Hayashi (1993)* estimates 30000 FRP boats built each year in Japan alone. Since disposal of these boats at the end of their life-cycle is expensive (estimated to exceed 940 Euro per boat just for the mechanical crushing, and more than 1250 Euro per boat when transport costs are included), illegal disposal of FRP boats along rivers, canals and in ports is a problem.

Traditionally, the most economical end-of-life options for composites were landfill disposal and waste incineration. However, since 2004, landfill disposal of composites has been forbidden in most European Union (EU) member states. Incineration of plastics is problematic due to the toxic byproducts. The EU End-of-Life Vehicle directive, adopted in 2003, requires 95% of each vehicle manufactured after January 2015 must be reused or recovered. These political constraints drive the dynamic evolution of a composite recycling industry. Naval architects can benefit from practice in other industries that have extensive experience with composites, namely the automotive and the aerospace industries. "Recycling and disposal of composites create issues that must be addressed. One such issue concerns end-of-life aircraft structures that contain carbon fiber composites coated with hexavalent chromium primer. These composites that are coated with hexavalent chromium can be classified as hazardous waste and thus may not be disposed on land due to possible leaching of the chrome into the ground.", *N.N. (2003)*. Indeed, the cost to dispose of a hazardous waste can be more than 20 times the disposal cost of a non-hazardous solid waste in EU. Thus, materials should be disassembled and sorted to reduce those parts containing hazardous substances to a minimum.

Recycling and disposal

General considerations

The following waste hierarchy is suggested for waste management:

- **Reuse or product recycling:** The product is kept in its shape, dismantled and reused, sometimes after an upgrade involving energy input and additional new material. For composite structures, this could mean cutting large (flat) panels from the hull structure to be reused in other structures. Problematic paint coatings need to be removed by sand blasting or affected parts of the structure are not reused. Reuse means material continuing to circulate. It is then important to have control on hazardous materials contained. Only part of the structure can be reused. The remaining part must then be treated according to one of the following methods.
- **Material recycling:** Composite recycling efforts in the past mainly concerned grinding, shearing, chipping, or flaking the composite into suitable size to be used as filler material in new molded composite parts, e.g. as filler mixing with cement or forming plates similar to plywood.
- **Chemical recycling:** The waste is decomposed into its original raw materials or directly transformed into other petrochemical raw materials. The waste is generally first mechanically crushed to increase the material surface. This results in a higher efficiency of the chemical process. Technically viable processes for composites are pyrolysis, hydrolysis and gasification. Pyrolysis is most frequently discussed. In pyrolysis, the polymeric component is thermally decomposed into smaller hydrocarbon molecules, which can be used as fuel. Remaining material (fibers, metallic parts) are then further recycled. Pyrolysis keeps thus fibers largely unbroken. However, this pyrolysis is expensive and only practicable to a certain plate size. Hydrolysis is used e.g. for PVC cores in sandwich panels. At present, none of the chemical recycling options are economically viable for commonly used glass fiber composites in the marine industry.
- **Energy recovery:** The waste is incinerated in appropriate installation recovering energy. The option depends on the caloric value of the waste. A threshold value higher than 11 MJ/kg is required in Europe to allow incineration for energy recovery. Carbon and aramide

fiber composites are well above this level, many glass fiber composites are below this level. Mixing with other material to increase the caloric value is not allowed. For carbon fiber composites, proper precautions must be taken to avoid the release of small fibers into the environment that may cause electrical interference problems, *N.N. (2003)*.

- **Disposal:** Waste may be disposed in waste incineration plants or landfills. Disposal of high-caloric waste in landfills is forbidden in the European community since 2005.

The capability to sort dissimilar materials, composites from metals, is the first step in recycling composites. Composites should be sorted by different reinforcement and filler/matrix materials. The composition of the composites determines the further processing. More valuable carbon reinforced composites, for example, will be recycled extracting the carbon fibers, while glass fiber reinforced composites may still end up in landfills (in some countries).

Aluminum

Aluminum is often called a material of perfect recyclability since the secondary metal is recovered using only 3% of the energy consumed in the production of virgin metal by electrochemical purification, www.world-aluminium.org. Practical aluminum alloys, however, include various additives such as silicon, iron, copper, manganese, magnesium, zinc, etc. Accordingly, while recycling of scrap has progressed considerably with cast products which allow a large amount of additives, rolled and shaped products which permit only a small amount of additives have been manufactured preferably from raw materials rather than recycling products. Research is active to extend also the recycling of aluminum alloys into rolled and shaped products. For the shipbuilding industry, the approach is straight-forward. The aluminum alloys in the ship structure are on record, disassembly follows standard procedures, and after sorting the different alloys, the aluminum alloy parts can be recycled in dedicated recycling facilities. The value of the scrap depends on a number of factors. Coated plates require additional processing prior to recycling and this reduces the amount paid for this scrap.

Glass-fiber composites

Glass fiber composites are the most popular composites in the boat industry. While glass can be easily recycled, the recyclate is not commercially viable due to the already low price for virgin material.

Some glass fiber composites (with lower glass fiber content) have enough caloric value to be used in energetic recycling. The main benefit is heat which may be used for district heat, steam generation, electricity generation or directly in chemical, steel or cement plants. Additional byproducts are gypsum and slag with a high content of molten glass. These are widely used in construction materials, e.g. concrete and aerated concrete. Slag without glass content may need further processing to remove hazardous substances, slag with glass content usually is unproblematic as the hazardous substances are bound in the glass. In addition to gypsum and slag, considerable amounts of ash are created. The disposal of this ash (typically in landfills) is expensive. In summary, energetic recycling of glass fiber composites is problematic due to their low caloric value and the large amount of residual ash.

At present, there are no economically viable options for chemical recycling of glass fiber composites, although it is technically feasible, as shown e.g. by *Hayashi and Yamane (1998)* for FRP boats.

In mechanical recycling, the recyclate is mainly used as filler material. Recycling glass fiber composites in Sheet Moulding Compounds (SMC) and Bulk Moulding Compounds (BMC) has been successful. These techniques allow relatively high degrees of recycled composite materials as filler, but involve high pressures and high temperature. Applications include electrical equipment, car components (headlights), and housings for electrical appliances. Recyclates have been used also for outdoor construction materials, e.g. for road cover, road markers and insulation panels. However, the amount of waste from glass fiber

composites exceeds so far largely the demand in recycling products with the applications found so far.

Fig.7a. Building material from recycled composites. Glass foam plates

Fig.7b. Building material from recycled composites. Gypsum blocks

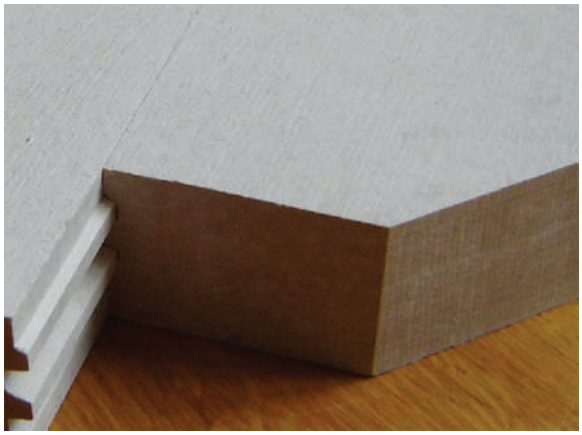

Fig.7c. Building material from recycled composites. Headlight

Glass fiber composites with high polyester content (60% unsaturated polyester) can be used in the cement industry. Process complications appear with the glass fibers blocking filters and dust generation requiring good filters for work place protection. Otherwise this application appears attractive as it leaves almost no residues, but it requires a large constant supply for the production plant. An estimated 10000 to 20000 t/a will be needed as supply.

Carbon-fiber composites

Carbon-fiber composites offer more attractive options for recycling. Acid digestion could be used to reclaim the carbon fibers, but appears to be impractical from an environmental point of view. Acid digestion uses hazardous chemicals and creates a mixture that will require further processing. Adherent Technologies Inc. (ATI), www.adherenttech.com, have been successful in separating carbon fibers from carbon fiber-reinforced epoxy composites and reclaiming valuable carbon fibers, Fig.8 and Fig.9, *N.N. (2003).*

Fig.8. Reclaimed carbon fibers, *N.N. (2003)*

Fig.9. Microscopic view of reclaimed carbon fibers, 99.8% pure, *N.N. (2003)*

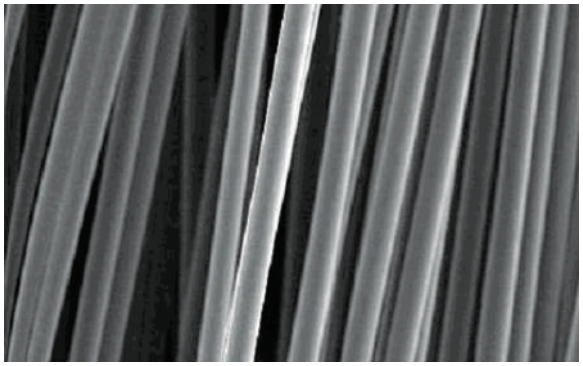

ATI employs catalytic conversion to recycle composites. Catalytic conversion produces chemicals or fuels from scrap or waste products. By-products generated include phenolic compounds used in certain adhesives. The reclaimed carbon fibers have very similar properties to virgin fibers, but are shorter. Reclaimed carbon fibers cannot be reused in applications requiring longer, continuous carbon fibers. However, the demand for chopped and milled carbon fiber is growing. Applications for such recycled carbon fibers are for example housings of cellular phones and laptop computers. "Methods exist today by which carbon fibers and prepregs can be recycled, and the resulting recyclate retains up to 90 percent of the fibers' mechanical properties. In some cases, the method enhances the electrical properties of the recyclate because the carbon recyclate can deliver performance near to or superior to virgin material. All that remains is to create demand for recycled fiber by packaging it in a form useful to end-users," *Davidson (2006)*. In summary, once the carbon fiber composite has been singled out and sorted, recycling is possible by dedicated facilities.

Sandwich panels

Before cutting composite or sandwich structures, embedded electrical equipment and metallic inserts as well as the content and nature of hazardous material need to be known. The position of metallic parts is indicated in technical drawings. Hazardous content and position will have to be documented, according to the current draft convention from IMO.

The processes of dismantling and further mechanical preparation for recycling (like crushing and milling) involve potential health risks due to exposure to dust, smoke, gas, sharp fibers and other sharp material parts, and noise. For example, hydrochloric acid and isocyanates are generated when heating the PVC core in sandwich structures. These risks can be contained through proper workplace and personal protection, as regulated by national occupational health and safety regulations, but implementation throughout the ship recycling processes might remain difficult due to different circumstances (climate conditions, accessibility and additional need of space when wearing or carrying personal protection equipment, etc.).

Hedlund-Aström et al. (2005) discuss the various options for recycling and disposal of sandwich structures in ships:

- Reuse: Cutting large panels from the hull structure allows reusing sandwich material. Hazardous material bound in the core may be safe to cut and transport, but authorities like environmental agencies should be consulted. Metallic equipment or inserts not removed during disassembly are either dismantled or cut away during cutting to final size.
- Mechanical material recycling: Milling the complete sandwich has been applied to a sandwich structure consisting of a face of glass-fiber reinforced polyester and Divinycell core, *Hedlund-Aström and Olsson (1997)*. The recycled sandwich mixture was blended with polyurethane. Plates similar to plywood or chipboard were manufactured through expansion in a form.
- Recycling by pyrolysis and hydrolysis were discussed. While technically feasible, they do not appear to be economically viable options.

Disassembly

There are various ways to cut composites during disassembly:

- Mechanical cutting with power saws or other cutting tools, Fig.10. The generated dust may in most cases require appropriate protection for the workers. The tools are cheap and can be portable.
- Water-jet cutting which is another form of purely mechanical cutting using a jet of water at high velocity and pressure, or a mixture of water and an abrasive substance, Fig.11. The process is essentially the same as water erosion found in nature but accelerated and concentrated by orders of magnitude, able to cut thin metals and composites. The technology is used in aerospace and other industries. The advantage is that there is no heat and no chemical process involved. Portable water-jet cutters are available on the market.

Fig.10. Mechanical cutting of boat hull

Source: www.slashbuster.com

Fig.11. Water-jet cutting

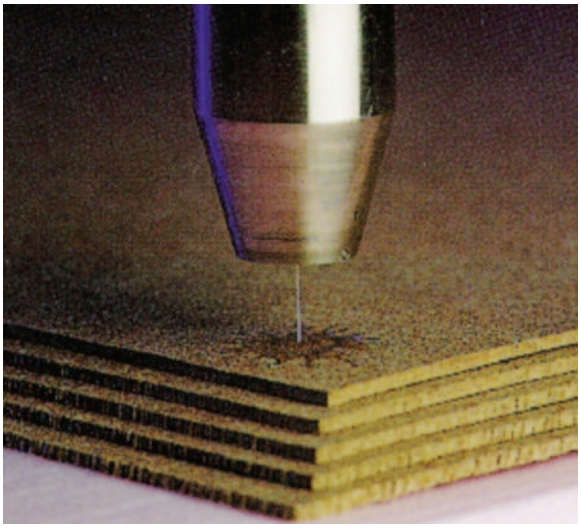

Source: wikipedia

- Thermal cutting using oxy-acetylene; this method is frequently used for cutting steel structures in ships. The approach is problematic for most composites due to potential toxic by-products in burning plastics.
- Plasma cutting; the cutting is usually performed under water reducing dust and fumes problems, but installation are not always portable and relatively expensive, though cheaper then laser cutting. The cutting speed is relatively low compared to thermal cutting, which is an important factor for cost effective ship dismantling.
- Laser cutting; the heat is highly focused reducing health hazards, but installations are expensive and not portable.

Problems to address

Identification of material

To maximize the recovery of material and generate the best financial return, the materials must be efficiently sorted before post-processing. A significant concern in recycling and disposal is the proper identification of various materials in ships to be scrapped, and how to sort and recycle this mix.

Recycling companies must know what they shall recycle. It could be a basic epoxy matrix composite, or it could be a brominated resin matrix, with all the associated toxic complications. At present, no sophisticated and reliable knowledge/experience exists. In newbuildings, this could be documented from the start in a material database. In the large fleet of existing ships of different age, we will be commonly faced with information gaps concerning the material composition.

Just before disassembly, material samples can be taken and analyzed. However, this type of destructive testing is usually not an option while the ship is still in service. Non-destructive testing of composites is subject to research, e.g. at the Fraunhofer research centers in Germany, and is expected to drift into industry practice in due time.

An example may illustrate the scope of work needed in compiling the variety of multi-layered composites found in modern ships. The example shows extracts of the files for the cruise vessel AIDA Diva: The deck structures use sandwich panels similar in structure to those of the walls. These panels consist of stone wool as core material and zinc plates as covers, lacquered or covered by foils. The files do not give the thickness of the cover plates; the density of the core material is 130 to 150 kg/m^3. Decks, hull and bulkheads are equipped with insulation against noise, fire and heat. This insulation consists mainly of mineral wool (stone, glass). The floor of the Captain's Cabin 1001 is equipped with a fire-resistant insulating floor of type A 60. This floor insulation is labeled Tefrolith M. Furthermore, there is a layer below the carpet labeled IMO Lay.

Product alternatives

The automotive industry has investigated composites based on natural organic materials (cellulose, sisal, jute, hemp, etc.) as alternatives to classical glass or carbon fiber composites, *Marek et al. (2000)*. These reinforcements are reusable, good insulator of heat and sound, degradable and cheap. They are less fire resistant and their quality varies naturally more, moisture may cause fibers to swell and price may fluctuate according to yield of crop. Despite these shortcomings, natural fiber composites are expected to see wide use in the automotive industry, due to their light weight compared to glass fibers and their recycling properties. Little is known about natural fiber composites in the shipbuilding industry. The moisture problem and uncertainties about the long-term behavior of natural fiber composites make them unlikely candidates for the marine industry.

Markets and logistics

Energy recovery is at present not a viable option for the popular glass-fiber composites. However, it is technically feasible. *Hayashi and Yamane (1998)* present for example a movable disposal system for FRP boats. The movable system, installed on two trailers, reduces transportation costs and allows decentralized service. The system is set up to incinerate most boats at original size, avoiding the pre-processing cost of crushing. The resulting stone-like solid with high silicone content are compact and can be used as stone pavement, cement, or core material for various insulation material. However, although a prototype was presented 10 years ago, the idea failed due to economic aspects. Considerable process improvement to reduce cost or subsidies would be required to change this.

The industry needs a network of specialized recycling facilities for composite structures. The decommission shipyard will typically focus on breaking the ship apart, sorting and channeling the individual items and materials for further processing by dedicated subcontractors or buyers. The task of the shipyard in this respect is identifying the composite, disassembling to the appropriate level using the appropriate technology, sorting and seeing that it gets to the appropriate dedicated specialist. While networks for more traditional materials like metals are established in shipbuilding, networks for composites still need to evolve. The relatively small amount of composite material processed in shipbuilding industry necessitates using networks and facilities developed by related industries (aeronautical, automotive, mechanical engineering).

Dissemination

Training and dissemination of knowledge concerning the problems and procedures will be a key issue for the transition of the industry towards a life-cycle management approach, particularly for the less familiar and more problematic materials in shipbuilding, like composites. Disposal and recycling add aspects for consideration already in the design stage. Besides aspects like 'Design for production', 'Design for operation' and 'Design for maintenance', we should then train engineers to consider aspects of 'Design for recycling', *Lamb (2003). Marek et al. (2000)* recommend considering two fundamental aspects for 'Design for recycling',

- Structural design (Is the item easy to disassemble?)
- Material selection (Can materials difficult to recycle be replaced by alternatives easy to recycle?)

VDI (2002) discusses Design for Recycling in more detail, drawing on experience for diverse mass production industries in Germany. Generally applicable guidelines for Design for Recycling are:

- Avoid problematic materials
  Regulated or restricted materials may require expensive disposal at the end of the life-cycle. Materials incompatible for recycling will have to be separated at considerable expense. Painting of parts generally contaminates parts. For composites, it is often preferable to use colored plastic resin.
- Use 'Design for recycling' materials
  Wherever possible, use recycled material and use recyclable material. In composite structures, use compatible adhesive bonding to allow recycling. Suitable combinations

may be found in discussion with experts for adhesives. Use materials which can be recycled as a mixture.
- Reduce complexity
  Reduce the number of material types used.
- Make disassembly and sorting easy
  Use route wiring. Use modular design. Make components of different recyclable material easy to separate. Mark plastic parts according to standards, *ISO (2000)*, and in a way that allows the marking to be read even after 30 years in a maritime environment.

Many of the general guidelines coincide with advice given for Design for Production.

Landamore et al. (2007) show how assessing the disposal costs in the design stage may influence material selection, applying life cycle cost analysis to inland leisure craft.

Conclusion

Unless markets for recycled composites materials evolve, the options for certain composite materials at the end of the life-cycle are limited:

- Export of this 'problematic' waste to countries with more lenient legislation. However, there are efforts to restrict this export both on national level of developing countries and on international level. It may not be a long-term option.
- Incineration or landfill with special permit and subject to a fee or tax.

As a consequence, these composites may then reduce the value of a decommissioned ship.

Acknowledgements

Many colleagues have supported this paper with their special expertise, supplying text and/or figures, namely André Fuhrmann, Saskia Greiner, Shinya Hayashi, and Thomas Korbel.

References

BEAUCHAMPS, B.; BERTRAM, V. (2006), *Quo vadis, navy – Trends for future high-performance naval platforms*, 5th Conf. High-Performance Marine Vehicles (HIPER), Launcerston, pp.364-373

BRYCE, R. (2005), *Recycling high speed ferries and ideas for the future*, RINA Conf. Recycling of Ships and Other Marine Structures, London, pp.107-114

DAVIDSON, J. (2006), *Carbon fiber composite recycling – An industry perspective*, Composites World, http://www.compositesworld.com/hpc/issues/2006/September/1410

FACH, K. (2002), *High Speed Craft in service*, 3rd Conf. High-Performance Marine Vehicles (HIPER), Bergen, pp.145-152

FACH, K.; ROTHE, F. (2000), *Classification experience with lightweight ship structures*, RINA Conf. Lightweight Construction Latest Developments, London

FUHRMANN, A.; GREINER, S.; KORBEL, T. (2007), *Entsorgung von Faserverbundwerkstoffen und Einsatz der Rezyklate*, Report for MaVeFa, Hochschule Bremen (in German)
http://www.faserverbund-verwertung.de/mavefa.php?site=mavefa

GRAMANN, H.; KÖPKE, M.; FLÜGGE, M.; GRAFE, W. (2007), *Data management for better ship-care and recycling*, 6th Conf. Computer and IT Applications in the Maritime Industries (COMPIT), Cortona, pp.33-41

HAYASHI, S.; YAMANE, K. (1998), *Study on the development of the recycling technology of waste FRP boats*, Papers of Ship Research Institute 35(3) (in Japanese)

HAYASHI, S. (1989), *Floating disposal system for waste FRP boats*, 16th Joint Meeting UJNR Marine Facilities Panel, Washington, pp.115-122

HAYASHI, S.; YAMANE, K. (1994), *Development of movable disposal system for waste FRP boats*, 19th Joint Meeting UJNR Marine Facilities Panel, Tokyo, pp.224-231

HEDLUND-ÅSTRÖM, A.; LUTTROP, C.; REINHOLDSSON, P. (2005), *Environmentally friendly recycling of FRP-sandwich ship hulls*, RINA Conf. Recycling of Ships and Other Marine Structures, London, pp.119-126

HEDLUND-ÅSTRÖM, A.; OLSSON, K.A. (1997), *Recycling and LCA studies of FRP-sandwich structures*, 2nd North European Engineering and Science Conf. – Composites and Sandwich Structures, EMAS Ltd, Stockholm

IMO (2007a), *Recycling of ships – Draft guidelines for the development of the Inventory of hazardous materials*, MEPC 56/3/2

IMO (2007b), *Recycling of ships – Draft guidelines for the development of the Inventory of hazardous materials*, MEPC-ISRWG 2/2

IMO (2007c), *Ship recycling*, IMO guidelines for ship recycling, IMO-I685E

ISO (1996), *Plastics – Symbols and abbreviated terms*, ISO 1043:1996

ISO (2000), *Plastics – Generic identification and marking of plastic products*, ISO/DIS 11469:2000

LAMB, T. (2003), *Design/production integration*, Ch.14 in Ship Design and Construction (Ed. T. Lamb), SNAME

LANDAMORE, M.J.; BIRMINGHAM, R.W.; DOWNIE, M.J.; WRIGHT, P.N.H. (2007), *Sustainable technologies for inland leisure craft*, J. Eng. for the Maritime Environment 221/M3, pp.97-114

MAREK, A.; BOLZE, K.; JOACHIM, T.; JUNG, O.; WIDDECKE, H. (2000), *Recycling von Verbundwerkstoffen im Automobilbau*, Workshop Kunststoffrecycling im Automobilbau, Wolfsburg (in German)

MÜLLER, L. (1990), F*aserverstärkte Kunststoffe im Boots- und Schiffbau*, Handbuch der Werften XX, Hansa-Verlag Hamburg (in German)

N.N. (2003), *Composite recycling and disposal* – An environmental R&D issue, Boeing Environmental Technotes 8/4

UMAIR, S. (2006), *Environmental impacts of fiber composite materials – Study of life cycle assessment of materials used for ship superstructure*, Master Thesis, Royal Institute of Technology, Stockholm

VDI (2002), *Recyclingorientierte Produktentwicklung (Recycling oriented product development)*, VDI Guideline 2243, VDI-Verlag

Accreditation of Hydrodynamic Channels in use in Naval Modeling

Acreditación de Canales Hidrodinámicos de Uso en Modelación Naval

Jorge Freiria[a]

Abstract

This work considers a Quality System applied to a specific environment, the Hydrodynamic Towing Tanks or Channels, following the International Towing Tank Conference (ITTC) guidelines, gathered in turn from the international regulations, and it focuses the assessment of uncertainty in the experimental outcomes from the hydrodynamic tests called Test to resistance, as well as in determining which of the variables are those that have greater incidence on the mentioned outcomes.

Key words: Ship resistance, uncertainty evaluation, hydrodynamic tests

Resumen

En este trabajo se considera un Sistema de Calidad aplicado a un entorno específico, los Canales o Tanques de Ensayos Hidrodinámicos, siguiendo las directrices de la International Towing Tank Conference (ITTC), recogidas a su vez de la normativa internacional, y se centra en la evaluación de las incertidumbres en los resultados experimentales del ensayo hidrodinámico que se denomina Ensayo de Resistencia al Avance, y en la determinación de cuales variables son las que tienen mayor incidencia en dichos resultados.

Palabras claves: Buques, resistencia, incertidumbres, ensayos

[a] Facultad de Ingeniería Instituto de Mecánica de los Fluidos e Ingeniería Ambiental
e-mail: jfreiria@fing.edu.uy

Introduction

Research with physical models begins to be developed as a scientific instrument starting from the dimensional analysis theoretical development. Lord Rayleigh's studies are the Pi theorem conceptual basis, which credit is done to E. Buckingham in 1914, (White, 1999). This way, the solution to hydraulic problems begins to be approached through its physical modeling to reduced scale. One of these problems, perhaps one of the most important problems of those times, given the fact that the economies of the nations depended upon the exchange of commodities by means of maritime transportation, was the decrease of resistance on the ships hulls.

William Froude was a pioneer in the fluid mechanics, applied to the determination and the reduction of this resistance. Froude realized the practical need of separating the resistance in components from different nature, developing the procedure which makes compatible the physical modeling with the dynamic similarity. In 1868 he published his paper "Comparison Law" establishing that the ratio between the ship's residual resistance (due mainly to the waves formation) of similar dimensions were equal to the cube of the ratio of the linear dimensions, if their velocities were in an inverse ratio of the square root of their magnitudes. The need of knowing the frictional resistance or of viscous origin made him carry out research using flat plates completely submerged, finding an empirical formulation which permitted the development of the modeling and extrapolation of results to the prototype methodology (Todd 1967), with the construction of a test channel considered as being today's existing installations forerunner.

The introduction of computing tools in the fluid mechanics field has generated a substantial change in the simulation of runoff phenomena in general, and in particular in the fluids associated to the movement of a ship (Pérez Rojas, 1994). There are still some difficulties for its application due to a limitation imposed by the capacity of the machines used for its processing and post processing or the incorporation of more accurate models for the turbulence phenomena. The outcomes brought up through the numerical modeling with computers by means of the new CFD (Computational Fluid Dynamics) techniques, require in their development stage, a mechanism which permits the assessment of their degree of accuracy, generating new working lines which improve the output of the codes arriving even to propose different ways from those previously followed. The ideal tool for this action is to compare with the data obtained from the prototype itself. Nevertheless, this alternative is difficult to be implemented in the naval hydrodynamic field, which makes necessary to look into other information sources, in particular to outcomes brought up from the physical modeling carried out in test channels, being understood that these have proven their efficacy throughout the years, just as it has been previously mentioned.

As the capacity of the computers improves, the codes improve too, diminishing the modeling time and increasing their range, such as solving numerically Navier – Stokes' equations with turbulence models. This, together with the improvement in the mesh systems, has permitted, evidently, to diminish those errors in connection with the results available in the hydrodynamic channels; this substantial improvement in the quality of the CFD outcomes generates an increasing exigency about the Test Channels outcomes, which is the source where the information for assessment of numerical models are provided from, demanding greater definitions and the assessment of errors or uncertainty in connection with the experiments. The assessment of these uncertainty, as well as the need of establishing a Quality Management System, demand the incorporation of the Test Channels to a universal Accreditation System.

Fig. 1. Representation of runoff on a hull (CFD)

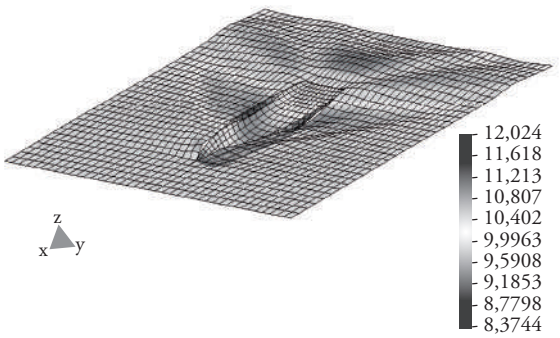

Acreditation

Accreditation is the procedure through which an authorized Institution recognizes in a formal manner that an organization is competent to carry out a specific assessment activity. These institutions are in charge of assessing and carrying out an objective statement that the services and products meet some specific requirements. The Testing and Gauging Laboratories, the certification institutions (of products, of management systems, of people), the inspection institutions, and the environmental inspectors are examples of Competence Assessment Institutions.

Under the Quality outlines, for example, ISO 9000, the Certification or Registration terms, that point fundamentally to transparency in their procedures, for both the internal operation as well as for external relation. Otherwise, Accreditation requires, in addition, a level of competence in the performance of activities, which differentiates it from Certification or Registration. An example is the norm ISO/IEC 17025, "Requirements for competence of test and measurement laboratories", which presents requirements of a higher degree of technical competence which include de determination of uncertainties.

Accreditation brings benefits to Management, since it offers an organization which is specialized and independent from the market interests that acts based on exclusively technical criteria. It puts to its disposal a valuable resource, a set of assessors who have proven their technical competence. It also strengthens the public's confidence on the basic services (public health laboratories, safety of food, etc.). For the assessors, the benefit of Accreditation is the contribution that the logo "Accredited" offers as a distinguishing feature in the market, being an integrity and competence guarantee, hence increasing the trade opportunities. Nowadays it is an indispensible requirement in most activities, becoming a basic requirement in order to offer technical assessment services, such as measuring, certification of quality systems, etc.

Acreditation of Test Channels

The Test Channels utilized for hydrodynamic tests must be considered as Laboratories, where tests with physical models are carried out. This immediately suggests the incorporation of them into a quality and specific competence system, just as it is stated, for example, by the norm ISO 17025. Signs of involvement with this aspect of the measurement process are beginning to be observed, pressed, on one hand by the pressure exerted when quality systems are being implemented, and on the other hand due to the need of adjusting the uncertainty margins on the measures in order to validate the modeling outcomes carried out in CFD.

Leadership of this process has been for the International Towing Tank Conference (ITTC) that at the 22nd Conference indicates, in a formal manner, the need of the implementation of a quality and uncertainty in measurement estimation system. By means of their Quality Committee they establish an approximation to the issue through a clarifying document about the range and terms in connection with the assessment of uncertainty in measurement.

Historically the ITTC has proposed to go through the path of an improvement of the outcomes in order to ensure the required validation conditions, path which later on led to the certification of quality implementing a universal analogue system to that one developed in other areas, applied specifically to the Test Channels, their management and quality of outcomes.

The ITTC efforts towards improving the quality and validation of the information go back to 1960, when at the 9th Conference research with models normalized by some channels (ITTC, 1960, 2005) was promoted, and the submission of outcomes to the Committee of Resistance in accordance with the established in the Report was recommended. These installations agreed the test with these normalized models in order to determine variations in the measured resistance, and despite of the fact that some error sources were detected, errors were

not determined, the dimensions of the models were not controlled and finally the effort was unsuccessful.

This issue is retaken at the 16th Conference, where four hulls were defined to carry out a joint research. These hulls were the Wigley, which is a hull with parabolic lines or mathematical careening, hull of series 60 with a 0.6 block coefficient, a Hamburg Ship Model Basin (HSVA) Tanker, and the Athena, a fast ship, a Cooperative Experimental Program (CEP) was established which would be working until arriving to the 18th Conference in 1987.

October 21, 1985 remains registered as the date of the creation of the Working Validation Party whose main task is to establish recommendations about that subject to the Committee, briefly outlining the foundations of the uncertainty calculation (ITTC, 1987).

At the 19th Conference, in 1990 the Validation Panel submits the "Guidelines for the Uncertainty Analysis in Measures" (ITTC, 1990) based on the norm ISO / ANSI together with examples related to tests in towing tanks.

The recommendations arisen from the Validation Panel are taken by the 20th Conference. Fundamentally, the responsibility for the activities related to the validation of data and the uncertainty calculation is transferred to the working parties, creating a Group whose action was focused mainly towards the establishment of a quality system in accordance with the norm ISO 9000. This Group was denominated Quality Control Group (ITTC, 1993).

The QCG's task at the 21st Conference is focused on progressing on the concepts handled in a quality system, including examples of implementation (ITTC, 1996).

At the 22nd Conference, the problem of calculating the uncertainty and the validation is presented with more emphasis; in the Final Report and Recommendations, the Committee of Resistance states the following in its Chapter 5- "Analysis of Uncertainties in Experimental Fluid Mechanics" - (ITTC, 1999):

> "The report of uncertainty in experiments continues to be a problem for the ITTC..... Those problems include the implementation of procedures, documentation and the submission of results. The estimation of the uncertainty associated with the experiments is indispensible for estimating the risks in design, not only when such information is utilized directly, but also, when it is used in the calibration and/or validation of other methods."

Similarly, the Group submits a quality manual (ITTC, 2001) based on the norm ISO 9000, proposal which is submitted to the consideration as recommended procedure; in this manual procedures for calculating uncertainty in accordance with the normative developed by the American Institute of Aeronautics and Astronautics (AIAA) in 1995 are introduced based on the methodology described in Coleman & Steele (1989), being it an up-dating of the previous normative ANSI / ASME (1985), and of the international normative ISO GUM (Guide to the expression of Uncertainty in Measurement)

The Committee of Resistance adopts the recommended procedures about methodologies for the assessment of uncertainty, guidelines for the conduction of experiments in towing tanks and examples for the resistance tests presented in the Quality Manual: 4.9 – 03 – 01 – 01 "Uncertainty Analysis in EFD, Uncertainty Assessment Methodology"; 4.9 – 03 – 01 – 02 "Uncertainty Analysis in EFD, Guidelines for Resistance Towing Tank Tests"; 4.9 – 03 – 02 – 01 "Resistance Tests"; 4.9 – 03 – 02 – 02 "Uncertainty Analysis, Example for Resistance Test"

The 23rd Conference tells about the experience carried out by three laboratories, which taking into account the recommendations proposed at the previous call, carried out resistance tests, sinking and trim, and wave elevation, using models of the same geometry and test conditions, but of different scales; starting from these experiences,

comparative data emerge for the variables utilized in the reduction equation and for determining reduction and for determining uncertainty. This work did not have enough details, did not take into account some effects affecting the total uncertainty, which meant the need of making new efforts in order to improve the individual uncertainty estimates (ITTC, 2002). Then, it is suggested a common methodology expressed through a series of procedures for the uncertainty analysis in the resistance tests, sinking and trim, wave profile and height, both for the simple tests as well as for the multiple ones. These procedures were included in the Quality Manual: 4.9 – 03 – 02 – 03 "Uncertainty Analysis Spreadsheet for Resistance Measurements"; 4.9 – 03 – 02 – 04 "Uncertainty Analysis Spreadsheet for Speed Measurements"; 4.9 – 03 – 02 – 05 "Uncertainty Analysis Spreadsheet for Sinkage and Trim Measurements"; 4.9 – 03 – 02 – 06 "Uncertainty Analysis Spreadsheet for Wave Profile Measurements". This Conference recommends the carrying out of comparative tests between ITTC members, in order to identify systematic errors, action which was concreted at the 24th Conference, in which opportunity the laboratory members are invited to participate with such a purpose. An inter-comparison exercise was designed where two scales would be available (Geosims) of the model developed at the David Taylor Model Basin (DTMB) DTMB 5415, with length overalls of 5.720 m and 3.048 m respectively, which will be utilized by two groups of institutions for their tests and analysis. The DTMB 5415 is a model which represents a modern ship of "Combatant" type, widely used for CFD codes validation and uncertainty determination in EFD (Experimental Fluid Dynamics) selected in Gothenburg 2000 as a benchmark for validation of numerical models (ITTC, 2002, 2005).

Each one of the models will complete a pre–determined schedule which will take them to different laboratories, beginning at those laboratories where they were constructed, being these the Hydrodynamic Experiences Channel of El Pardo (CEHIPAR) in the case of model with a length of 5.720 m, and the CEHINAV of the ETSIN, for the model with length of 3.048 m (ITTC, 2005).

Uncertainty Determination - ITTC

The procedure adopted by the ITTC is based on the methodology defined by the AIAA in the Norm AIAA S – 071A - 1999 (1999) and by ANSI / ASME (1998), both founded on "Experimentation and Uncertainty Analysis for Engineers", by Coleman, H.W. and Steele, W.G., as all of the methodologies and procedures source of reference and discussion.

It is necessary to introduce the concepts where the calculation of uncertainty on measurements is supported. Terms such as measure, error, uncertainty, can lead to misinterpretations or confusing interpretations if not clearly defined.

The definitions of the terms related to measurements are developed in the norm ISO/IEC/OIML/ BIPM (1984) "International vocabulary of basic and general terms in metrology" (VIM), while the statistical concepts come from norm ISO 3534 "Statistics – Vocabulary and symbols" (ISO 1992,1999, 2006; AIAA, 1999; Schmid, 2000).

Measure: it is the subject attribute to measurement of a specific physical phenomenon which can be identified and valued. The clear identification of the measure and its detailed description from the point of view of the variables which take part in its definition is one of the main points in question. An incorrect or deficient definition could lead to failure in the measurement procedure.

Error: it is the discrepancy between a measurement and the true value of the measure. Two components are assigned to this magnitude, one component of random nature which is called "precision error" supposing that there are unpredictable variations affecting the measurement, and other one which reflects other aspects of the measurement which produce a slant and which is normally associated to non random effects, which is indicated as "systematic error".

Uncertainty: doubt, fluctuation, irresolution, insecurity; in the case of the measurements it is applied with the sense of doubt or lack of certainty in the accuracy of the measurement outcomes. It

is a parameter which characterizes the dispersion of values which can be attributed to the measure, reflecting the lack of an exact knowledge on the value of the measure. The contributions to uncertainty are attributed to several sources, being inevitable its existence; improvement of the measurement procedures can lead to diminishing the magnitude of the uncertainty, although they never disappear completely.

It is necessary to have a perfect knowledge of the principle of the measurement, this is, of the scientific foundation used in measurement, of the method or manner in which it must be carried out, and of the specific procedure for applying the proposed method. An inadequate knowledge of any of these aspects can lead to erroneous estimates both of the quantity measured and of its uncertainty. Among the possible uncertainty causes, supposing that both the measure and the method of measurement have been well defined and that the latter has been adequately executed, the following can be mentioned: incomplete knowledge of the environmental effects on the measure, personal predisposition of the observer in connection with a manipulation or reading of instruments, assigned values to constants, parameters used by the algorithms of the reduction equations, reference materials, etc., assumed hypothesis in the model and incorporated into the measurement system, repetition of experiments in conditions apparently identical.

Spreading of errors: Usually the desired magnitude is not measured directly but rather other variables which relate to one another, by means of the reduction equation, end up defining the desired value. The way in which such uncertainty affects the final measurement is called spreading of errors, and each one of its components must be assessed.

Type of Errors

The error is assumed to be integrated by two components, the first one associated to deviations in the procedures of measurement or "systematic errors", while the remaining one attributed to countless aspects which in a random manner act during the procedure, is called "precision errors".

Systematic Error: it is the total error component due to deviations or slants in the measurement procedure, for instance a slipping of the scale, influence of one of the magnitudes on the others, etc. There are three categories of systematic errors: associated to the calibration of the instrument or measurement system, to the gathering of data, and to the reduction of data. Within each category there can be several elemental sources which force the systematic deviation. The total value of the systematic error estimate is calculated using the root sum square (RSS). For example, for the variable X_i there are $_J$ elemental sources of systematic errors identified by their estimators as $(B_i)_1$, $(B_i)_2$, ...$(B_i)_J$, with which the systematic error in the variable X_i can be calculated as:

$$B_i = \sqrt{\sum_{k=1}^{j} (B_i)_k^{\,2}} \qquad (1)$$

Where B_i is the estimate of the systematic error associated with the variable X_i and $B_{i,k}$ are the estimates of the systematic errors which contribute the total systematic error; values $(B_i)k$ must be estimated for each variable X_i utilizing the available information of the moment.

Spreading of Systematic Errors: the general expression of the uncertainty estimate due to the spreading of systematic errors of variables X_i in the experimental measurement of magnitude r defined as $r = r(X_1, X_2, \ldots\ldots\ldots\ldots, X_k)$ is given by the expression:

$$B_r = \left[\left(\frac{\partial r}{\partial X_1} \cdot B_1 \right)^2 + \left(\frac{\partial r}{\partial X_2} \cdot B_2 \right)^2 + \cdots \left(\frac{\partial r}{\partial X_k} \cdot B_k \right)^2 \right]^{1/2}$$

$$= \left[\sum_{i=1}^{k} (\theta_i \cdot B_i)^2 \right]^{1/2} \qquad (2)$$

where B_r is the systematic error corresponding to an experimental magnitude r and $\theta i = \partial_r / \partial X_i$ is denominated coefficient of sensibility, describes

how sensible the measure is with respect to the variations of the corresponding input magnitude. Constants or properties of materials: the systematic errors associated with constants will be considered void since such data does not generate uncertainty. In the case of properties of materials which appear in the phenomena of reduction equations, when they are given in the tables or curves in according to a variable of definition. It will be assumed as systematic error in this case the error itself in the generation of such data. In case of not having access to this information, some criterion must be assumed, for example, considering the last meaningful figure of the values in the table.

Equations of calibration: The equation of calibration is an equation which relates a measurement or output value to the measurement of a magnitude or input value:

$$X_k = f\,(y_1, y_2, \cdots\cdots\cdots\cdots y_N) \qquad (3)$$

This equation must be treated as a reduction equation, and due to this, its treatment will be similar to that one given in equation [2]:

$$B_i = \left[\left(\frac{\partial X_K}{\partial y_1} \cdot B_1 \right)^2 + \left(\frac{\partial X_K}{\partial y_2} \cdot B_2 \right)^2 + \cdots\cdots \left(\frac{\partial X_K}{\partial y_N} \cdot B_N \right)^2 \right]^{1/2} \qquad (4)$$

Precision Errors: the precision errors have their origin in an endless number of circumstances which cause different answers before the same measurement; these causes are always present and cannot be avoided completely. They include the operator and his/her answer facing each measurement, the instruments, the variations inherent to the energy supply, the environmental conditions which can produce variations in the answers of the instruments, etc.

Estimate of precision errors: the precision error can be estimated in the measurement r as:

$$P_r = t \cdot S_r \qquad (5)$$

where t is the limit to the variable normalized for the established interval of confidence, known as range factor; for $N>10$ it is assumed a value $t = 2$ and S_r is the standard deviation of the sample of N *readings*.

Spreading of precision errors: it has been previously established that the sources of precision errors are difficult to identify and are connected to different aspects of a very varied nature; however, it can be established that those errors have an absolutely random and Gaussian distribution.

Assuming that M sources of precision errors have been identified for variable j; the general expression of the uncertainty estimate due to the spreading of precision errors is given by the following expression:

$$Pj_i = \left[(P_j)_1^2 + (P_j)_2^2 + \cdots\cdots (P_j)_M^2 \right] = \left[\sum_{k=1}^{M} (P_j)_k^2 \right] \qquad (6)$$

In the experiments whose results are obtained from a sole test, the precision limit of each variable X_i *must* be determined. In order to do this, several ways must be taken into account: repeated measurements, auxiliary tests, previous experience, estimate starting from the data of the scale, etc.

When multiple samplings are carried out, averaged values of the M sets of measurements $(X_1, X_2, \ldots\ldots X_j)_k$ can be determined, in the same conditions of the experimentation, from which it is deducted

$$r = \frac{1}{M} \cdot \sum_{k=1}^{M} r_k \qquad (7)$$

The limit of the precision error of the set of samples is transformed into

$$P_r = \frac{t \cdot S_r}{\sqrt{M}} \qquad (8)$$

being S_r the standard deviation of the sample

$$S_r = \frac{1}{M-1} \cdot \sum_{k=1}^{M} (r_k - r) \qquad (9)$$

Test Channels: Uncertainty in measurements in the Resistance Test

The resistance test consists in conducting a model to a predetermined speed with the finality of determining the value of the resistance of the careening. To these effects, the resistance of the model as well as the velocity must be measured in a simultaneous way (ITTC, 2002). Once the total resistance has been determined the component denominated residual resistance must be deducted, which is that one which keeps the same in model and prototype if Froude's conditions of modeling of equality of number are respected; with this value and the estimate of the viscous component the total resistance in the prototype is finally determined.

The resistance is the horizontal component of the opposite force that the fluid exerts on the hull, and it is determined through the measurement of the tension force. To measure this quantity different methods are used, for example, mechanical or electronic dynamometers, load cells, etc.

The advance velocity of the model cannot be measured or it is very difficult to measure directly, for this reason, it is decided to measure the velocity of the dynamometric car, which is generally obtained through an encoder. This could be directly coupled to one of the wheels of the car or to one device bound to the car which can rotate without slipping by one of the third rails.

The density and viscosity of water affect the outcomes of the test, so they must be defined each time. Their determination is done in an indirect manner, by means of the measuring of the water temperature corresponding to the moment the test is being executed.

The measurement of the coefficient of resistance is expressed in a dimentionaless way which is being given by the equation

$$C_{TM} = \frac{R_{TM}}{1/2 \cdot \rho_M \cdot S_M \cdot V_M^2} \qquad (10)$$

where R_{TM} is the measured resistance, ρ_M is the density of water during the test, S_M is the model wet surface and V_M is the measured velocity, corrected by blockage if necessary.

The value of the determined residual component, dependent upon Froude's number, whose calculation is carried out using the expression

$$C_{RM} = C_{TM} - C_{FM} \cdot (1 + k) \qquad (11)$$

where C_{TM} is the sample coefficient of resistance, C_F is the frictional coefficient of resistance given by the model – ship Correlation Line adopted by the ITTC in 1957, k is the form factor deducted by the Prohaska method (ITTC 1966).

The tests are designed for a nominal velocity V_{nom}, but this velocity can hardly be obtained in an accurate form in the tests, hoping to find very close values in a normal distribution which will depend upon the quality of the equipment, of the calibration of the same, and the expertise of the operator. Given the fact that in this exercise the outcomes for the pre-established nominal velocity must be compared, the true velocity V_M must be corrected, taking into account that for little variations of same, the fact that the resistance is proportional to the square of the rate between velocities (ITTC, 2000).

$$C_{TM}^{nom} = C_{TM} \cdot \left(\frac{V_{nom}}{V_M} \right)^2 \qquad (12)$$

$$C_{FM} = \frac{0.075}{(\log Re - 2)^2} \qquad (13)$$

being $Re=(V_M \cdot L_M)/\nu_M$ Reynolds' Number for the test conditions, where V_M is the velocity of the model, L_M is the length of the model and ν_M is the viscosity of water.

In addition, the ITTC establishes the need of using a normalized temperature for the submission of outcomes due to the great dependency of the resistance on the viscosity (ITTC, 2002, 2005). In the case of the tests carried out for third parties, it is recommended to normalize to the medium temperature of the set, while in comparison exercises such the one proposed, the temperature will be corrected to a normalized temperature of

$$C_{TM}^{15^\circ} = C_{RM} + C_{FM}^{15^\circ} \cdot (1+k) \qquad (14)$$

where C_{RM} is the residual resistance and $C_{TM}^{15^\circ}$, $C_{FM}^{15^\circ}$ are the corrected coefficients for the normalized temperature.

The frictional resistance is dependent on the temperature, but not so the component of resistance by wave formation, which is calculated using the data as they come from the corrected tests for the nominal velocity. Equation (14) can be expressed in the following manner taking into account (11)

$$C_{TM}^{15^\circ} = C_{TM} + (C_{FM}^{15^\circ} - C_{FM}) \cdot (1+k) \qquad (15)$$

where $C_{TM}^{15^\circ}$ is the total normalized coefficient of resistance, $C_{FM}^{15^\circ}$ is normalized coefficient of friction and k is the factor or form.

Experimental determination of coefficients in exercise proposed by the ITTC

The outline of the tests, which were carried out in five consecutive days, is shown in detail in Table 1. The initial run will only be taken into account for generating an initial movement of the water in the tank. In Table 2 to Table 4 experimental outcomes obtained with model DTMB 5415, are shown. This model has been designated by the ITTC as a test model (benchmarking), at the Channel of Naval Hydrodynamic Experiences (Canal de Experiencias Hidrodinámicas Navales (CEHINAV)) at the Naval Engineers Superior Technical School (Escuela Técnica Superior de Ingenieros Navales (ETSIN) in the Universidad Politécnica de Madrid (UPM), participant in the international comparison exercise. This model has the following principal dimensions at the floating: length 3.048 m, beam 0.410 m, draft 0.132 m.

The first three columns represent the gross data obtained from the tests, while in column 4 the values of resistance corrected for the nominal speed are shown, and finally in the last column, the values of the coefficient of resistance normalized for a temperature of 15º are transcribed. Once the set of coefficients has been determined, depuration through the application of statistical methods is carried out. (Eliminated data in bold).

Analysis of Systematic Errors

In order to determine uncertainty in the resistance outcomes, the limit of the systematic errors must be established for the following set of variables:

Table 1. Velocities and Froude's Numbers of tests

	V1	V2	V3	V4	V5	V6	V7	V8	V9	V10
Fr	0,28	0,10	0,28	0,41	0,10	0,28	0,41	0,10	0,28	0,41
V (m/s)	1,530	0,547	1,530	2,241	0,547	1,530	2,241	0,547	1,530	2,241

Source: Author

Fig. 2. CAD Representatiosn of the model DTMB 5415

Table 2. Data of Resistance Test for Fr 0.10

R_X (N)	V (m/s)	Temperature (º)	$R_{X\,norm}$ (N)	$C_T^{15º}$
0,94	0.54602	15.5	0,941	0,004580
0,94	0.54604	15.6	0,946	0,004610
0,99	0.54605	15.7	0,996	0,004855
0,97	0.54602	15.7	0,973	0,004742
0,97	0.54600	15.7	0,975	0,004754
1,01	0.54604	15.9	1,018	0,004967
0,98	0.54603	15.7	0,979	0,004770
0,97	0.54603	15.8	0,977	0,004766
0,96	0.54598	16.0	0,967	0,004719
1,03	0.54604	15.9	1,029	0,005018
1,01	0.54604	16.0	1,012	0,004939
1,00	0.54601	16.0	1,003	0,004894
0,92	0.54606	16.0	0,921	0,004499
0,98	0.54603	16.1	0,982	0,004797
0,95	0.54602	16.3	0,955	0,004670

Source: Author

Table 3. Data of Resistance Test for Fr 0.28

R_X (N)	V (m/s)	Temperature (º)	$R_{X\,norm}$ (N)	$C_T^{15º}$
8,44	**1.52812**	**15.5**	**8,460**	**0,005273**
8,50	1.52809	15.6	8,521	0,005313
8,47	1.52799	15.7	8,487	0,005294
8,48	1.52805	15.7	8,498	0,005300
8,50	1.52819	15.7	8,523	0,005316
8,54	1.52806	15.9	8,565	0,005346
8,49	1.52818	15.7	8,506	0,005305
8,49	1.52814	15.8	8,515	0,005313
8,51	1.52807	16.0	8,532	0,005327
8,50	1.52811	15.9	8,519	0,005317
8,53	1.52805	16.0	8,556	0,005342
8,57	**1.52812**	**16.0**	**8,593**	**0,005365**
8,50	1.52810	16.0	8,518	0,005319
8,60	**1.52804**	**16.1**	**8,622**	**0,005385**
8,47	1.52807	16.3	8,492	0,005308

Source: Author

Table 4. Data of Resistance Test for Fr 0.41

R_X (N)	V (m/s)	Temperature (º)	$R_{X\,norm}$ (N)	$C_T^{15º}$
27,9	2.23716	15.5	28,033	0,008116
27,9	2.23716	15.6	27,954	0,008095
28,1	2.23734	15.7	28,142	0,008151
27,9	2.23746	15.7	27,964	0,008100
28,1	2.23737	15.7	28,163	0,008157
27,9	2.23743	15.9	27,981	0,008108
27,7	2.23699	15.7	27,846	0,008066
27,9	2.23721	15.8	27,982	0,008107
28,2	**2.23693**	**16.0**	**28,261**	**0,008191**
27,8	2.23687	15.9	27,933	0,008095
27,9	2.23708	16.0	27,953	0,008102
28,0	2.23721	16.0	28,131	0,008154
28,0	2.23696	16.0	28,101	0,008145
27,9	2.23717	16.1	28,028	0,008126
27,8	2.23725	16.3	27,893	0,008090

Source: Author

Table 5. Resistance: variables for calculating uncertainty

Variable	Symbol	Variable	Symbol
Length	L_M	Density	$\rho(T)$
Wet Surface	S_M	Viscosity	$v(T)$
Velocity	V_M	Coefficient of Frictional Resistance	$C_{FM}(Re)$
Resistance	R_X	Coefficient of Total Resistance	C_{TM}
Temperature	T	Factor of Form	$1+k$

Length: It is assumed that in the confection of the model an error of ± 1 mm is made when the machine for carving the model on wood starts the process, for example, on the fore end, and another error exactly the same when it finishes on the opposite end, due to an error in the positioning of the cap. The systematic error would be $B_{L1} = 2.000E\text{-}03\ m$.

Wet Surface: we will have contributions due to errors transmitted by the weighing of the model generating an error in estimating the displacement, and due to the errors made in the linear dimensions which act in the same direction, completing a systematic error $B_S = 4.154E\text{-}03\ m^2$.

Velocity: the velocity is the measurement through an encoder coupled directly to the dynamometric car motive system. Since there were not up-dated data on how it functioned, data on calibration of the system were handled, finding out that the errors combined of calibration and of the reduction equation ($V=d/t$; d is the distance and t is the time in covering such distance) are:

Table 6. Systematic error of the velocity

Froude's Number	BV (m / s)
0.100	**1.538E-03**
0.280	**1.553E-03**
0.410	**1.574E-03**

Source: Author

Resistance: The resistance is measured through the load cell which is connected by means of a flexible link directly to the model. In this case there appear components of error associated with calibration of the cell itself and different sources in the acquisition of data (misaligning of the load cell, analogous - digital conversion of the measuring and trim equipment of the model). The composition of these errors determines a systematic error B_R = *4.361E-02 N*.

Temperature: it is measured with a microprocessor thermometer which consists of a calibrated termistor. The temperature termistor is linearized by means of a microprocessor fitted in the instrument. The range of the measurement is between –50º and 150º, being its resolution 0.1º and its precision ± 0.4º. This value is considered as an estimate of the error in this case, being then B_t = *4.000E-01º*.

Density: it is calculated according to the tables provided in the ITTC "7.5-02-01-03 procedures. Density and Viscosity of Water", whose values can be represented by the correlation:

$$\rho = 1000.1 + 0.0552 \cdot t - 0.0077 \cdot t^2 + 0.00004 \cdot t^3 \qquad (16)$$

where *t* is the temperature of the water channel measured in ºC; part of the systematic error is associated with the equation of reduction of the phenomenon, while the adjustment curve of the experimental data contributes with another component. Finally the estimation of the error will be B_ρ = *7.816E-02 kg/m³*.

Viscosity: analogously like in the case of density, viscosity is calculated according to the tables provided in the ITTC "7.5-02-01-03 proceedings. Density and Viscosity of Water", whose values can be represented by the correlation:

$$\nu = (6.83E-04 \cdot t^2 - 5.228E-02 \cdot t + 1.768) \cdot 10^{-6} \qquad (17)$$

where *t* is the temperature of the water of the channel measured in ºC. The components of error are conceptually equivalent, completing in this case a value of Bρ= *2.001E-08 m²/s*.

Frictional Coefficient: it is calculated through equation 13, being the error limited to that one associated with the equation of reduction:

$$B_{C_F} = \left[\left(\frac{\partial C_F}{\partial V} \right)^2 \cdot B_V^{\,2} + \left(\frac{\partial C_F}{\partial L} \right)^2 \cdot B_L^{\,2} + \left(\frac{\partial C_F}{\partial \nu} \right)^2 \cdot B_\nu^{\,2} \right]^{1/2} \qquad (18)$$

being its values according to the velocity the following:

Table 7. Systematic Error in the frictional coefficient of resistance

Froude's Number	B_{CF}
0.100	1.628E-05
0.280	1.189E-05
0.410	1.067E-05

Source: Author

Total Coefficient of Resistance: it is calculated through equation 10, and its systematic error is also associated with this equation of reduction like in the previous case:

Table 8. Systematic Error in the total coefficient of resistance

Froude's Number	B_{CT}
0.100	2.140E-04
0.280	3.322E-05
0.410	2.980E-05

Source: Author

Form Factor: this factor was estimated in an experimental form according to the established in the ITTC, 1999; the reduction equation of these data leads to an estimate of its systematic error shown in the following table:

Table 9. Systematic Error of the form in f(Fr)

Froude's Number	B_{1+k}
0.100	6.114E-02
0.238	3.820E-02
0.316	5.474E-02

Source: Author

Coefficient of total resistance: it is calculated through equation 16, and like in the previous cases the estimate of the systematic error is associated with this reduction equation, being the values

Table 10. Systematic Errors for Coefficient of Total Resistance Normalized

Froude's Number	B_{CT15^o}
0.100	2.155E-04
0.238	3.819E-05
0.410	3.427E-05

Source: Author

Analysis of Precision Errors

In order to determine the resistance, the magnitudes which show the random variation are: velocity, resistance, and temperature.

Table 11. Precision Errors

Froude's Number	P_{CT15^o}
0.100	7.571E-05
0.280	9.007E-06
0.410	1.479E-05

Source: Author

However, when correcting the experimental values to velocities and temperatures, the only variable affected by the precision errors will be the resistance. Given the fact that multiple tests have been carried out for each velocity, it is necessary to consider as a multivariable experiment, according to which we will have that the precision rate must be calculated in accordance with the formulation established in equations 8 and 9. The processed data for the three velocities are detailed in tables 2 to 4. The criterion adopted for dropping observations out of the range was to consider, in order to eliminate them, those measurements which exceeded $\pm 2\sigma$ the average [34], eliminating three records Fr = 0.28 and one for Fr = 0.41 (shown in bold). [σ represents the standard deviation of the sample]

Uncertainty in $C_T^{15^o}$

The uncertainty associated with the coefficient to total resistance normalized, UCTM15º, is calculated using the quadratic mean (root sum square) applied to the quantities which are involved in the phenomenon, the estimate of the systematic error , BCT15º, and the estimate of the precision error, PCT15º. In the last column of Table 12, how much the uncertainty calculated with respect to the total value of coefficient represents is shown with respect to the total value of coefficient CTM15º (second column).

Spreading of Errors: Analysis of Sensibility

Complementary to the estimate of uncertainty, the need of having, on one hand, an automated procedure which permits the assessment of uncertainty in real time, and on the other hand, to

Table 12. Total Uncertainty

Froude`s Number	$C_{TM}^{15^o}$	$B_{CT}^{15^o}$	$P_{CT}^{15^o}$	$U_{CTM}^{15^o}$	% $C_{TM}^{15^o}$
0.100	4.772E-03	2.155E-04	7.571E-05	**2.294E-04**	4.81
0.280	5.317E-03	3.819E-05	9.007E-06	**3.934E-05**	0.74
0.410	8.115E-03	3.427E-05	1.479E-05	**3.735E-05**	0.46

Source: Author

count on, with tools which permit the measuring of the influence the errors from the different variables have on the total value, was presented, generating useful information for the improvement of the processes or instruments (Longo y Stern, 2005).

The basic idea of this procedure can be explained through the description of the complex system of variables which is involved in the experimental tests and which is shown in Fig. 3. A first level is constituted by environmental variables completely independent; in this group we can distinguish environmental variables which define the environment of the experimented, other variables which define the dimensional frame, and finally those which are involved with the adjustment of the system of the collection of data and operation of the system.

Fig. 3. Diagram of spreading of errors

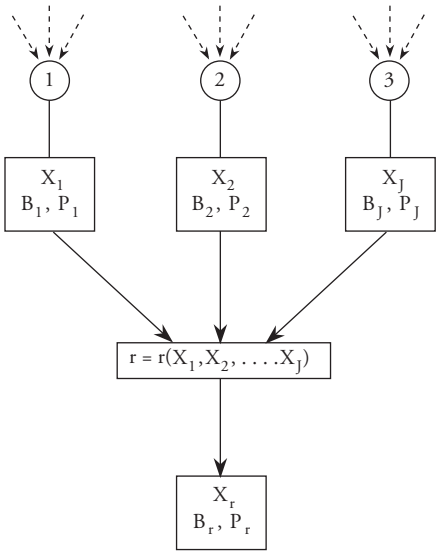

The set of variables of the first level act determining of conditioning those of the middle level which are those which have been identified as direct responsible for the variation of the magnitude which is intended to me measured. These latter determine the outcome of the experiment or test through a superior level or directly in its incidence in an equation of reduction, which is a mathematical model developed in order to quantify the phenomenon.

In this equation of reduction normally emerges from a process of an dimensionaless analysis evaluated at the light of experimental data. In these cases, the determination of uncertainty in the resulting measurement is a high complexity task, where the errors associated to the measuring of the variables of the initial level are transmitted to the recording variables, and the composition of uncertainty of these latter define through the equation of reduction the uncertainty of the final outcome.

Assessment of uncertainly in "linked steps"

The proposition of using the outline described calculating the systematic errors of the elemental variables or of initial level, using these outcomes to next calculate the corresponding errors in the recording variables, finishing the process through calculating the systematic error in the control magnitude using the previous values, all through an automated process so that a variation in any initial value is automatically reflected in the final outcome.

The proposed outline applied to the resistance test is described below, beginning from the superior level. The outcome of the resistance test is the resistance coefficient normalized $C_{TM}^{15o} = f(C_{TM}, C_{FM}, C_{TM}^{15o}, k)$. This coefficient is described in the equation of reduction according to other test variables, which represent the physical phenomenon, being this the superior level of the "linked steps" analysis. Each one of the factors involved in the previous equation represents the variables of the middle level: $C_{TM} = f_1 (R_{TM}, \rho, S_M, V_M)$, $CFM = f_2 (Re)$, k (defined experimentally), which depend upon the quantities measured or recorded: resistance, density, etc. Finally, these latter are determined by elemental variables which depend upon external factors: from the process of elaboration of the model (L), from the environmental conditions, $\rho = f_3 (T)$, $\nu = f_4 (T)$, or from the operational aspects such as the system of gathering of information in the case of R_{TM} or the calibration of the measuring system of velocity V.

Analysis of Sensibility for tests at the CEHINAV

In order to demonstrate how the variation of the systematic error influences the outcome of a variable, a test velocity corresponding to *Fr = 0.280* as reference, has been chosen, including each time the modifications compared to the values determined in the tests (Table 13).

Table 13. Coefficient and Systematic Error of Total Resistance for Fr = 0.280

Fr	C_T 15º	B_{CT} 15º	% C_T 15º
0,28	5,317 E-03	3,819 E-05	0,72

Source: Author

Table 14. Variation of the Systematic Error in the Length

B_L	Fr	C_T 15º	B_{CT} 15º	% C_T 15º
0,000 E-03	0,28	5,317 E-03	3,819 E-05	0,72
2,000 E-03	0,28	5,317 E-03	3,819 E-05	0,72
4,000 E-03	0,28	5,317 E-03	3,819 E-05	0,72

Table 15. Variation of the Systematic Error in the Temperature

B_T	Fr	C_T 15º	B_{CT} 15º	% C_T 15º
0,000 E-01	0,28	5,317 E-03	3,628 E-05	0,68
4,000 E-01	0,28	5,317 E-03	3,819 E-05	0,72
8,000 E-03	0,28	5,317 E-03	4,344 E-05	0,82

Table 16. Variation of the Systematic Error in the Weighing of the Model

B_W	Fr	C_T 15º	B_{CT} 15º	% C_T 15º
0,000 E-01	0,28	5,317 E-03	3,723 E-05	0,70
2,624 E-01	0,28	5,317 E-03	3,819 E-05	0,72
5,247 E-01	0,28	5,317 E-03	4,085 E-05	0,77

Table 17. Variation of the Systematic Error in the Load Cell

B_{R1}	Fr	C_T 15º	B_{CT} 15º	% C_T 15º
0,000 E-021	0,28	5,317 E-03	2,977 E-05	0,56
3,853 E-02	0,28	5,317 E-03	3,819 E-05	0,72
7,706 E-02	0,28	5,317 E-03	5,635 E-05	1,06

Table 18. Variation of the Systematic Error in the Analogous- Digital conversion of the Data Adquisition

B_{R2}	Fr	C_T 15º	B_{CT} 15º	% C_T 15º
0,000 E-02	0,28	5,317 E-03	3,603 E-05	0,68
2,042 E-02	0,28	5,317 E-03	3,819 E-05	0,72
4,084 E-02	0,28	5,317 E-03	4,406 E-05	0,83

Table 19. Simultaneous variation Load Cell / Data Adquisition

$B_{R1/R2}$	Fr	C_T 15º	B_{CT} 15º	% C_T 15º
VOID	0,28	5,317 E-03	2,694 E-05	0,51
COMBINED	0,28	5,317 E-03	3,819 E-05	0,72
DOUBLE	0,28	5,317 E-03	6,048 E-05	1,14

Table 20. Variation of the Systematic Error in the Velocity

B_V	Fr	C_T 15º	B_{CT} 15º	% C_T 15º
0,000 E-03	0,28	5,317 E-03	3,106 E-05	0,69
1.553 E-03	0,28	5,317 E-03	3,819 E-05	0,72
3,106 E-03	0,28	5,317 E-03	4,253 E-05	0,80

Source: Author

The values of the systematic errors of the selected variables are modified manually in the calculation program. Using the analysis procedure, those errors are forced in two opposite situations, duplicating them in first place and then reducing them to zero. The results of these modifications are shown below:

Analyzing the data presented for the variations of systematic errors and their incidence on the total uncertainty it can be established that the combination of two factors, the load cell and the data finder, supposes the most important factor to take into account in view of the limitation of the uncertainty. On their side, the variation of the error in the temperature, the weighing of the model, and the velocity have meaningless incidence, while the variation in the error made in determining the length is significant.

Conclusions

Assessment of uncertainty associated to the coefficient of resistance in the Test of Resistance for the experimental installation involved in the uncertainty determination exercise at an international level was presented. Basic aspects of the theories and procedures involved in such calculation were included.

This work is intended for the spreading of practices involved in the Accreditation of experimental laboratories as well as to promote the Test Channels which are not involved in instances such as the ITTC and to include them in their procedures.

On the other hand, the importance that the operator has in the identification of the systematic errors is presented, including the bases of an automated procedure which has been denominated "analysis in linked steps", becoming a tool which not only permits the determination in real time of the uncertainty associated to each one of the tests in particular, but also as an objective means of identification of the elements of greater weakness of the procedure or of the installation in order to be able to act on them as well as to improve the measurement system.

References

[1] TURSINI, L. Transactions INA, vol 95, 1953.

[2] WHITE, F.M. *Fluid Mechanics*. McGraw – Hill, 1999.

[3] TODD, F. H. *Resistance and propulsion*. Principles of Naval Architecture, 1967.

[4] PÉREZ ROJAS, L. *Los CFD como herramienta en Hidrodinámica*. Aulas del mar. Universidad de Murcia, Cartagena, Septiembre 1994

[5] CURA, A., BERTRAM, V. *Métodos de CFD en modelación naval*. Facultad de Ingeniería, Montevideo, Uruguay. 1995.

[6] ITTC. 9th International Towing Tank Conference. *Proceedings; Decisions and Considerations* 725. Paris, Francia. 1960.

[7] ITTC. 17th International Towing Tank Conference. *Proceedings* 79 - 88. Gotenburgo, Suecia. 1984.

[8] ITTC. 18th International Towing Tank Conference. *Proceedings* 311 - 316. Kobe, Japón. 1987.

[9] ITTC. 19th International Towing Tank Conference. *Proceedings V1*. 578 - 603. Madrid, España. 1990.

[10] ITTC. 20th International Towing Tank Conference. *Proceedings V1*. 79 - 103. San Francisco, USA. 1993.

[11] ITTC. 21th International Towing Tank Conference. *Proceedings V1*. 315 - 337. Trondheim, Noruega. 1996.

[12] ITTC. 22th International Towing Tank Conference. *Resistance Committee: Final Report and Recommendations to the 22nd ITTC*. Seul, Japón. 1999.

[13] ITTC. 22th International Towing Tank Conference. *Sample Quality Manual*. Seul, Japón. 1999.

[14] ITTC 22nd. International Towing Tank Conference, *Resistance Committee Report*, ITTC, 1999. Seoul, Corea.

[15] ITTC. QM Recommended Procedures. *Performance, Propulsion; 1978 ITTC Performance Prediction Method*. 1999.

[16] ITTC. 23th International Towing Tank Conference. *Proceedings; Resistance Committee: Final Report and Recommendations*" 17 - 87. Venecia, Italia. 2002.

[17] ITTC. QM Recommended Procedures. *Testing and Extrapolation Methods; Resistance; Resistance Test*. 2002.

[18] ITTC. QM Recommended Procedures. "*Resistance Uncertainty Analysis, Example for Resistance Test*". 2002.

[19] ITTC. 24th International Towing Tank Conference. *Proceedings V1*. 313 - 321. Edimburgo, Inglaterra. 2005.

[20] ITTC. 24th International Towing Tank Conference. *ITTC Worldwide Series for Identifying Facility Biases*. Edimburgo, Inglaterra. 2005.

[21] INTERNATIONAL ORGANIZATION FOR STANDARDIZATION. ISO/IEC PRF Guide 99 *International vocabulary of basic and general terms in metrology* (VIM). 1999.

[22] INTERNATIONAL ORGANIZATION FOR STANDARDIZATION. ISO 3534 – 1 *Statistics – Vocabulary and symbols*. 2006.

[23] INTERNATIONAL ORGANIZATION FOR STANDARDIZATION. ISO/TAG 4/WG3: 1992. *Guide to the Expression of Uncertainty in Measurement*. 1992

[24] AMERICAN INSTITUTE OF AERONAUTICS AND ASTRONAUTICS. AIAA S-071 Standard. *Assessment of Wind Tunnel Data Uncertainty*. 1999.

[25] SCHMID, W. A.; LAZOS, R. J. *Guía para estimar la incertidumbre de la medición*. CENAM, El Marquez, Qro., México. 2000.

[26] COLEMAN, H. W.; STEELE, W. G. *Experimentation and Uncertainty Analysis for Engineers*; John Wiley & Sons, Inc., New York, NY. 1999.

[27]LONGO, J.; STERN, F. *Uncertainty Assessment for Towing Tank Tests with example for Surface Combatant DTMB model 5415*. Journal of Ship Research, Vol. 49, No. 1. Marzo 2005.

[28] CEDEX (Centro de Estudios y Experimentación de Obras Públicas) - Ministerio de Fomento (http://www.cedex.es/).

[29]ENAC. *Acreditación, una herramienta al servicio de la Administración y de la sociedad;* información institucional. Entidad Nacional de Acreditación (http://www.enac.es/)

[30]ENAC; *La Entidad Nacional de Acreditación*; información institucional. Entidad Nacional de Acreditación (http://www.enac.es/)

[31]ENAC. *Laboratorios Acreditados: la necesidad de estar seguro*; información institucional. Entidad Nacional de Acreditación (http://www. enac. es/)

[32]PEREZ ROJAS, L; VALLE CABEZAS, J.; SOUTO IGLESIAS, A. *The future in the experimental ship hydrodynamics*. ETSIN. 2nd International Conference on Maritime Transport and Maritime History: Maritime Transport 2003, Barcelona, España. Noviembre 2003.

[33]LÓPEZ GONZÁLEZ, L. A.; PEREZ ROJAS, L. *Estimación de la incertidumbre en la medida del hundimiento y trimado del modelo Serie 60*. Universidad Politécnica de Madrid, ETSIN. Madrid, España. Octubre 2002.

[34]CERNUSCHI, F.; GRECO, F. I. *Teoría de errores de mediciones*. Editorial Universitaria de Buenos Aires. Buenos Aires, Argentina. Junio 1974.

[35]*Proyecto Bajel: Informe de los ensayos de resistencia realizados con el modelo de la carena del buque "Serie 60"*. Estudios de Incertidumbre. Departamento de Arquitectura y Construcciones Navales, Canal de Ensayos Hidrodinámicos, ETSIN. Noviembre 2000.

[36]BADANO, P.; GUARGA, R. *Las técnicas de modelación en canales de prueba navales: estudio de la viabilidad de su aplicación en el Canal Hidrométrico del IMFIA*. Facultad de Ingeniería, Montevideo, Uruguay. 1990

[37]PROHASKA, C. W. *A simple method for the evaluation of the Form Factor and Low Speed Wave Resistance*. Proceedings 11th ITTC, 1966.

Editorial Regulations for Authors

Thematic

The *Ship Science and Technology* Journal accepts for publication original engineering contributions on ship design, hydrodynamics, dynamics of ships, structures and materials, vibrations and noise, technology of ship construction, marine engineering, standards and regulations, ocean engineering and port infrastructure, results of scientific and technological researches. Every article shall be subject to consideration of the Editorial Council of *The Ship Science and Technology* Journal deciding on pertinence of its publication.

Typology

The *Ship Science and Technology* Journal accepts publishing articles classified within following typology (Colciencias 2006):

- *Scientific and technological research article*. Document presenting detailed original results of finished research projects. Generally, the structure used contains for important parts: introduction, methodology, results and conclusions.
- *Reflection Article*. Document presenting results of a finished research as of an analytical, interpretative or critical perspective of author, on a specific theme, resorting to original sources.
- *Revision Article*. Document resulting from a finished research in the field of science or technology in which published or unpublished results are analyzed, systemized and integrated in order to present advances and development trends. It is characterized for presenting an attentive bibliographic revision of at least 50 references.

Format

All articles must be sent to editor of The *Ship Science and Technology* Journal accompanied by a letter from author requesting its publication. Every article must be written in Microsoft word processor in single space and sent in magnetic form. Articles must not exceed 9,000 words (7 pages). File must contain all text and any tabulation and mathematical equations; this file must not contain graphs. Additionally, all mathematical equations must be made in Microsoft Word Equations Editor. File must not include graphs.

Content

All articles must contain following elements that must appear in the same order as follows:

Title
It must be concise with appropriate words so as to give reader a slight idea of content.

Author and Affiliations
Author's name must be written as follows: name, initial of second name and surnames. Affiliations of author must be specified in following way and order:

- Business or institution (including department or division to which he/she belongs).
- Mail address.
- City (Province/State/Department).
- Country.
- Telephone, fax and e-mail.
- Specify name and e-mail of correspondent author.

Summary
Short essay of no more than one hundred fifty (150) words specifying content of work, scope and results. It must be written in such a way so as to contain key ideas of document.

Key Words
Identify words and/or phrases that help recover relevant ideas in an index.

Introduction
Text must be explanatory, clear, simple, precise and original in presenting ideas. Likewise, it must be organized in a logic sequence of parts or sections, with clear subtitles that guide reader. The first part of document is the introduction. Its objective is to present the theme, objectives and justification of why it was elected. Likewise, it must contain sources consulted and methodology used as well as a short explanation of status of research if it were the case and form in which the rest of article is structured.

Body Article
It is made up of the theoretical framework supporting the study, statement of theme, status of its analysis, results obtained and conclusions.

Equations, Tables, Charts ang Graphs
All of these elements must be numbered in order of appearance according to its type and have at the foot, that is, exactly underneath of chart, graph or picture, the source from where data was taken and who made it.

Equations must be numbered on the right hand side of column containing it, in the same line and in parenthesis. Body of text must make reference of it as "(Equation x)". When the reference starts a sentence it must be made as follows: "Equation x".

Equations must be written so that capital letters can be clearly differenced from small letters. Avoid confusions between letter "l" and number one or between zero and small letter "o". All subindexes, superindexes, Greek letters and other symbols must be clearly indicated.

All expressions and mathematical analysis must explain all symbols (and unit in which it is measured) that have not been previously defined in the nomenclature. If work is extremely mathematical by nature, it would be advisable to develop equations and formulas in appendixes instead of including them in body of text.

Graphs (lineal drawings, tables, pictures, etc.) must be numbered according to order of appearance and should include the number of graph in parenthesis and a brief description. As with equations, in body of text, reference as "(Graph X)", and when reference to a graph is the beginning of a sentence it must be made as follows: "Graph x".

Charts, graphs and illustrations must be sent in modifiable vector file format (Microsoft, Excel, Microsoft Power Point and/or Microsoft Visio). Pictures must be sent in Tif format files, separate from main document in a resolution higher than 1000 dpi.

Foot Notes
We recommend their use as required to identify additional information. They must be numbered in order of appearance along the text.

Acknowledgment
Acknowledgments may be made to persons or institutions considered to have made an important contribution and not mentioned in any other part of the article.

Bibliographic References

Quotations
They may be made in two ways: at the end of text, in which case last name of author followed by a comma, year of publication followed by a comma and number of page, in the following manner:

"With modernity there was eagerness for accuracy, preciseness and 'clear' demonstration of all human life scopes" (Cianciardo, 2004, p.30).

The other way is:
Cianciardo (2005, p.30) manifests that "With modernity there was eagerness for accuracy, preciseness and 'clear' demonstration of all human life scopes".

List of References
Bibliographic references of original sources for cited material must be numbered at the end of article in alphabetical order and according to following parameters:

Books
Last name of author followed by a comma, initial(s) of name followed by a period, the year of publication of book in parenthesis followed by a comma, title of publication in italics and without quotation marks followed by a comma, city where published followed by a comma and name of editorial without abbreviations such as Ltd., Inc. or the word "editorial".

Basic Form:
Last name, I.N. (Year), Las claves del futuro. Economía y conflicto en Colombia, Bogota, Oveja Negra.

Author must remember that differently from Spanish, titles of books in English have all initial letters in capital letters, except for connectors. For example:

Kirzner, I.M: (1996), *Perception, Opportunity and Profit*, Chicago, University of Chicago, Press.

In the event of more than one author, separate by commas and the last one by an "and". If there are more than four authors write the last name and initials of first author and then the abbreviation "et al.".

If a corporate author
Write complete name of entity and follow the other standards.

Basic form:
Institution (year), *Title of publication*, city, editorial.

Example:
Fundacion Compartir (2005), *Nuestros mejores maestros. Experiencias educativas ejemplares*, Bogota, la Fundación.

Please note that if it is the same entity who edits book, you repeat name or write its abbreviation by initials or acronym. In the event that work has been made by a different editorial, follow the first example.

When book or any publication have as author an entity pertaining to the state, write name of country first.

Basic form:
Country, entity pertaining to the state (year), *Title of publication*, City, Editorial.

Example:
Colombia, Departamento Nacional de Planeación (2003), *Construcción de un futuro para Colombia desde sus territorios*, Bogota, DNP.

Journal Article
Last name of author followed by a comma, initial(s) of name(s) followed by a period, year and months separated by a hyphen in parenthesis. If publication specifies days write them too, followed by a comma, title of article in round letters and with simple quotation marks, the word "in" followed by name of publication in italics and without quotation marks, followed by a comma and then the year, volume (if any) number and pages of article.

Basic form:
Last name, I.N. (year, month-month), 'Title of article', in *Name of publication*, year, v, n.º, xx, pp. yy-zz.

Example:
Samper, D. (2006, September-November), 'La lengua esta quebrada… ¿con que la curaremos?, in *Number*, n.º 50, pp. 30-32.

Without author. Basic form
Name of publication, (year, date-date), 'Title of article', n.º xx, pp. yy-zz.

Example:
Semana (2006, July 31-August 7) 'Odisea en La Macarena', n.º 1.265, pp. 40-43.

Graduation Work
Last name of author followed by a comma, initial(s) of name(s) followed by a period, year when thesis was defended in parenthesis followed by a comma, title of work in italics and without quotation marks followed by a comma; between brackets and in small letters write the type of work (graduation monograph, master's degree thesis, etc.), followed by a comma, city where university is located followed by a comma, complete name of university followed by a comma and complete name of career.

Basic form:
Last name, I.N. (year when defended), *Title of work*, [type of work], City, University, Academic Program.

Example:
Salazar, N. (2006), *Inseminación artificial en jaguares,* [type of work], Bogota, Universidad Nacional de Colombia, Veterinary Career.

Internet
Last name of author followed by a comma, initial(s) of name(s) followed by a period, year of publication in parenthesis followed by a comma, that is, when it was "put up" in the network (if there is one) followed by a comma, title of work in round letters and simple quotation marks followed by a comma, "on-line" in between brackets followed by a comma, the expression "available at" with colon, complete address of page, followed by a comma, the word "recovered" followed by a colon and complete date when it was looked up.

Basic form:
Last name, I.N. (year), 'Title of article', [on-line], available at: http://www.direccion completa.com, recovered: day of month of year.

Example:
Semana (2006, November 11), 'Conocer la sociedad nacional en su reinado', [on-line], available at: http://www..semana.com/ wf_ InfoArticulo.aspx?IdArt=98125, recovered: 5 November of 2007.

Acceptance

Articles must be sent by e-mail to editor of The *Ship Science and Technology* Journal to revista@cyt-buques.com or in CD to mail address of journal, accompanied of the "Declaration of Originality of Work Written " included in this journal. Author shall receive acknowledgement of receipt by e-mail. Comments and evaluations made by the journal shall be kept in confidentiality. Receipt of articles by The Ship Science and Technology Journal does not necessarily constitute acceptance for publishing. If an article is not accepted it shall be returned to the respective author.

Opinions and declarations stated by authors in articles are of their exclusive responsibility and not of the journal. Acceptance of articles grants The Ship Science and Technology Journal the right to print and reproduce these; nevertheless, any reasonable petition by author to obtain permission to reproduce his/her contributions shall be attended.

SHIP
SCIENCE & TECHNOLOGY
CIENCIA & TECNOLOGÍA DE BUQUES

Statement of Originality of Written Work

Title of work submitted

_____

_____

_____

I hereby certify that work submitted for publication in The *Ship Science and Technology* journal, of Science and Technology for the Development of Naval, Maritime and Riverine Industry Corporation, Cotecmar, was written by me, given that its content is product of my direct intellectual contribution. All data and references to material already published are duly identified with its respective credit and included in the bibliographic notes and quotations highlighted as such.

I therefore declare that all materials submitted for publication are completely free of copyrights; consequently, I make myself responsible for any lawsuit or claim related with Intellectual Property Rights thereof.

In the event that article is chosen for publication by The *Ship Science and Technology* journal, I hereby state that I totally transfer reproduction rights of same to Science and Technology for the Development of Naval, Maritime and Riverine Industry Corporation, Cotecmar. In retribution for present transfer I agree to receive five issues of the journal where my article is published.

In witness thereof, I sign this statement on the _____ day of the month of _____ of year _____, in the city of _____ .

Name and signature: Identification document:

_____ _____

www.cotecmar.com/cytbuques/

www.cotecmar.com/cytbuques/